DUACS Level-3 SWOT KaRIn (L3_LR_SSH)
User Handbook

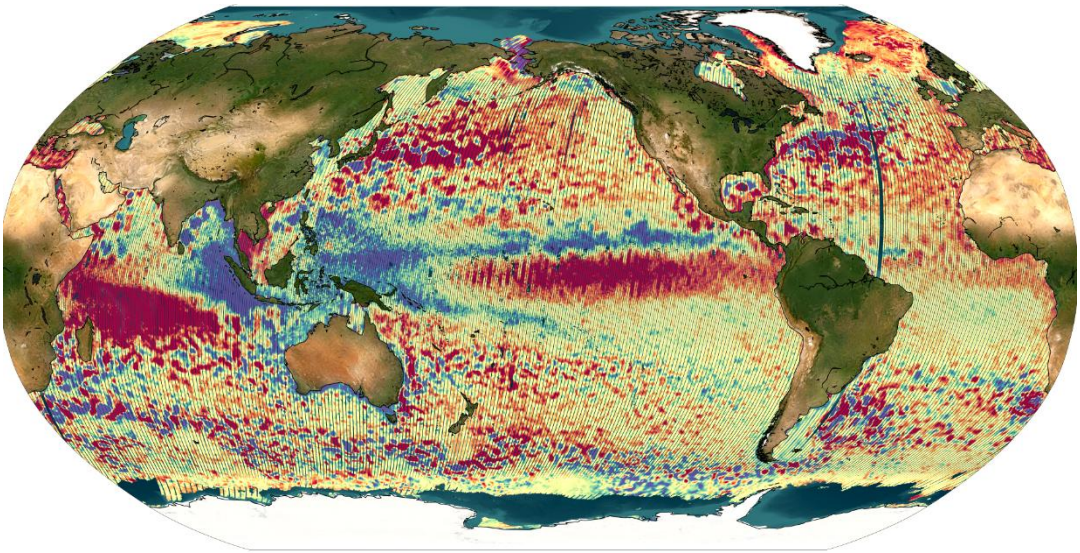

Nomenclature: SALP-MU-P-EA-23629-CLS
Issue:3.0

Date: October 2025

Chronology Issues:		
Issue:	Date:	Reason for change:
1.0	September 2023	First issue
1.1	May 2024	Updated product release (V1.0)
1.2	June 2024	Addition of Unsmoothed products
1.3	September 2024	Add product versions changes V1.0.1 and V1.0.2 (Basic and Expert datasets)
1.4	October 2024	Add Unsmoothed v1.0.2 Complete information on V1.0.2 temporal availability
1.5	January 2025	Add V2.0 Basic and Expert datasets
2.0	March 2025	Add v2.0.1 Basic and Expert and Unsmoothed products
2.1	May 2025	Update Unsmoothed product temporal availability
3.0	October 2025	Add v3.0 Basic and Expert and Technical products

List of Acronyms

Aviso+	Archiving, Validation and Interpretation of Satellite Oceanographic data
CLS	Collecte, Localisation, Satellites
CNES	Centre National d'Etudes Spatiales
SLA	Sea Level Anomaly
DAC	Dynamical atmospheric correction
L2	Level-2 product
L2P	Level-2+ product
L3	Level-3 product

Table of Contents

1 Introduction

This user manual describes the products named “Swot L3 KaRIn”. The Level-3 (L3) products are formally part of the Science Team Project DESMOS and funded by the French Early Adopter Program (i.e. PIA). Those products are lightweight, simple, and usable out-of-the-box; moreover, Nadir altimeter & KaRIn measurements are displayed in one single image.

The Value-added compared to SWOT L2 KaRIn (L2_LR_SSH) products are:

- State of the art research-grade upgrades (incl. very recent & submitted papers)
- Multi-mission calibration (SWOT is consistent with other altimeters)
- Noise-mitigation for SSHA derivatives (experimental, AI-based)
- Pre-made sophisticated editing procedure KaRIn and nadir instruments blended into a single image
- L3 has new layers (optional) that can blend with L2 fields

4 types of files are distributed: Basic, Expert, Technical and Unsmoothed.

- Basic L3_LR_SSH includes only SSHA (Sea Surface Height Anomaly) and mean dynamic topography (MDT) on the 2km KaRIn grid.
- Expert L3_LR_SSH includes the backscatter coefficient (sigma0), the mean sea surface (MSS) and geostrophic currents (absolute and anomalies) in addition to SSHA and mean dynamic topography (MDT). It also integrates algorithms, corrections and external models as separate layers. It is available on the 2km KaRIn grid.
- Technical L3_LR includes additional parameters and geophysical fields that may be of interest for certain applications or that provide an alternative solution to those used in the core (Basic/Expert) product. It is available on the 2 km KaRIn grid.
- Unsmoothed L3_LR_SSH includes the MSS, MDT and geostrophic currents (absolute and anomalies) in addition to the SSHA and MDT on the 250-m KaRIn native grid. Like the Expert subproduct, it also integrates a quality flag, corrections and external models as separate layers.

Publications should include the following statement in the Acknowledgments:

Citation Basic L3_LR_SSH:

"The SWOT_L3_LR_SSH product, derived from the L2 SWOT KaRIn Low rate ocean data products (L2_LR_SSH) (NASA/JPL and CNES), is produced and made freely available by AVISO and DUACS teams as part of the DESMOS Science Team project". AVISO/DUACS., 2023. SWOT Level-3 SSH Basic (v3.0) [Data set]. CNES. https://doi.org/10.24400/527896/A01-2023.017 “

Citation Expert L3_LR_SSH:

"The SWOT_L3_LR_SSH product, derived from the L2 SWOT KaRIn low rate ocean data products (L2_LR_SSH) (NASA/JPL and CNES), is produced and made freely available by AVISO and DUACS teams as part of the DESMOS Science Team project". AVISO/DUACS, 2023. SWOT Level-3 SSH Expert (v3.0) [Data set]. CNES. https://doi.org/10.24400/527896/A01-2023.018 “

Citation Technical L3_LR_SSH:

"The SWOT_L3_LR_SSH product, derived from the L2 SWOT KaRIn low rate ocean data products (L2_LR_SSH) (NASA/JPL and CNES), is produced and made freely available by AVISO and DUACS teams as part of the DESMOS Science Team project". AVISO/DUACS, 2023. SWOT Level-3 SSH Technical (v3.0) [Data set]. CNES. https://doi.org/10.24400/527896/A01-2025.009 ”

Citation Unsmoothed L3_LR_SSH:

"The SWOT_L3_LR_SSH product, derived from the L2 SWOT KaRIn low rate ocean data products (NASA/JPL and CNES), is produced and made freely available by AVISO and DUACS teams as part of the DESMOS Science Team project". AVISO/DUACS, 2024. SWOT Level-3 KaRIn Low Rate SSH Unsmoothed (v3.0) [Data set]. CNES. https://doi.org/10.24400/527896/A01-2024.003 “

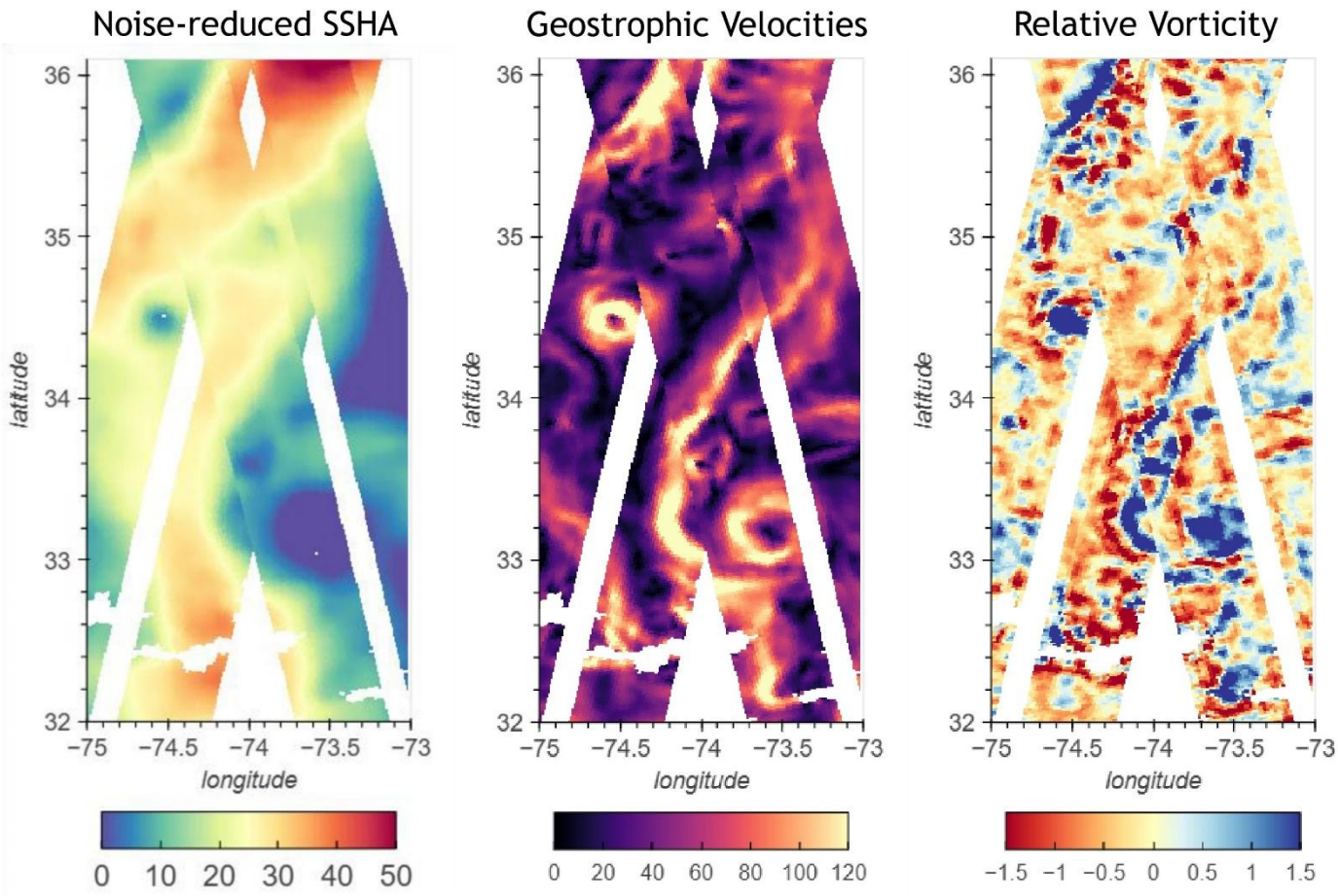

Figure 1: Example of SSHA (after noise reduction) (left), geostrophic velocities (middle) and relative vorticity (right) obtained with SWOT measurements contained in the SWOT L3 KaRIn oceanproduct. (cycle 502, tracks 9 and 22, 2023-04-26)

1.1 Data Policy and conditions of use

The SWOT L3 KaRIn ocean product is available free of charge for scientific studies and commercial activities.

2 Processing

This section describes the processing of the SWOT L3 KaRIn (L3_LR_SSH) product. This product contains the KaRIn measurements as well as the Nadir measurements (only in Expert and Basic products): KaRIn and Nadir instruments are blended into a single image.

Note that a presentation dedicated to the processing named “SWOT Level-3 Overview and link with L2 products”, from Dibarboure et al., have been presented at the SWOT Science Team in June 2024.
The processing methodology for SWOT level 3 products is outlined in a paper by Dibarboure et al. (2024).

The following figure provides an overview of the system for the generation of the SWOT L3 KaRIn ocean product. The Nadir component follows the same processing as the other altimeters as described in Pujol et al., 2023, and the L3 KaRIn processing sequence is given. The resultant L3 KaRIn ocean product contain both KaRIn and Nadir measurements.

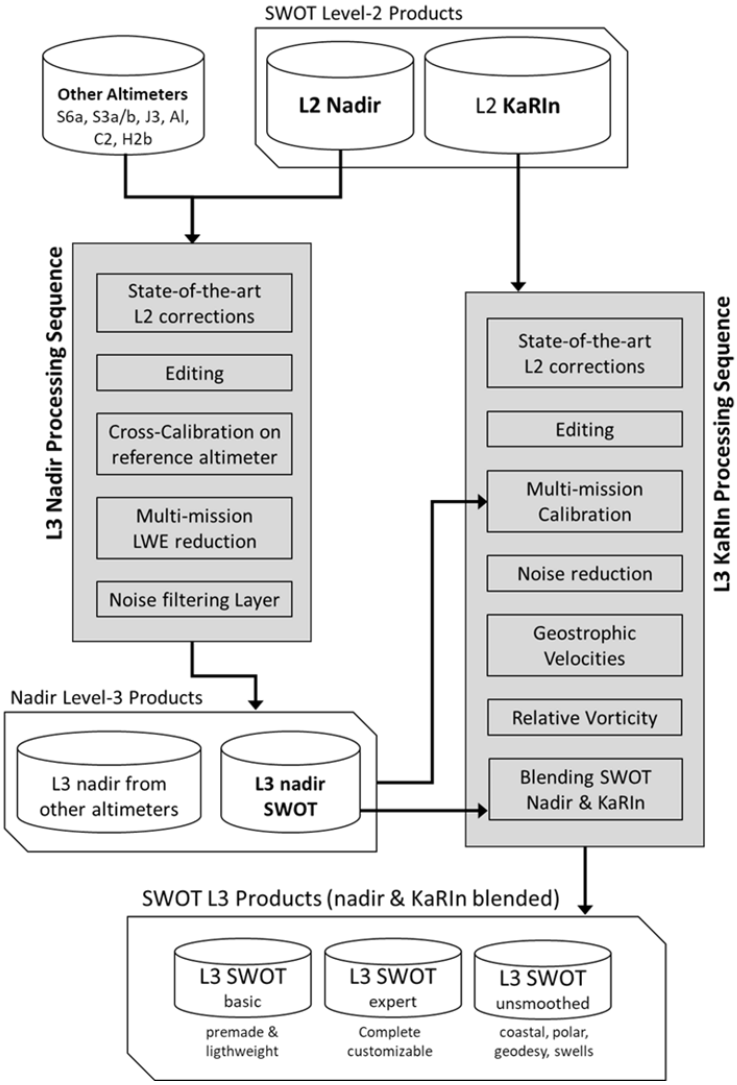

Figure 2: DUACS and SWOT L3 KaRIn and Nadir system processing

2.1 Input data

The input data used to compute the SWOT L3 KaRIn ocean product is the SWOT L2_LR_SSH, defined with a 2x2km or 250x250m spatial posting rate and distributed by the CDS-AVISO (https://doi.org/10.24400/527896/a01-2023.015). The version of these products evolves with time. The Table 1 lists the L2_LR_SSH product version used in the L3_LR_SSH production.

2.2 250m swath reconstruction

The L2 LR 250m product presents the data into separated 'left' and 'right' swaths, and including different holes in the swath grid definition. A specific acquisition aims to consolidate the product into a unified format compatible with other LR products.

The acquisition and preprocessing of the L2 LR 250m product performs several crucial steps to achieve this unification:

- **Swath Merging**: The unsmoothed products contain distinct data groups for the left and right instrument swaths. A core function **merges** these two sections into a single, continuous 2D array. This involves flipping the left swath and concatenating it with the right. A **39-pixel gap** is inserted at the center to represent the nadir gap, ensuring a continuous cross-track dataset.
- **Time Synchronization**: The script reads and validates the time vectors from both swaths. It then computes a single, unified time vector for each measurement line, typically by averaging the left and right timestamps.
- **Data Masking**: Invalid measurements are meticulously filtered out. A Boolean mask is generated based on valid latitude and time values, ensuring that only robust data points are processed and stored.
- **Variable Reading**: Data loading is primarily handled by a **variable reader**. This function iterates through a list of specified product files and reads the designated variables. The valid data mask is consistently applied to all variables, guaranteeing uniform dimensions across the dataset.
- **Geolocation Interpolation**: For **longitude** and **latitude** variables, a dedicated function interpolates any gaps in the geolocation data. This step is vital for constructing a complete and continuous swath.
- **Generating Supplemental Variables**: To maintain compatibility with standard LR products, the script can generate variables not present in the original unsmoothed files:
    - cross_track_distance: Calculated by a function based on a predefined instrument geometry.
    - valid_location_flag: Generated by a function to indicate whether the geolocation at each pixel is original or was filled via interpolation.
- **Metadata Extraction**: Essential metadata, such as cycle_number and pass_number, are extracted directly from the product filenames using a **regular expression pattern**.

2.3 Up-to-date standards

The measurements are then updated with the standards as follows:

	SWOT L3_LR_SSH v1.0	SWOT L3_LR_SSH v1.0.2	SWOT L3_LR_SSH v2.0 and v2.0.1	SWOT L3_LR_SSH v3.0
Product standard ref	PGC0 before 23/11/2023 PIC0 after	PGC0 before 10/01/2024 PIC0 after (see section 4)		PGC0 before 10/01/2024 PIC0 between 10/01/2024 and 06/05/2025 (c032 / p223) PID0 after
Orbit	POE-F			
Ionospheric	GIM model computed from vertical Total Electron Content maps (Chou et al. 2023) rescaled on the orbit altitude with IRI95 model (https://irimodel.org/)			
Wet troposphere	Model computed from ECMWF Gaussian grids			
Sea State Bias	Non-parametric SSB from AltiKa GDR-F (Tran 2019)		Non-parametric SSB from AltiKa GDR-F (Tran 2019) with corrected SWH MFWAM model field	
Mean Profile/ Mean Sea Surface	Hybrid MSS (SIO22,CNES/CLS22,DTU21) (Schaeffer et al. 2023; Laloue et al. 2024)			MSS CNES_CLS_2025 (beta release, Charayron et al. 2025)
Mean Dynamic Topography	MDT CNES_CLS_2022 (Jousset and Mulet 2020; Jousset et al. 2022) available on AVISO+ https://doi.org/10.24400/527896/a01-2023.003		MDT CNES_CLS_2022 (Jousset and Mulet 2020; Jousset et al. 2022) with a -5cm offset	
Dry troposphere	Model computed from ECMWF Gaussian grids (new S1 and S2 atmospheric tides are applied)			
DAC	DAC v4.0: TUGO forced with ECMWF pressure and wing fields (S1 and S2 were excluded) + inverse barometer computed from rectangular grids			
Ocean tide	FES2022: (Lyard et al. 2023; Loren Carrère et al. 2023) (https://doi.org/10.24400/527896/a01-2024.004)			FES2022: (Lyard et al. 2023; Loren Carrère et al. 2023) (https://doi.org/10.24400/527896/a01-2024.004) from unstructured grid when available and completed with cartesian grid
Internal tide	(Zaron 2019) (HRETv8.1 tidal frequencies: M2, K1, S2, O1)		(Zaron E. et Elipot S. 2024) (blend of HRET14 & HRET8.1; tidal frequencies: M2, K1, S2, O1, N2)	
Pole tide	(Desai et al. 2015)& Mean Pole Location			
Solid earth tide	Elastic response to tidal potential (Cartwright et Edden 1973; Cartwright et Tayler 1971)			
Loading tide	FES2022: (Lyard et al. 2023; Loren Carrère et al. 2023)			

Table 1: Altimeter standards used in the L3 KaRIn production

2.4 Cross Calibration

The correction is computed with the XCAL algorithm. The reference for the XCAL algorithm is Dibarboure et al., June 2022, SWOT Science Team meeting, SWOT simulated Level-2 and Level-3 data-driven calibration and Dibarboure et al., Sep 2023, SWOT Science Team meeting, Crossover Calibration Status and Examples.

The Level-3 calibration correction aims to reduce systematic errors in KaRIn and ensure its measurements are consistent with L3 products from other altimeter missions. Therefore, data from operational nadir altimeters are used in the KaRIn calibration process. KaRIn systematic errors are first estimated over ocean areas using pre-selected KaRIn measurements. The residuals, relative to multi-mission nadir data, are decomposed into roll errors and phase-screen errors. The resulting calibration correction is then interpolated over invalid measurement areas, including fe holes over ocean, continents and polar areas. This calibration is estimated using LR 2x2km upstream data.

The correction applied on the 250x250m product is an interpolation of the solution computed using 2x2km data.

The methodology has been refined through successive versions of L3 products.

In the L3 V1.0 version, the calibration has been improved with an updated phase screen correction with two components (varying with beta angle and in-orbit position) and an improved interpolation method for short segments

In the v2.0 version, the calibration has been improved with the aim of reducing the leakage of the ocean dynamic signal and taking into account the improvements made to the data selection processing: A large part of the data selection is newly applied before calibration

- Data eclipse transition segments are used in the calibration
- Fewer degrees of freedom are used
- (L3 pseudo phase screen corrections remain unchanged w.r.t v1.0.2)

In the V3.0 version, the calibration has been improved with a better estimation of the roll errors by adding harmonics on the day frequency; the use of an optimal interpolation methodology to estimate the roll correction in areas where direct estimation is not possible; and update of the static phase screen component for the PID product version.

2.5 Editing

The editing process mainly consists in applying the flags that are in the L2_LR_SSH input files. The variables taken into account are:

- ancillary_surface_classification_flag (to keep only ocean data),
- ssha_KaRIn_2_qual (L2 product flags)
- ssh_KaRIn_uncert (measurement uncertainty)
- distance_to_coast (for the coastal flag)
- cross_track_distance (distance from the nadir)
- Ice_concentration (for the polar flag)
- sig0_karin_2 (for the sea-ice classification of the Unsmoothed product)
- rain_rate_rf (for the rain flag)

From the L3_LR_SSH v1.0, a flag expert was created. Its content is refined through successive versions of L3 products as summarised in the following table. It gives the different flag values available for the different product versions.

Each step of the editing process can be activated or deactivated.

Quality flag values in v1.0	Quality flag values in v2.0 and v2.0.1	Quality flag values in v3.0
• Flag #102: No SSHa values available • Flag #101: Pixels over land. • Flag #100: Edges of swath. Only values between 10 to 60 km to the nadir are considered as valid data. • Flag #70: Pixels impacted by spacecraft events. • Flag #50: Abnormally high SSHA values. • Flag #30: SSHA pixels out of the expected statistical distribution. • Flag #20: Suspected sea-ice pixels. • Flag #10: Suspected coastal pixels. • Flag #5: SSHA pixels out of the local distribution. • Flag #0: Valid data.	• Flag #102: No SSHa values available • Flag #101: Pixels over land. • Flag #100: Edges of swath. Only values between 10 to 60 km to the nadir are considered as valid data. • Flag #70: Pixels impacted by spacecraft events. • Flag #50: Abnormally high SSHA values. • Flag #30: SSHA pixels out of the expected statistical distribution. • Flag #20: Sea-ice pixels • Flag #19: Unsure sea-ice pixels (only for the unsmoothed product) • Flag #18: Unsure ocean pixels in polar areas (only for the unsmoothed product) • Flag #10: Suspected coastal pixels. • Flag #5: SSHA pixels out of the local distribution. • Flag #3: Eclipses. • Flag #0: Valid data.	• Flag #102: No SSHa values available • Flag #101: Pixels over land. • Flag #100: Edges of swath. Only values between 10 to 60 km to the nadir are considered as valid data. • Flag #70: Pixels impacted by spacecraft events. • Flag #50: Abnormally high SSHA values. • Flag #30: SSHA pixels out of the expected statistical distribution. • Flag 25: Rain Cells • Flag #20: Sea-ice pixels • Flag #19: Unsure sea-ice pixels (only for the unsmoothed product) • Flag #18: Unsure ocean pixels in polar areas (only for the unsmoothed product) • Flag #10: Suspected coastal pixels. • Flag #5: SSHA pixels out of the local distribution. • Flag #3: Eclipses. Flag #0: Valid data.

Table 2: Quality flag values in L3 KaRIn products

More details about each flag are available in Dibarboure et al (2024) and evolutions are detailed in section 4. The following figures show some cases of use of the flag expert. For most studies, we recommend keeping only flag #0 to flag #3.

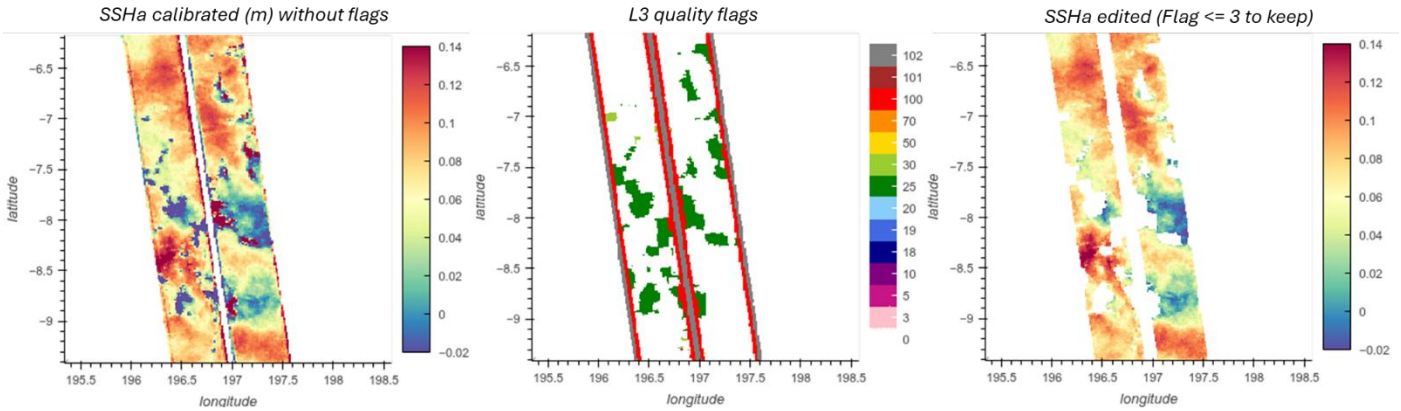

Figure 3: Example of editing of the rain cells (C19 P556). Keeping flags #0 to #3 (from v2.0.1) is recommended.

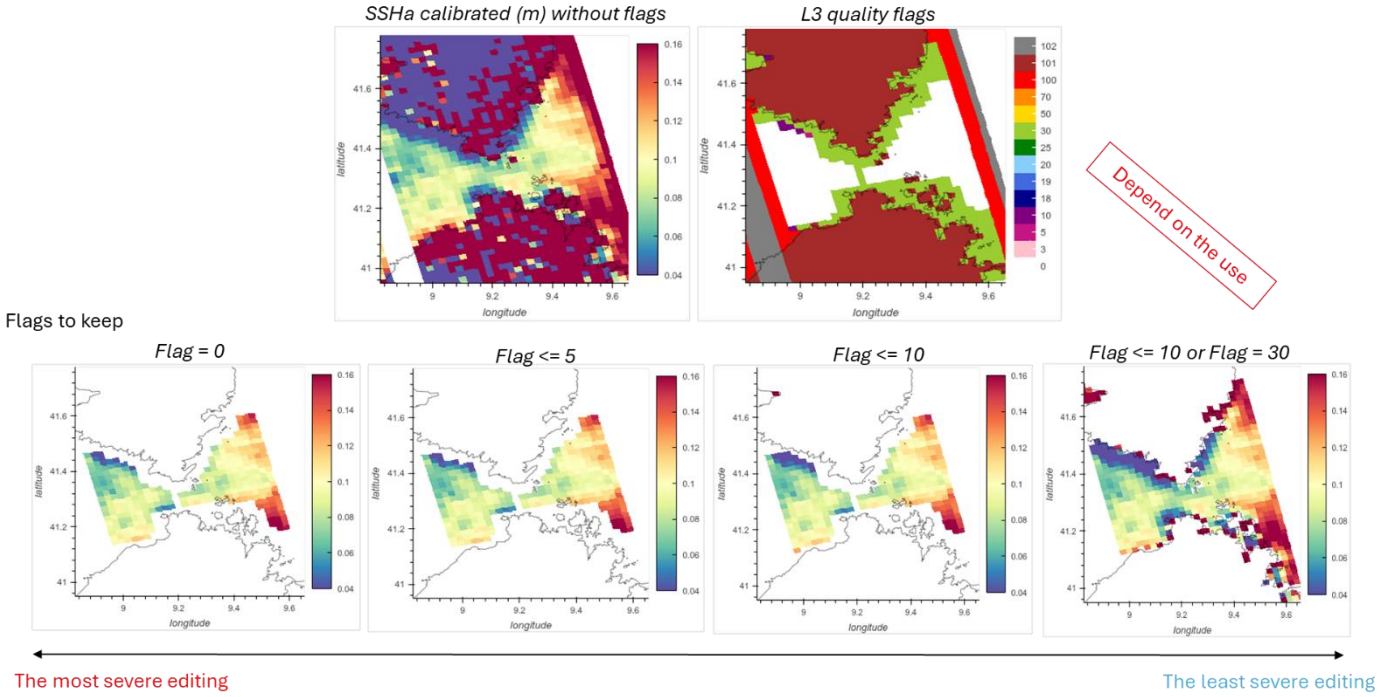

Figure 4: Example of editing of coastlines (C19 P542) in v3.0

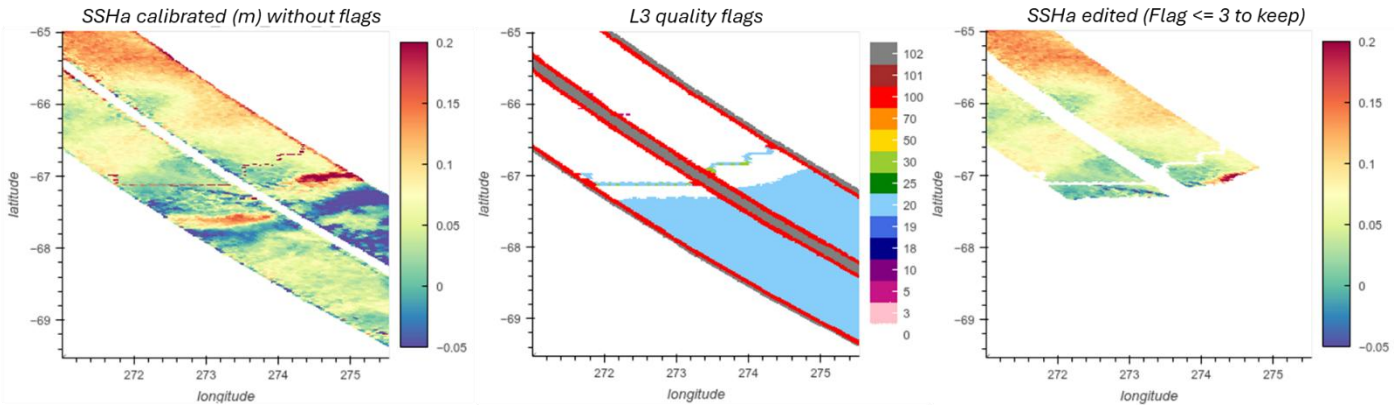

Figure 5: Example of editing of polar (C19 P552) areas in v3.0

2.6 Denoising and Filtering

Despite its unprecedented precision, SWOT's Ka-band Radar Interferometer (KaRIn) still exhibits a substantial amount of random noise. A denoising method is then applied, it is described in Treboutte et al., 2023. It consists of a Neural Network which is based on a U-Net architecture and is trained and tested with simulated data from the North Atlantic. The following table presents the denoising differences between the different versions of the L3_LR_SSH products :

	Version 0.3	Version 1.0, 1.0.1, 1.0.2,2.0 and 2.0.1	Version 3.0
Training dataset	Based on the eNATL60 ocean model without tides Noise generated by the SWOT simulator	Based on the eNATL60 ocean model with tides Correlated Noise generated by style transfer to be as realistic as possible	Based on the eNATL60 ocean model with tides. Realistic editing from L3 real swaths is applied on simulated swaths. No style-transfer
Use of the [Gomez et al, 2020] algorithm	Yes after the UNet	No	No

Table 3: Filtering method applied for the SWOT L3_LR_SSH v1.0,v2.0 and v3.0

More details about the training dataset are available in Dibarboure et al. (2024).

The Figure 6 shows the impact of the filtering in the resultant current and the vorticity.

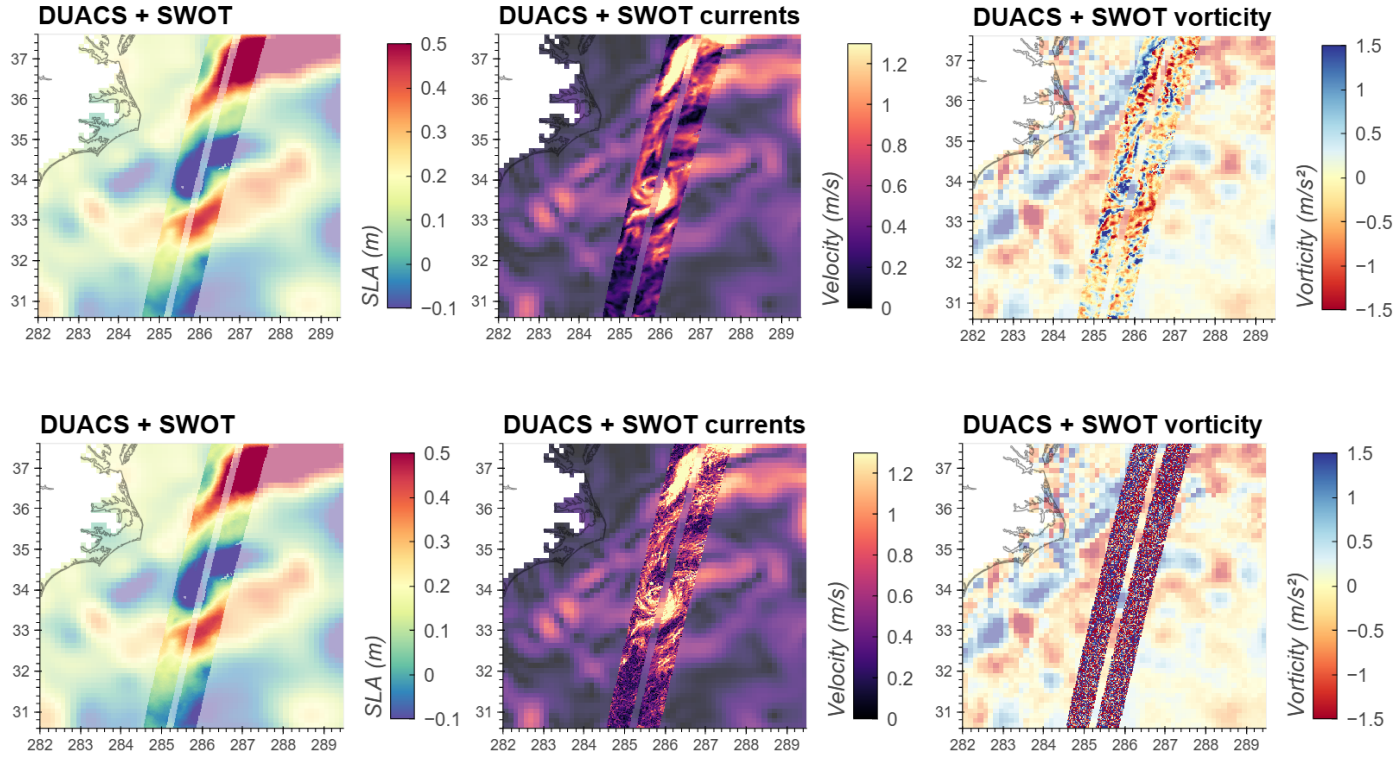

Figure 6: Sea Level Anomalies of DUACS and SWOT L3 v3.0 measurements (left), deduced current (middle) and vorticity (right) with the denoising applied (top) and without (bottom)

2.7 SSHA derivates and geostrophic currents estimation

An estimation of the geostrophic currents is proposed in L3 KaRIn products. The methodology used to compute the anomaly of the currant is presented in the following table. The mean currant is issued from the MDT field (Jousset et al. 2025)

Version 0.3	Version 1.0 and 2.0.1	Version 3.0
2-points stencil methodology from "denoised" SSHA. in along- and across-swath direction. The current is then interpolated on Northward and Eastward direction.	6-points stencil methodology from "denoised" SSHA (Arbic et al. 2012) in along- and across-swath direction. The current is then interpolated on Northward and Eastward direction. An estimation of the SSH gradients from "unfiltered" (raw) SSHA measurements is also proposed using the same methodology	2D spline fitting for "denoised" SSHA (Tranchant et al. 2025) An estimation of the SSH gradients from "unfiltered" (raw) SSHA measurements is also proposed using the same methodology

Know limitations:

The SSH measured by KaRIn is not just from mesoscale but also a synoptic view of unbalanced motions and barotropic residuals. Denoising/filtering processing applied may not allow to accurately extract the balanced motion. Specifically, geostrophy assumption might simply no longer be relevant for the smallest scales observed by KaRIn

3 SWOT L3 KaRIn (L3_LR_SSH) Products

3.1 Temporal availability

Table 4 indicates the first and last dates available (and the corresponding cycle number).

	V1.0	V1.0.2	V2.0	V2.0.1	V3.0
1-day CalVal phase	C474/T003 - C578/T004 28th March 2023 – 10th July 2023	C474/T003 - C578/T004 28th March 2023 – 10th July 2023	C474/T003 - C578/T004 28th March 2023 – 10th July 2023	C474/T003 - C578/T004 28th March 2023 – 10th July 2023	C474/T003 - C578/T004 28th March 2023 – 10th July 2023
21-day Science phase	C001/T149 - C017/T557 26th July 2023 – 8th July 2024	*(Basic/Expert)* C001/T149 - C27/T091 26th July 2023 – 16th January 2025 *(Unsmoothed)* C001/T149 - C016/T554 26th July 2023 – 17th June 2024	*(Basic/Expert)* C001/T149 – C029/T127 26th July 2023 – 28th February 2025	*(Basic/Expert)* C001/T149 – now 26th July 2023 – now *(Unsmoothed)* C001/T149 - C029/T379 26th July 2023 – 9th March 2025	*(Basic/Expert/Technical)* C001/T149 – now 26th July 2023 – now *(Unsmoothed)* not available

Table 4: Temporal availability of the SWOT L3 KaRIn time series

3.2 List of variables

3.2.1 L3 core products

The following table lists the different variables available in the last version of the L3 core product. Note that the name of the variable may change from a product version to the other (see specific "Release change notes" below). The standards used for some geophysical corrections may also change from a product version to the other (see chapter 2.3 for details).

Name of variable	Signification	Unit	product
time	Time of measurement in seconds in the UTC time scale since 1 Jan 1950 00:00:00 UTC.	s	All
longitude	Longitude	Degrees East	All
latitude	Latitude	Degrees North	All
ssha_unfiltered	sea surface height anomaly	meters	All
ssha_filtered	sea surface height anomaly without noise	meters	All
ssha_unedited	sea surface height anomaly without editing	meters	Expert/Unsmoothed
ocean_tide	geocentric ocean tide height (ocean + load tide)	meters	Expert/Unsmoothed
mdt	mean dynamic topography	meters	All
mss	mean sea surface height above the reference ellipsoid	meters	Expert/Unsmoothed
dac	dynamic atmospheric correction	meters	Expert/Unsmoothed
internal_tide	Coherent internal ocean tide	meters	Expert/Unsmoothed
ugos_filtered,vgos_filtered	Absolute geostrophic velocity: zonal and meridian component, derived from ssha_filtered and absolute mean current associated with MDT	meters/second	Expert/Unsmoothed
ugosa_unfiltered,vgosa_unfiltered	Geostrophic velocity anomalies derived from ssha_unfiltered: zonal and meridian component	meters/second	Expert/Unsmoothed
ugosa_filtered,vgosa_filtered	Geostrophic velocity anomalies derived from ssha_filtered: zonal and meridian component	meters/second	Expert/Unsmoothed
sigma0	normalized radar cross section (sigma0) from KaRIn	-	Expert/Unsmoothed
cross_track_distance	Distance of sample from nadir.	meters	Expert/Unsmoothed
calibration	phase screen + xcal	meters	Expert/Unsmoothed
i_num_line	alongtrack indice of the nearest KaRIn pixel from the nadir data	count	Basic/Expert
i_num_pixel	acrosstrack indice of the nearest KaRIn pixel from the nadir data	count	Basic/Expert
quality_flag	Quality flag (see section 2.5 for details)	-	Expert/Unsmoothed

Table 5: List of variables in the NetCDF core files for v3.0. 'All' means the variable is available in Basic, Expert and Unsmoothed datasets of the L3_LR_SSH product

3.2.2 L3 technical product

The following table lists the variable available in the technical product.

Name of variable	Signification	Unit	product
time	Time of measurement in seconds in the UTC time scale since 1 Jan 1950 00:00:00 UTC.	s	Expert_Technical
longitude	Longitude	Degrees East	Expert_Technical
latitude	Latitude	Degrees North	Expert_Technical
loading_tide_fes	Loading tide component from FES 2022 model. Allows to retrieve the dynamical part of ocean tides : « ocean_tide » variable in the core product providing the total geocentric tide. Dyn ocean tides = « ocean_tide » from core product – « loading_tide_fes22 »	meters	Expert_Technical
ocean_tide_got & loading_tide_got	Ocean tide solution from GOT5.8 (Ray R. 2025) # ocean_tide_got58 gives the total geocentric tide (ocean+load) # loading_tide_got58 gives the loading tide component	meters	Expert_Technical
internal_tide_zhao	Internal tide solution from (Zhao 2025)	meters	Expert_Technical
internal_tide_miost	Internal tide solution from MIOST-IT24 from (Tchilibou et al. 2025)	meters	Expert_Technical
rain_rate_itu	Precipitation rate proposed by (Picard et al. 2025)), based on Physically-based atmospheric attenuation model	meters	Expert_Technical
flag_rain_itu	Rain flag proposed by (Picard et al. 2025), deduced from thresholds applied on rain_rate_itu field	meters	Expert_Technical
rain_rate_rf	Precipitation rate proposed (Picard et al. 2025)), based on Supervised random forest algorithm	meters	Expert_Technical
calibration_low_frequency	Low frequenvcy componants of the calibration correction	meters	Expert_Technical
ugosa_filtered_stencil, vgosa_filtered_stencil	Geostrophic velocity anomalies derived from ssha_filtered: zonal and meridian component, using stencil derivate (from L3 v2.0.1 version). Note: is equivalent to velocities derived with 2D fit with reduced kernel	Meters/second	Expert_Technical
mss_compression_correction	MSS compression correction for KaRIn 2km product resolution. This correction is applied on MSS available in the expert product (variable «mss»). It can be removed to this MSS field to retrieve the full resolution (« uncompressed ») MSS. mss_uncompressed = mss from expert product - mss_compression_correction	meters	Expert_Technical

Table 6: List of variables in the NetCDF core files for v3.0 Technical dataset of the L3_LR_SSH product

3.3 Nomenclature of files

The nomenclature used for these products is:

SWOT_L3_LR_SSH_<FileIdentifier>_<CCC>_<PPP>_<DateBegin>_<DateEnd>_v<Version>.nc

Where:

FileIdentifier is ‘Basic’, ‘Expert’, ‘Unsmoothed’ or ‘Expert_Technical’

CCC is the number of cycle on 3 digits

PPP is the number of pass on 3 digits

DateBegin and DateEnd are the begin and end dates in UTC of the measurements in each file.

Version is ‘0.3’ or ‘1.0’ or ‘1.0.1’ or ‘1.0.2’ or ‘2.0’ or ‘2.0.1’

4 Releases change notes

This chapter presents the changes introduced by the successive new product versions

4.1 Version 1.0.0

This section is not exhaustive and does not reflect all the changes brought to the product from V0.3 to V1.0.0

4.1.1 Basic and Expert

4.1.1.1 Land sea mask

The mask provided in the L2 product is sometimes incorrect (known limitation, regionally dependent; example in Figure 7). A tentative improvement was made in v1.0 with the use of a mask derived from Open Street Map (OSM).

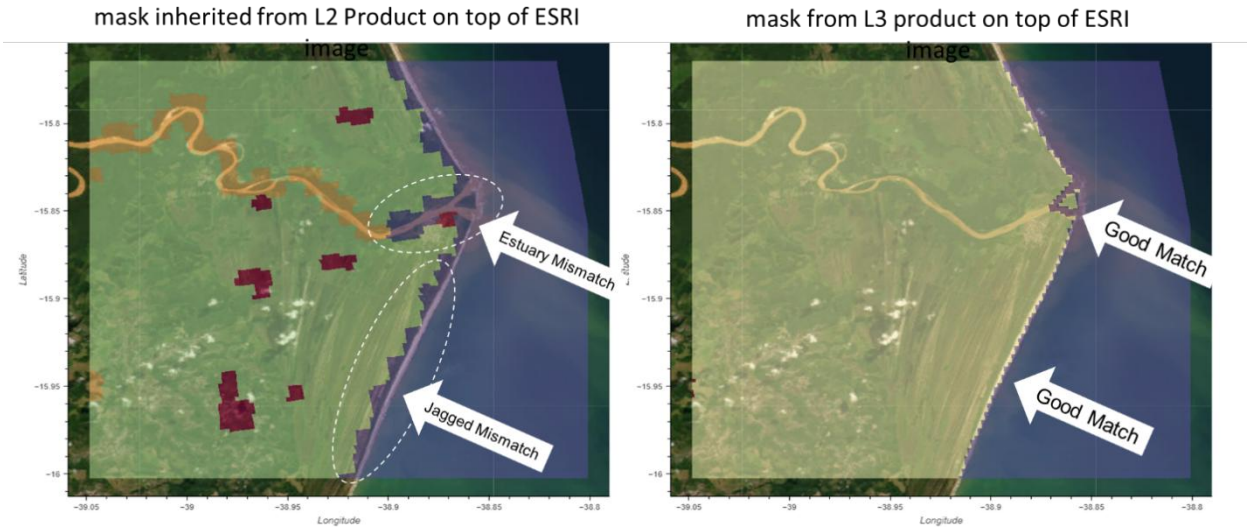

Figure 7: Example of Land-Sea mask from L2 KaRIn (left) and L3 (right) superimposed with ESRI image. Yellow to red pixels correspond to non-ocean surface type (i.e. rejected in L3)

A tentative improvement was made in v1.0 with the use of a mask derived from Open Street Map. If this version fixes most of the known L2 issues, albeit with some failures in estuaries (see 5.1).

4.2 Version 1.0.1

4.2.1 Unsmoothed

An anomaly was detected in the Unsmoothed V1.0 netcdfs. The geophysical corrections (ocean_tide, DAC), the MSS, MDT and sigma0 values in the product had an inverted sea/land mask.

Below is an illustration of the anomaly and its correction:

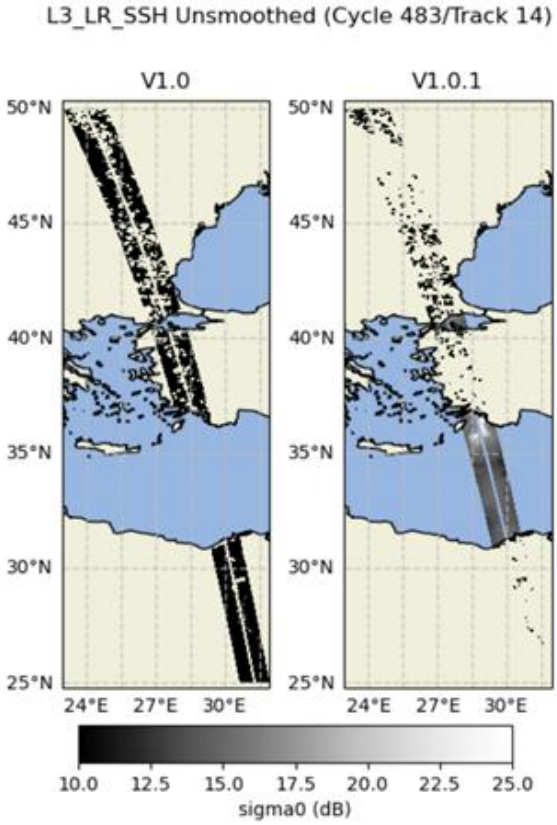

Figure 8: illustration of a badly filled field in V1.0 (left) and its correction in V1.0.1 (right)

4.3 Version 1.0.2

4.3.1 Basic, Expert and Unsmoothed

4.3.1.1 M0 wave removal

The M0 wave has been removed from the ocean tide correction FES2022 configuration. This change has a very small impact for users using the calibrated Sea Level Anomaly, because this large scale signal is absorbed by the calibration error in the V1.0.0.

The following figure illustrates the impact of removing the M0 wave over the ocean tide correction (left) and over the calibration (right). The patterns are similar, confirming the small impact over the calibrated Sea Level Anomaly.

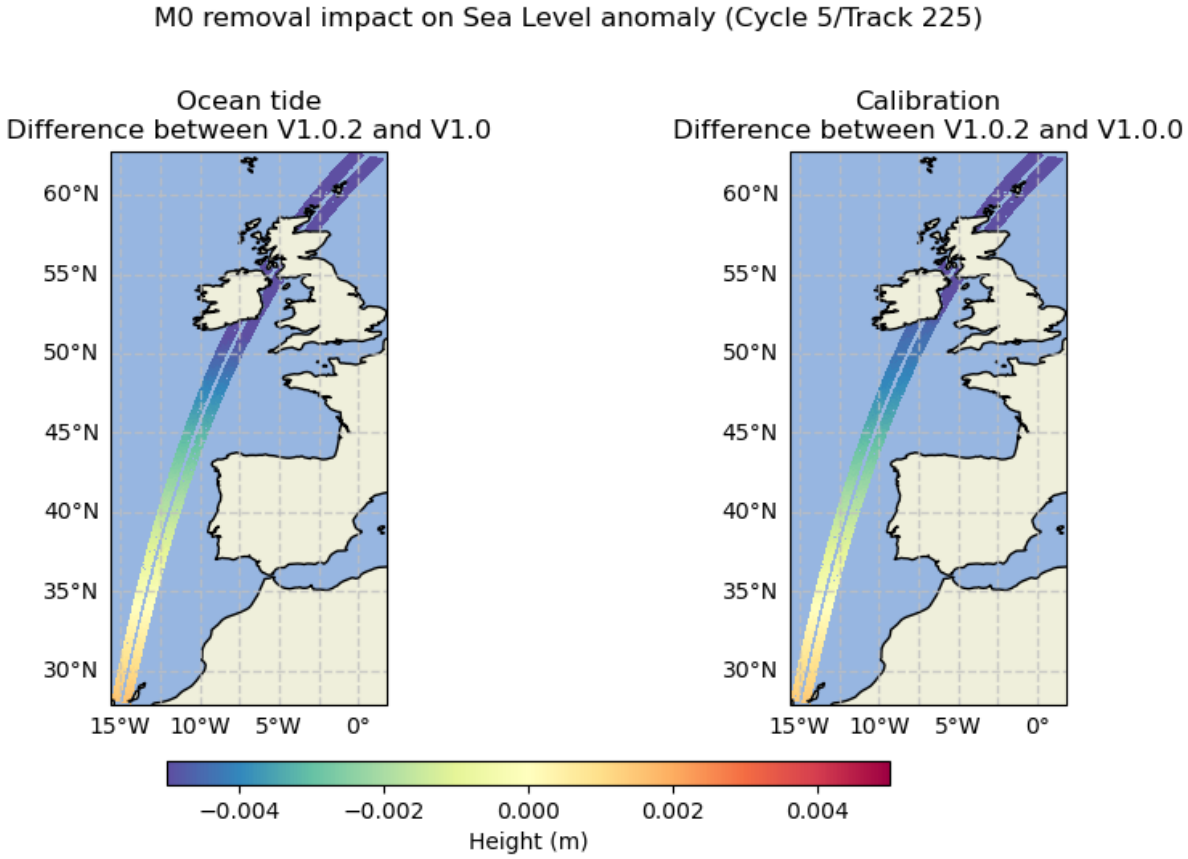

Figure 9: illustration of the M0 wave absorption by the calibration correction

4.3.2 Basic and Expert

4.3.2.1 Editing near the coast

The V1.0 introduced a newer and finer land-sea mask (Open street Map based). The editing parametrization for pixels near the coast was not properly adjusted, which can cause wrongly-edited lines in the quality flag near the coast. The new parametrization fixes this issue in the V1.0.2

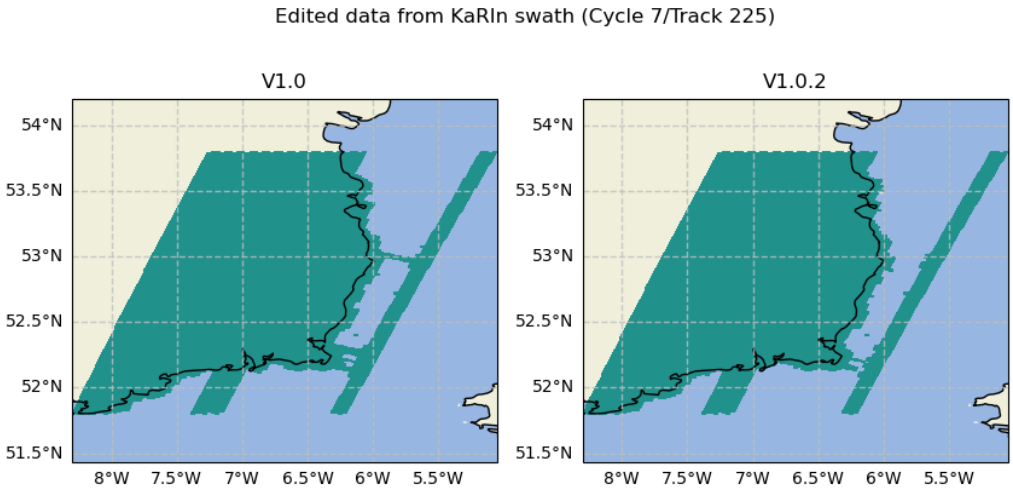

Figure 10: change in editing parametrization. The V1.0 (left) exhibits lines near the coast that should not by edited and are not present in the V1.0.2 (right)

4.3.2.2 Ocean tide in Sea Level Anomaly

For products based on PIC upstream data, the ocean tide correction has been wrongly applied. The ocean_tide field contains the expected FES2022 model, but the sea level anomaly has been corrected using an alternative FES2014 field. The V1.0.2 fixes the tide correction in the sea level anomaly.

This issue only impacts Basic and Expert datasets starting from cycle 7

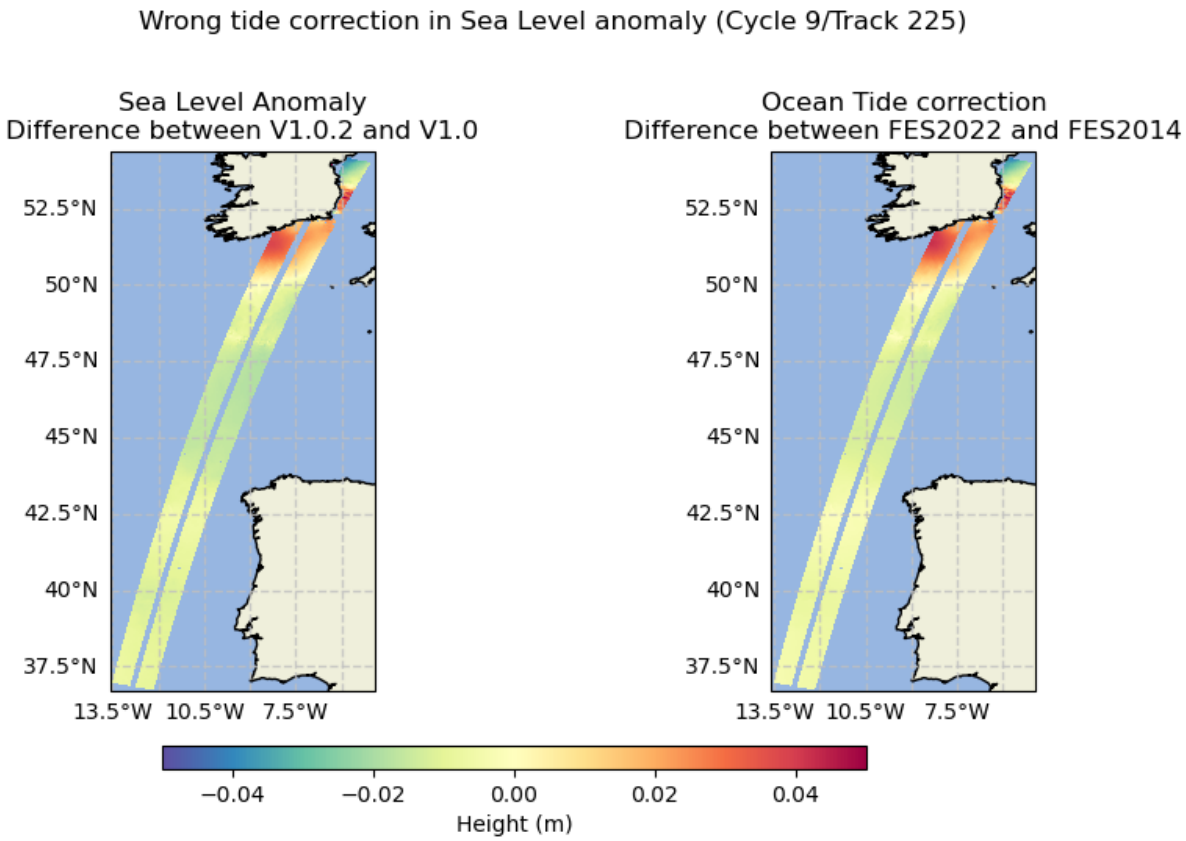

Figure 11: illustration of the Sea Level Anomaly change caused by a proper application of the ocean tide between V1.0 and V1.0.2

4.3.2.3 Sea state bias filling

Regions with ice have a default value for the Sea State Bias (SSB) correction. This default value introduced a bias on the non edited Sea Level Anomaly between the high latitudes and the rest of the ocean. This is of no consequence over the edited ssha or filtered Sea Level Anomaly ssha_noiseless because these regions are edited. However, this can be seen on the calibrated Sea Level Anomaly ssha_unedited. The SSB filling method has changed to mitigate this effect.

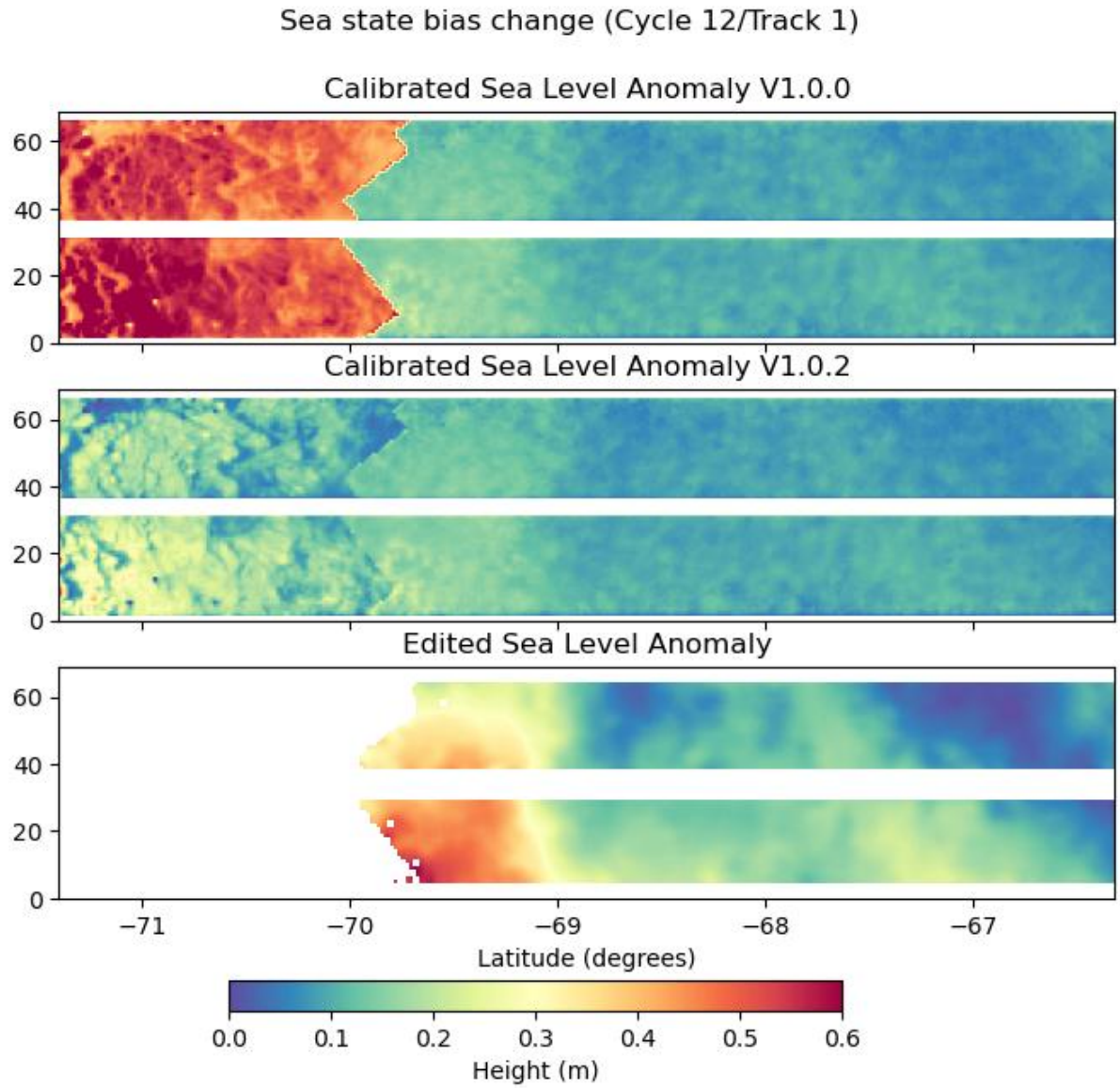

Figure 12: Sea State Bias filling method illustration

This change only affects the sea state bias correction in the Basic and Expert products. The Unsmoothed product still uses the old filling method.

4.3.2.4 PIC/PGC blending

Because the PGC does not cover the most recent periods, the L3_LR_SSH upstream data is a blending of two L2_LR_SSH versions: PIC and PGC. Previously, the PGC to PIC switch was at Cycle 7 but newly available data made it possible to use PGC data up to Cycle 9.

To summarize the upstream data versions:

- PIC0 starting from Cycle 9 / Track 388
- PGC0 up to Cycle 9 / Track 387 included, minus the exceptions listed in the following table

List of PIC half orbits (ranges are inclusive)

Cycle 7	[521-531], 533, [535-536], [538-542], [544-547]
Cycle 9	[335-336], [388, 584]

4.3.3 Unsmoothed

4.3.3.1 Missing half orbits with respect to Expert dataset

The calibration field is interpolated from the Expert product. This interpolation needs a consistent uncalibrated sea level anomaly between the two products. A version discrepancy between the Expert and Unsmoothed product means that the sea level anomalies are not consistent.

Due to production constraints, some half orbits have different upstream versions for the Expert and Unsmoothed products. These half orbits have been removed and will be retrieved in a future reprocessing.

List of missing half orbits due to upstream version discrepancy (range are inclusive)

Cycle 1	561
Cycle 3	322
Cycle 4	158, 160
Cycle 6	297, 298
Cycle 7	[532-534], 537, 543
Cycle 8	[244-245]
Cycle 9	[304-331], [337-387]
Cycle 11	[381-382], 384
Cycle 13	[261-262], [544-570]
Cycle 15	70, 72, 74, 135, 137

4.4 Version 2.0

4.4.1 Basic and Expert

4.4.1.1 Change of the geophysical standards

The SSB2 correction of the L2 PIC/PGC product is used in L3 production. This solution is based on MFWAM model output that shows limitation of definition in polar and coastal areas. Consequently, a known offset of 10cm is introduced in SSB2 in these areas, impacting the resulting SSHA with introduction of net discontinuities. In the L3_LR_SSH v2.0, the SSB2 correction is extrapolated towards 0 in polar areas to remove the SSH discontinuities that may limit polar studies (e.g., Figure 13). This was done assuming the in sea-ice leads SSB is close to zero (small waves), so we enforce continuous transition from open ocean to sea-ice leads. Nevertheless, this extrapolation does not yield a correct/geophysical SSB correction. This quick fix intends to remove only the SSB2 offset in a gradual way, but the SSHA remains biased (no wave height available in these regions = SSHA bias).

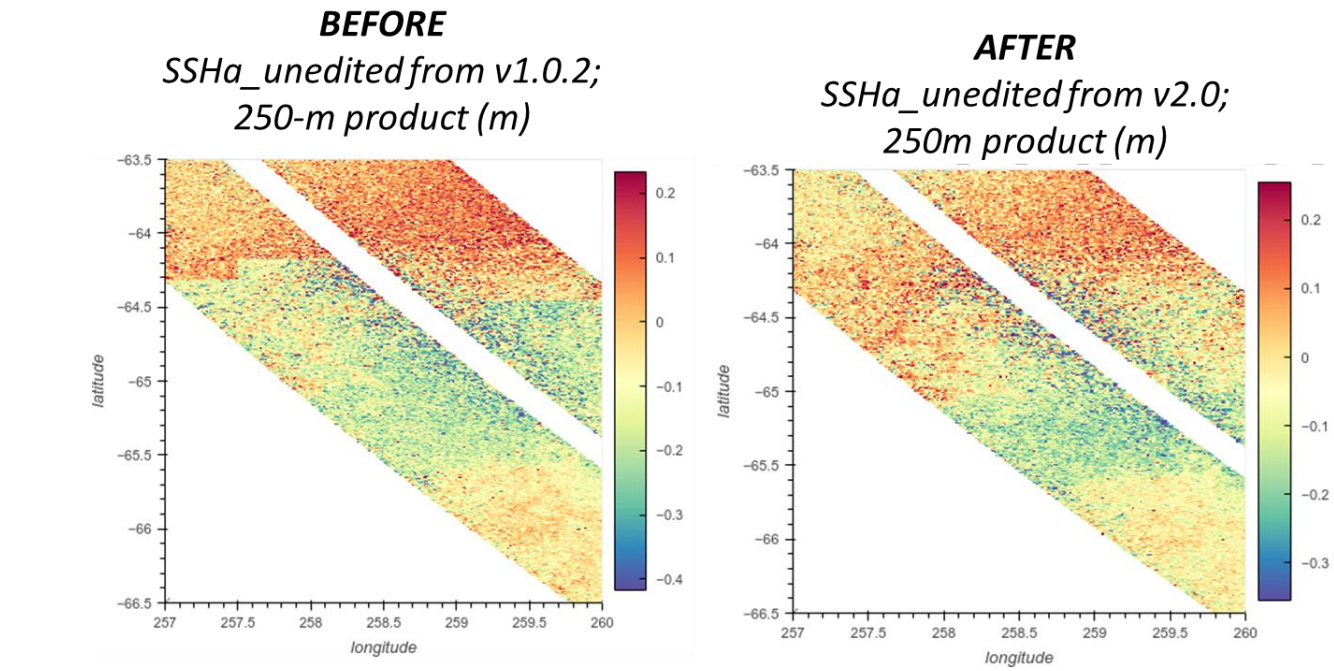

Figure 13: Example of SSB used in the L3_LR_SSH; v1.0.2 version (left) and v2.0 (right)

The internal tide correction is improved in v2.0 with the use of a blend solution between HRET14 & HRET8.1 model (Zaron, 2024), resolving the coherent tides for 5 different tidal frequencies (M2, K1, S2, O1, N2) when HRET8.1 (Zaron, 2019), resolving 4 tidal frequencies (M2, K1, S2, O1), was used in v1.0.2. The blend HRET solution is slightly more accurate than HRET 8.1 over most of the open ocean (3 mm RMS, locally 1 cm; Consistent numbers found with SWOT Nadir, SWOT KaRIn, Jason-3, Sentinel3A/B and Sentinel-6 MF missions, e.g., Figure 14). The gain is however not geographically homogeneous. As HRET8.1, the blend HRET solution is based on nadir altimetry and it does not correct for higher modes of internal tides, nonlinear waves, solitons, and non-stationary tides. The blend HRET solution is delivered in a dedicated variable of the L3_LR_SSH v2.0 product, allowing the user to uncorrect/replace it.

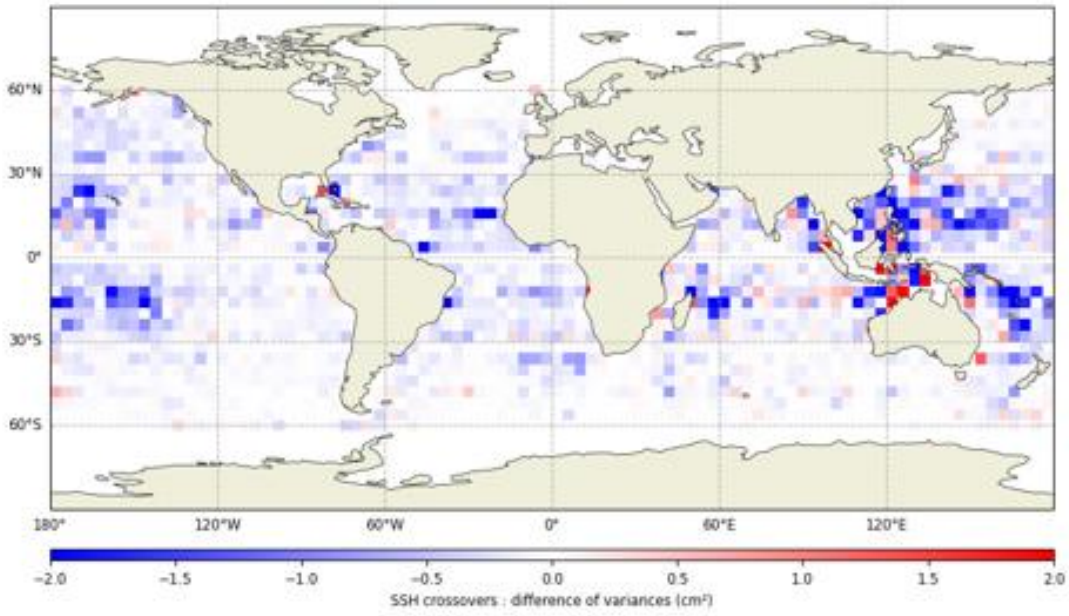

Figure 14: Difference of SSHA variance for HRET14 vs HRET8 measured with Sentinel-3A/B (cm²)

A -5cm offset was introduced in the MDT field model, and resulting ADT. This offset fixes known discrepancy between SWOT and other L3 products distributed by CMEMS. It was introduced in the DUACS/CMEMS production in 2014, following a change of the arbitrary altimeter reference period used ([1993, 1997] vs. [1993, 2012]).

4.4.1.2 Data selection changes - Spatial coverage improved

Eclipse transition segments are isolated from other SWOT mission events (e.g. maneuvers) and flagged with a specific value (flag 3; Figure 15). The performance analyses from the SWOT L2 Project CalVal and L3 teams did not observe any degradation for these segments. Consequently, the SSHA is now provided during eclipse transitions, improving the coverage by 4%. The users of expert and unsmoothed products can choose to remove these segments by using the specific flag value.

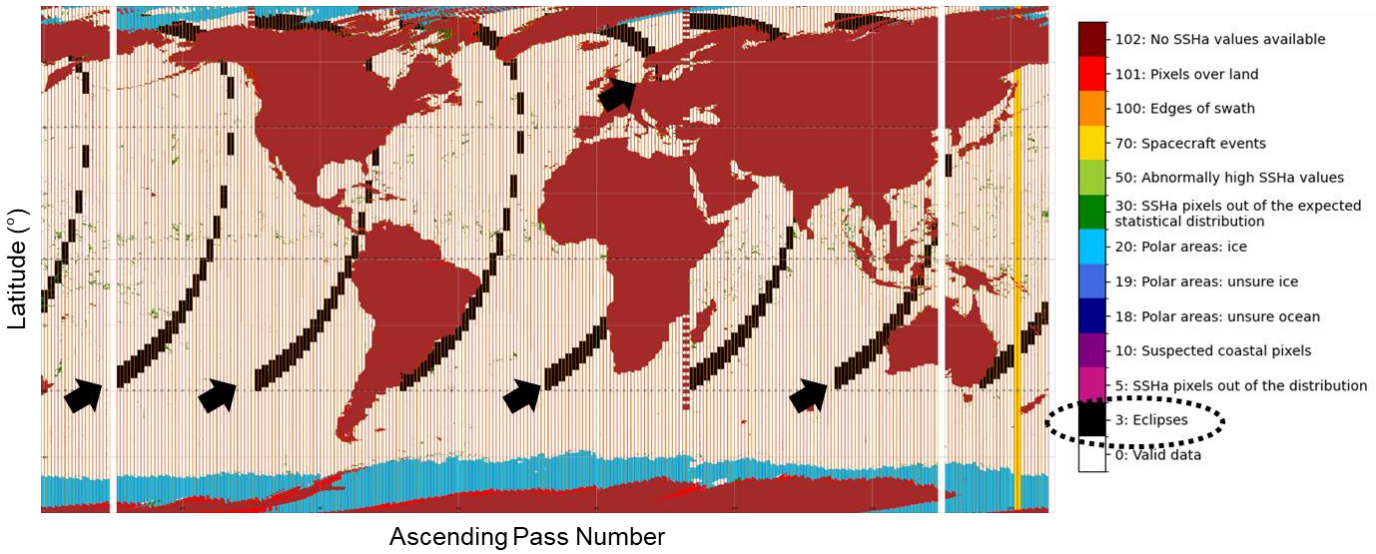

Figure 15: Example of KaRIn L3 quality flag for one cycle of ascending passes

The data selection was improved by using a new Land-Sea mask selection criterion. Due to the introduction of a new land sea mask in V1.0, some estuaries have been lost in the process (see 4.1.1.1). In the L3 v2.0, a revised mask with manual processing of 43 major estuaries is used to retrieve them. The quality flag is updated consequently. Nevertheless, estuaries with no SSHA in the L2 cannot be retrieved in the L3 (known PIC/PGC issue, not related to land mask), and retrieved SSHA can be rejected with other statistical criteria (e.g., Figure 16).

The selection flag algorithm was revisited to reduce the occurrence of ambiguous rejection criteria (e.g. rain vs coast; example Figure 17), and to consider areas better retrieved with revised L3 SSB2 (see previous section). In that last case, only pixels with an ice concentration higher than 60% and those on the edge of the polar ocean are flagged as “suspected sea-ice pixels” (flag 20, e.g., Figure 18)

The data selection sequence is also better integrated with the L3 calibration, improving the quality of the latest.

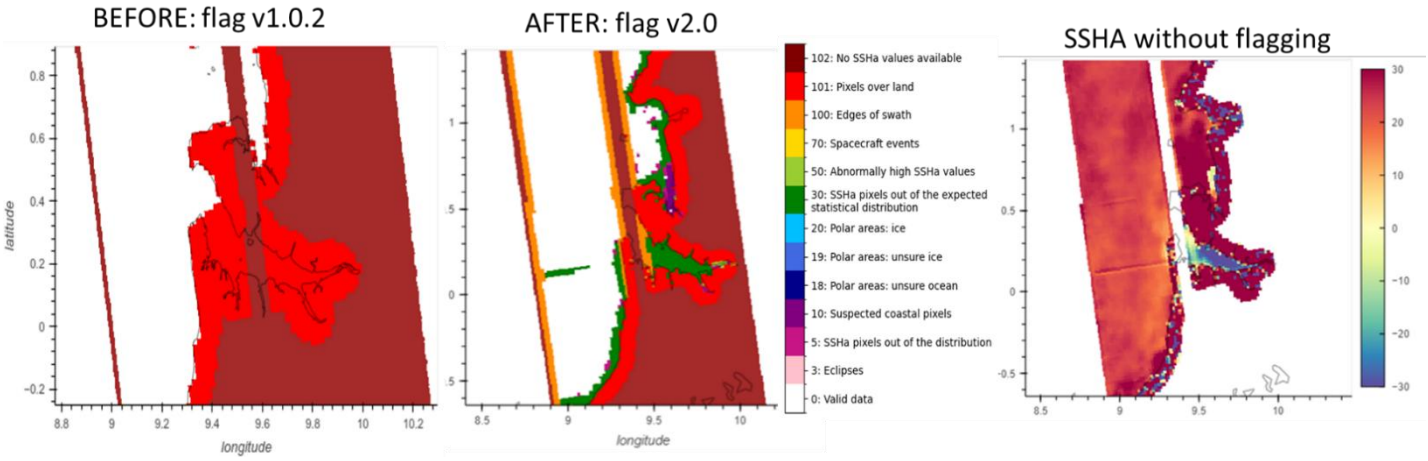

Figure 16: Example of data selection over the Gabon estuary. SSHA before selection (right), after selection in v1.0.2 version (left) and in v2.0 (middle). In that example, main part of the SSHA in the estuary is rejected on statistical criteria on SSHA (flag value 30: SSHA pixels out of the expected statistical distribution)

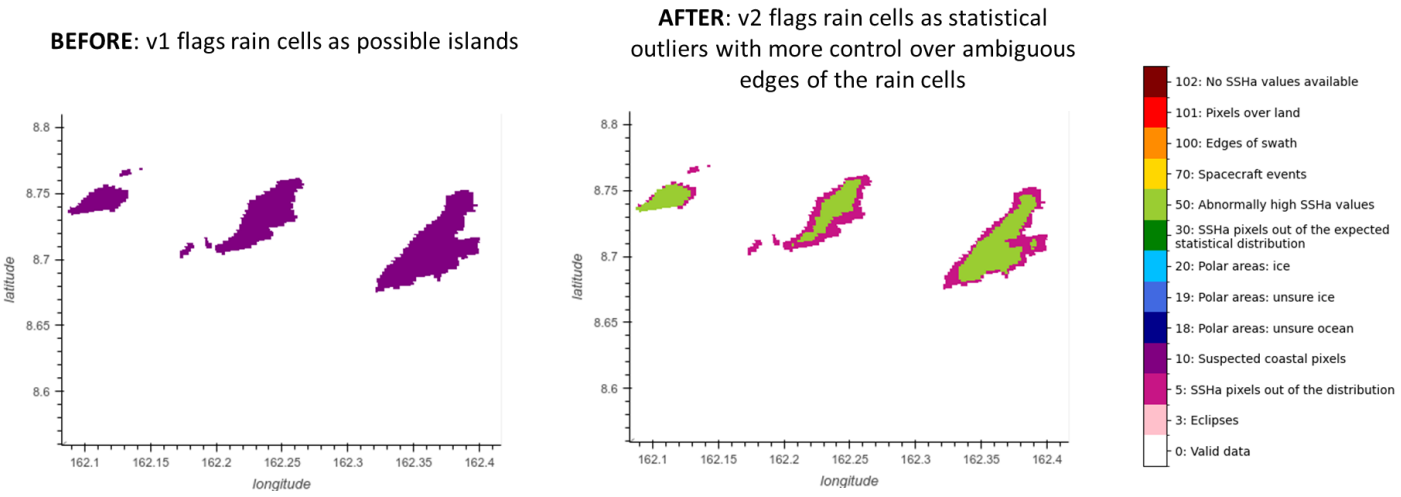

Figure 17: Example of data selection over rain cells. Flag defined in L3 v1.0 verstion (left) and v2.0 (right). In v1.0 the rain cells were identified with criteria rather representative of coastal pixels (flag 10); in v2, rejection cretaria rather rely on statistical analysis of SSHA value (flag 50: abnormally high SSHA values; and flag 5: SSHA pixels out of the local distribution)

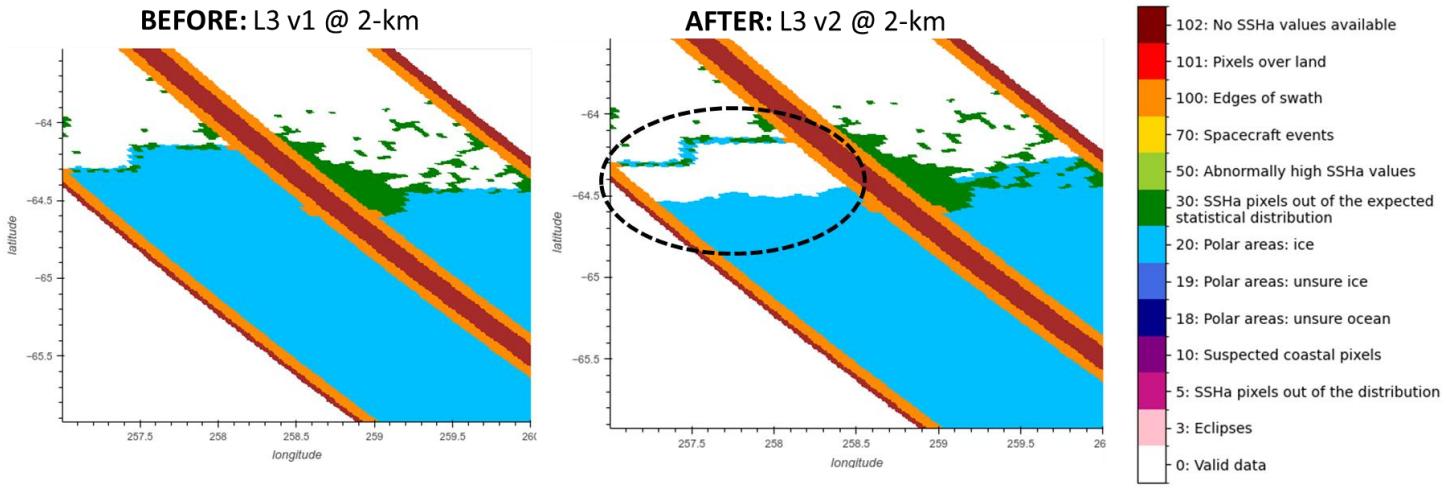

Figure 18: Example of data selection in polar areas impacted by extrapolated SSB_2 correction implemented in v2. Selection flag provided in v1 L3 version (left) and v2 (right)

4.4.1.3 Calibration

calibration v1 was absorbing other geophysical error residuals (see SWOTST 2024 Talk) and not just KaRIn systematic errors. The calibration algorytm and sequence was thus improved in v2.0 with the objective to reduce the leakage of ocean dynamical signal and consider improvement done on data selection processing:

- A large part of the data selection is newly applied before calibration
- Data eclipse transition segments are used in the calibration
- a more sophisticated handling of the bias/linear/quadratic terms and the orbital harmonics VS broadband interpolators: fewer degrees of freedom are used to calibrate only what is absolutely needed and ignore uncalibrated error sources when calibration is not possible / desirable.
- (L3 pseudo phase screen corrections remain unchanged w.r.t v1.0.2)

This results in better correction for the semi-enclosed / coastal / polar seas and Hydrology (e.g., Figure 19). On counterpart, more tidal, SSB and Wet troposphere residual signals may be observed in SSHA field.

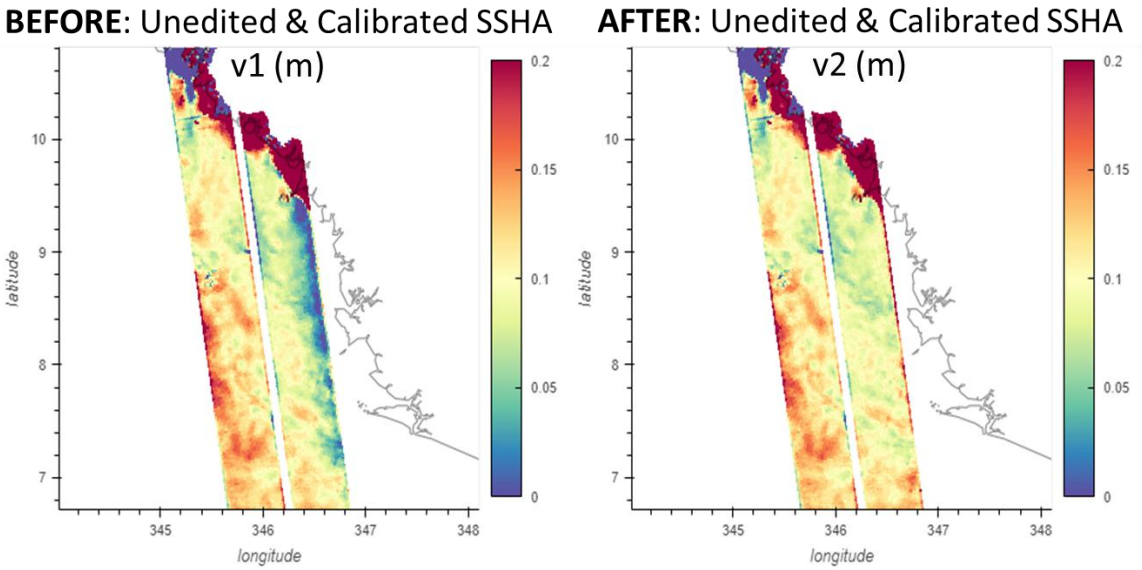

Figure 19: Example of SSHA calibrated in L3 v1.0 (left) and v2 (right). The new editing and more robust calibration implemented in v2.0 remove the coastal tilt previously observed in v1.0

4.4.1.4 Product format

Some variables are renamed, and new variables are added in the v2 product version. The evolutions are summarized in the following tables.

Variable name in v1.0.2 version	Variable name in v2.0 version
ssha	ssha_unfiltered
ssha_noiseless	ssha_filtered
ugsoa	ugosa_filtered
vgosa	ugosa_filtered

Table 7: Variable renamed in v2.0 version

Variable name in v2.0	Variable content
internal_tide	Internal tide solution applied to ssha contained in the product version (blend of HRET14 & HRET8.1 in v2.0)
ugosa_unfiltered	geostrophic velocities anomalies (zonal and meridian components) derived from the SSHA_UNFILTERED parameter (i.e. without denoising)
vgosa_unfiltered	
cross_track_distance	Distance between the swath position and the nadir position on the same line Only added in Unsmoothed dataset (already present in Basic and Expert)

Table 8: New variables added in the v2.0 version

4.5 Version v2.0.1

4.5.1 Basic, Expert and Unsmoothed

Some half orbits of the calval phase are not well calibrated and were not properly detected by the editing algorithm. The quality flag of these half orbits has been set to 30 to mark them as bad

Cycle	Half orbit range (inclusive)
567	[20-28]
568	[10-13]

Table 9: Newly edited half orbits

4.5.2 Basic and Expert

4.5.2.1 MDT and absolute derivatives near the coast

Due to a change in the MDT/MDU/MDV interpolator in the V2.0.0 (switched to bicubic), some points near the coast have been lost with respect to the V1.0.2 (cf figure).

In order to mitigate this issue, the source grids for MDT topography and associated absolute currents are filled using a Gaussian-Seidel method. This prevents the loss of points in the mdt, ugos and vgos fields. An example of impact is given in the following figure.

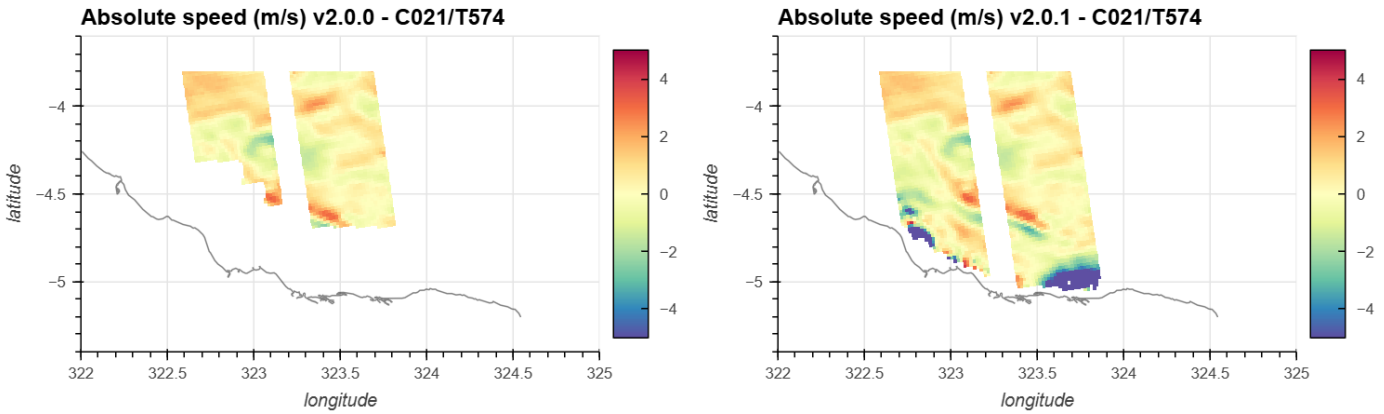

Figure 20: Example of anomaly of MDT interpolation in v2.0 and corrected field in v2.0.1

4.5.2.2 Wrong flag application in eclipses

The editing flag was wrongly applied on the sea surface height in the v2.0 netcdf products. Although the eclipses were present in the ssha_unedited field, they were wrongly removed in the ssha_unfiltered and ssha_filtered fields. This has been fixed in v2.0.1 and the eclipse data is properly available as announced in the v2.0 (see section 4.4)

4.5.2.3 Product format

Some variables are renamed in v2.0.1 product version to complete changes previously implemented in v2.0. The evolutions are summarized in the following table.

Variable name in v1.0.2 version	Variable name in v2.0 version	Variable name in v2.0.1 version
ssha	ssha_unfiltered	
ssha_noiseless	ssha_filtered	
ugsoa	ugosa_filtered	
vgosa	ugosa_filtered	
ugos	ugos	ugos_filtered
vgos	vgos	vgos_filtered

Table 10: Variable renamed in v2.0 and 2.0.1 version

4.5.3 Unsmoothed

4.5.3.1 Change of the geophysical standards

As for the basic/expert v2.0 product version, the unsmoothed v2.0.1 product benefits from the use of new altimeter standards and geophysical corrections. See section 4.4.1.1.

4.5.3.2 Land sea mask

In V1.0, we introduced a mask that fixes most of the known L2 issues (see 4.1.1.1). This mask was used in the Basic and Expert datasets but not in the Unsmoothed dataset. V2.0.1 aligns the land/sea masks between by using this mask in the Unsmoothed product. Note that the patch improvement introduced in V2.0 for the Basic and Expert datasets is also applied

4.5.3.3 Calibration

The same calibration than basis/expert v2.0 is applied for the unsmoothed v2.0.1 version. See section 4.4.1.3 for details.

4.5.3.3.1 Missing half orbits

The calibration field is interpolated from the Expert product. This interpolation needs a consistent uncalibrated sea level anomaly between the two products. A version discrepancy between the Expert and Unsmoothed product means that the sea level anomalies are not consistent.

The following table lists the passes for the unsmooth product for wich the calibrated correction is not available.

Table 11: List of half orbits for with calibration correction is missing

Cycle number	**Pass number**
26	341, 369, 397, 425, 453, 481
27	9, 37, 65, 93, 121, 456, 484, 512, 540, 568
28	12, 40, 68, 96, 124, 152, 180, 208, 236, 264, 292, 320, 348, 376, 404, 432, 460

4.5.3.4 Data selection changes - Spatial coverage improved

As for the basic/expert v2.0 version, the unsmoothed v2.0.1 benefits from an improved data selection:

- Eclipse transition segments are isolated from other SWOT mission events (e.g. maneuvers) and flagged with a specific value
- a new Land-Sea mask selection criterion is used: the land/sea mask used is now aligned with the basic/expert production (Open Street Map mask from v1.0 previously used)
- The selection flag algorithm was revisited to reduce the occurrence of ambiguous rejection criteria, and to consider areas better retrieved with revised L3 SSB2
- The data selection sequence is also better integrated with the L3 calibration

See section 4.4.1.2 for more details

In addition, specifically for the unsmoothed product, 21LEGOS has developed a sea-ice classification for polar areas. It provides several information:

- ocean (flag #0)
- ocean_unsure (flag #18)
- ice_unsure (flag #19)
- ice (flag #20)

Summer in the Arctic (May-September) is still exploratory because of the presence of melt-pounds on the sea ice. As this product is experimental, a few imperfections have been identified.

- Some passes contain mostly ‘unsure’ categories (Figure 22).
- Along-track lines due to radiation hits (more details in https://archive.podaac.earthdata.nasa.gov/podaac-ops-cumulus-docs/web-misc/swot_mission_docs/D-109532_SWOT_UserHandbook_20240502.pdf) may be visible and deteriorate the classification (Figure 23).
- Ice classification is only applied when the ice concentration exceeds 50%. Between 0 and 50% of ice concentration, the data is automatically edited with flag #20 (Figure 24).
- Pixels surrounding icebergs can be misclassified (Figure 25), as well as pixels in complex areas (**Figure 27**).

The SSHA denoised field is available on ocean pixels identified in polar areas. Although the results seem relevant (eg Figure 26), it is important to remember that the denoising algorithm has been designed and trained on open oceans and must therefore be used with care in degraded cases such as ice-covered areas, estuaries or misclassification (eg **Figure 27**).

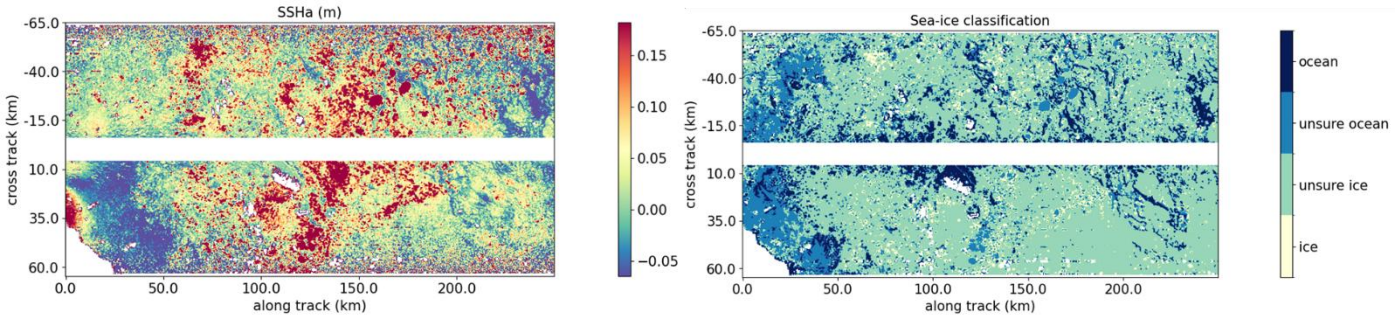

Figure 22*: Raw SSHA (left) and sea-ice classification (right) for KaRIn C484 P9*

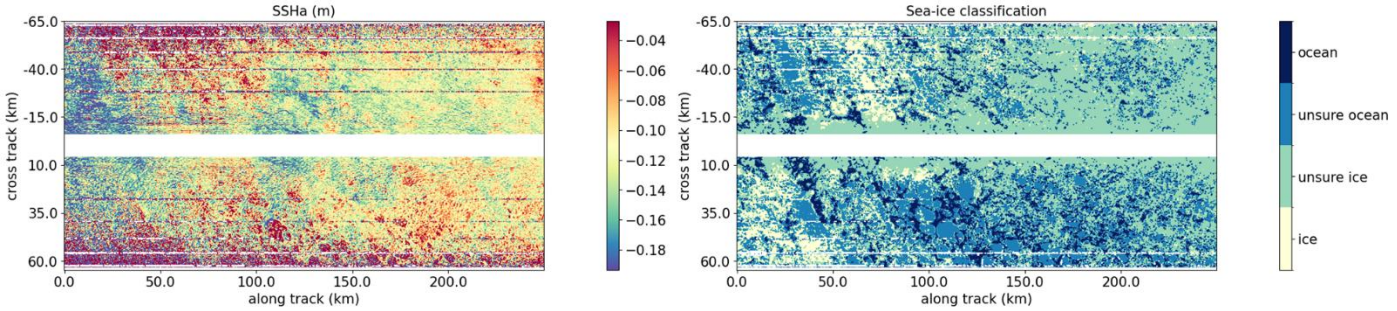

Figure 23: Same as previously, but for *C577 P24*

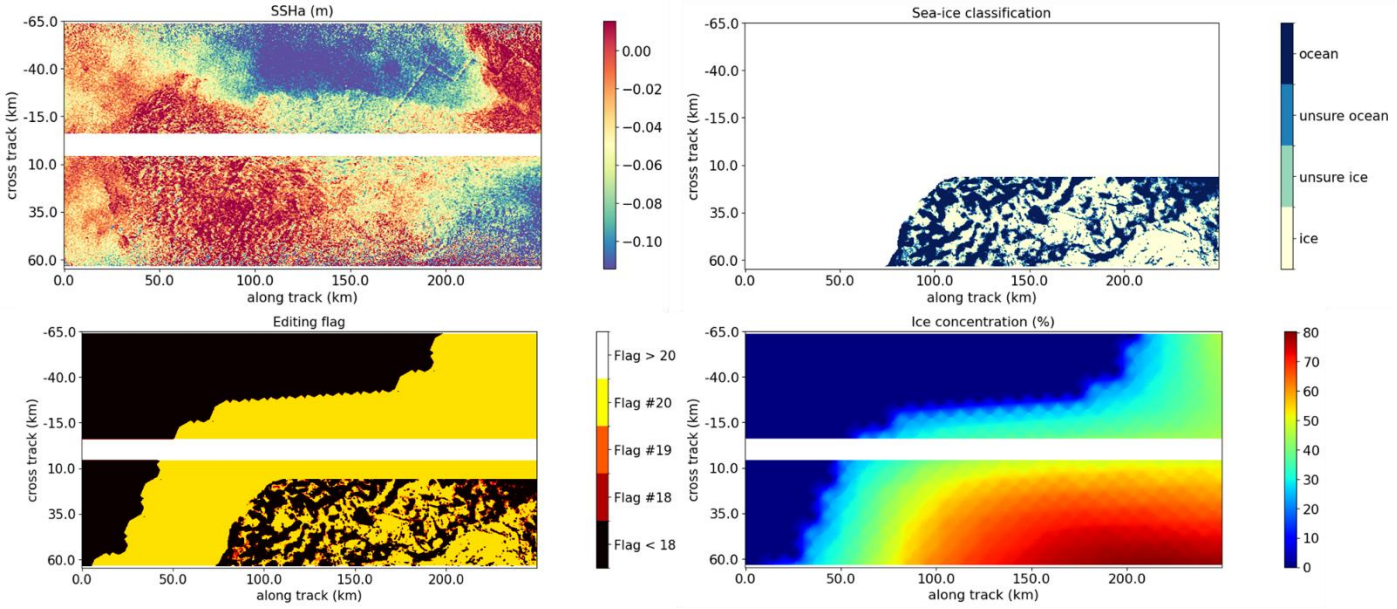

Figure 24: Raw SSHA (top left), sea-ice classification (top right), edinting flag (bottom left) and sea ice concentration (bottom right) for KaRIn C500 P2.

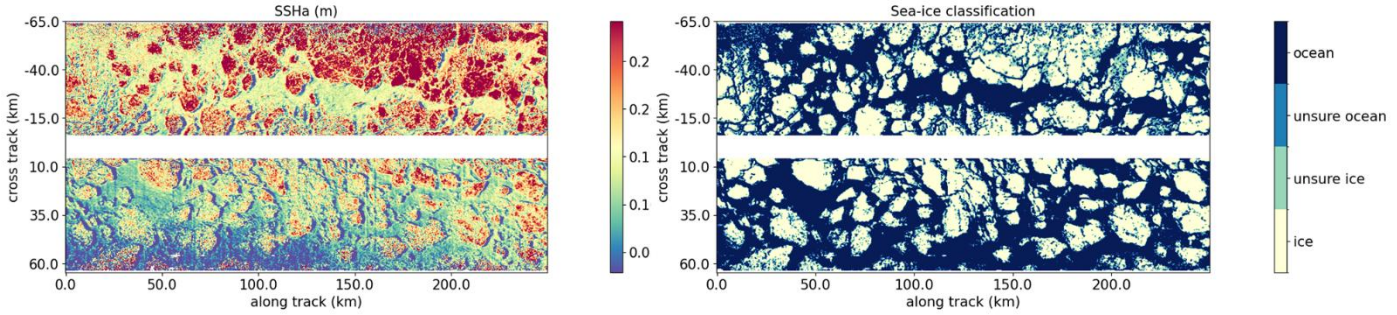

Figure 25: Same as Figure 22, but for *C474 P5*

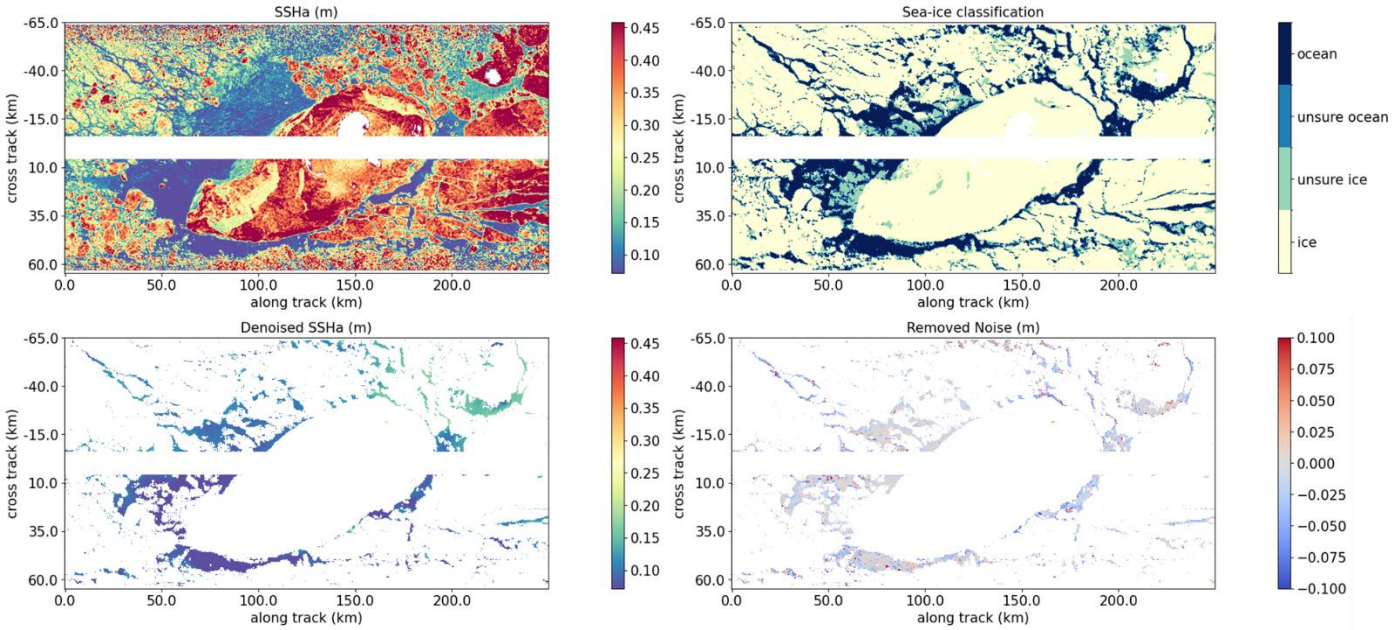

Figure 26: Raw SSHA (top left), sea-ice classification (top right), Denoised SSHA over ocean (bottom left) and Noise removed by denoising processing (bottom right) for KaRIn C507 P1

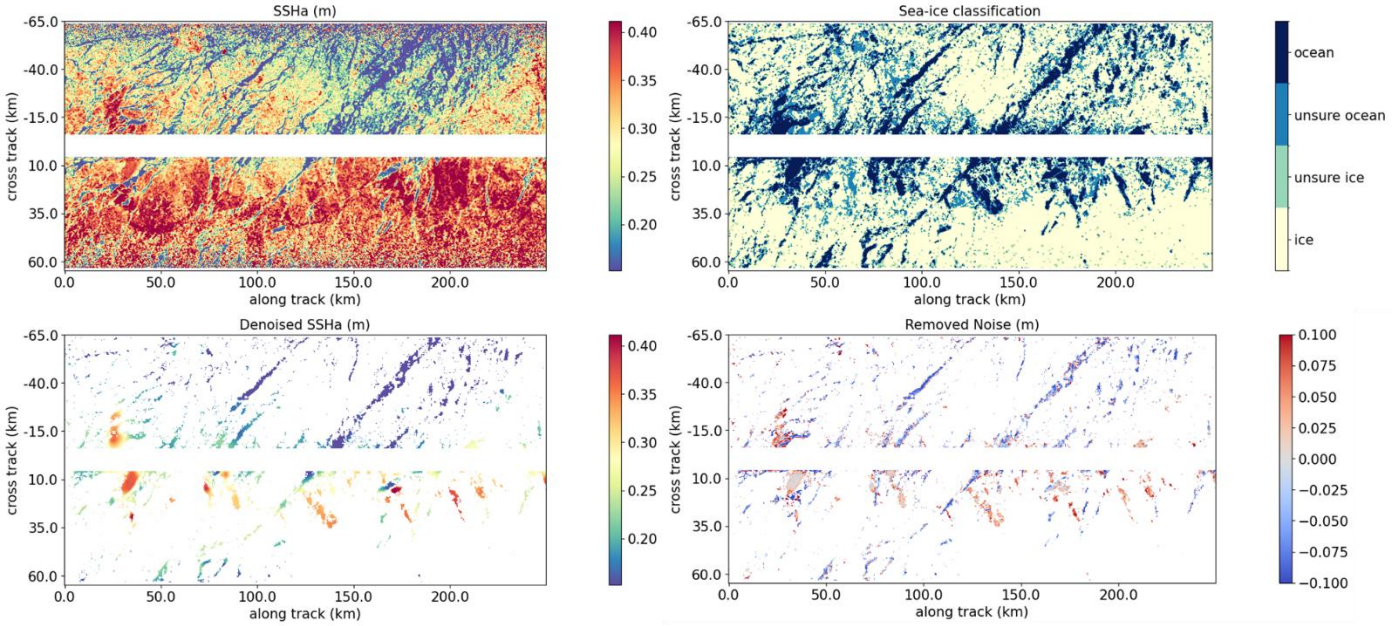

Figure 27: **Same as Figure 26, but for C474 P26**

4.5.3.5 Product format

Some variables are renamed, and new variables are added in the v2.0.1 product version. The evolutions are summarized in the following tables

Variable name in v1.0.2 version	Variable name in v2.0.1 version
ssha	ssha_unfiltered
ssha_noiseless	ssha_filtered
ugsoa	ugosa_filtered
vgosa	ugosa_filtered
ugos	ugos_filtered
vgos	vgos_filtered

Table 12: Variable renamed in v2.0.1 version

Variable name in v2.0	Variable content
internal_tide	Internal tide solution applied to ssha contained in the product version (blend of HRET14 & HRET8.1 in v2.0)
ugosa_unfiltered	geostrophic velocities anomalies (zonal and meridian components) derived from the SSHA_UNFILTERED parameter (i.e. without denoising)
vgosa_unfiltered	
cross_track_distance	Distance between the swath position and the nadir position on the same line Only added in Unsmoothed dataset (already present in Basic and Expert)

Table 13: New variables added in the v2.0.1 version

4.6 Version v3.0

The Version 3 (v3) release exclusively covers the 2×2 km resolution products, comprising the Basic, Expert, and newly introduced Technical product lines.

4.6.1 Basic and Expert

4.6.1.1 New MSS CNES_CLS_2025 used

The Mean Sea Surface (MSS) used for Sea Surface Height Anomaly (SSHA) construction has been updated in version 3. The MSS Hybrid 2023 (Laloue et al. 2024), previously used in version 2, has now been replaced by a beta version of the MSS CNES_CLS_2025, as presented by (Charayron et al. 2025). This MSS integrates 30 years of nadir altimetry data with 25 cycles of SWOT-KaRIn 2km measurements from the science orbit phase. A specific correction, identified as "MSS compression correction" is taken into account during the processing. It allows to mitigate the inconsistency between the SSH resolved scale by KaRin 2km and nadir 1Hz products and the resolved scales of the MSS directly interpolated on the measurement position. It allows to retrieve the full MSS signal from compressed altimeter measurements.

The use of DUACS DT-2024 multi-mission gridded products contributes to managing ocean variability and maintaining the 20-year reference period [1993–2012] for this new MSS. Additionally, the implementation of the MIOST mapping algorithm—which accounts for a dynamic internal tide mode (Ubelmann et al. 2022)—enhances the separation of KaRIn measurements between small-scale ocean variability and small-scale static MSS signals.

This results in a more accurate definition of MSS structures at scales below 100 km. Validation with independent measurements highlights a global mean SSHA variance reduction of 10% over wavelengths ranging from 10 to 125 km, with improvements reaching up to 20% around the 20–30 km scale. These gains are primarily concentrated along geodetic structures, where local reductions in variance exceed 1 cm^2.

The adoption of this new MSS significantly reduces the imprint of geodetic structures in the resulting SSH data (e.g., Figure 27).

Known limitations: The MSS CNES_CLS_2025 is not optimized for coastal areas or polar regions.

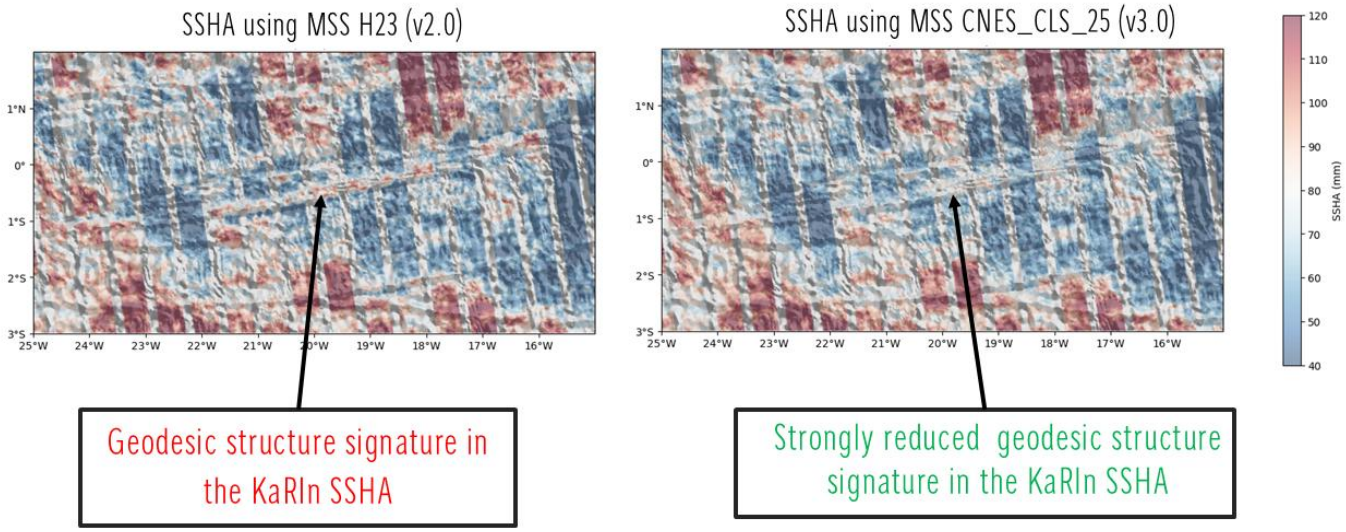

Figure 28: KaRIn SSHA from cycle #16 in the equatorial Atlantic area, over a transform fault. SSHA is superimposed with bathymetric gradients. SSHA in V2.0 (left) and V3.0 (right) product version. (no data selection applied).

4.6.1.2 Ocean tide estimation extended in estuaries areas

The ocean tide correction from the FES_2022 unstructured mesh, used in the version 2 product, is not defined across the full extent of certain estuarine areas. As a result, in most cases, the ocean tide correction and resulting corrected SSHA are missing in the extremities of estuaries. To address this limitation, the v3 product complements the ocean tide correction in these regions with the FES_2022 extrapolated structured grid solution. This enhancement enables retrieval of the SSHA solution across the entire estuarine domain sampled with KaRIn (e.g., Figure 29).

Known limitations: the blended ocean tide solution does not guarantee full continuity across the transition zones between the two combined solutions, and some discontinuities may be observed. Additionally, the accuracy of the ocean tide solution remains limited in such areas.

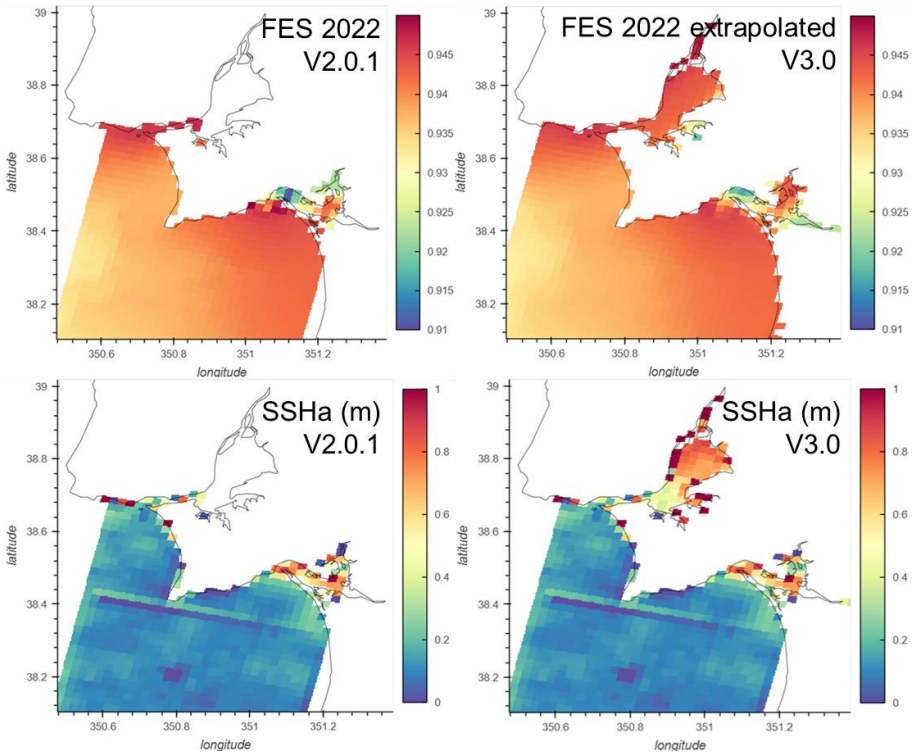

Figure 29: ***Example of the impact of the extrapolation of FES 2022. Case of an estuary in Spain – Only land sea mask data selection applied***

4.6.1.3 Data selection improved

Data selection was improved by introducing a new land-sea mask selection criterion. The retrieval of estuarine areas using a high-resolution land-sea mask, first initiated in version 2, has been generalized in version 3.0. To achieve this, OpenStreetMap (OSM) polygons defining coastal and estuarine regions were used to construct the land-sea mask implemented in version 3. This enhancement enables systematic retrieval of most estuaries (e.g. Figure 30).

Known limitations: OSM polygons remain imperfect, and narrow estuaries or their extremities may not be fully resolved—particularly when using the 2 km resolution mask. Additionally, some rivers and small inland surface water bodies near the coast may be misclassified as sea in this new version of the mask. A valid data selection flag is used to reject measurements over such areas.

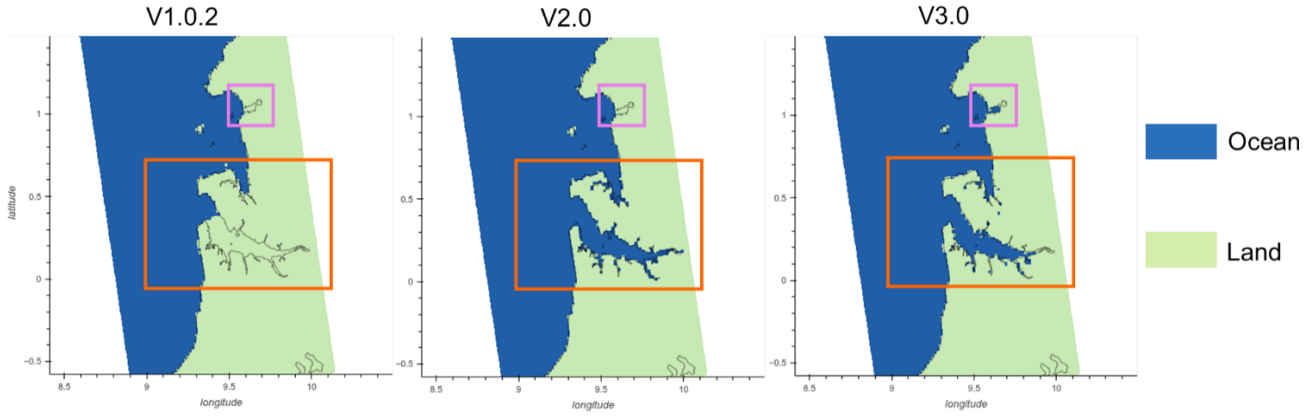

Figure 30: Example of land-sea masks used in V1 (left), V2 (center), and V3 (right). Orange boxes highlight an estuary that was not resolved in the V1 version, manually retrieved in V2, and automatically resolved in V3 using OSP estuary contours. Pink boxes show an example of an estuary not resolved in either V1 or V2, but retrieved in V3 thanks to OSP estuary contours.

Additionally, the data selection quality flag was improved near the coast to better detect remaining in-land pixels. In v2.0.1, some unedited pixels could remain very close to the coastline. In v3.0, these pixels are edited by flag 10.(e.g. Figure 31)

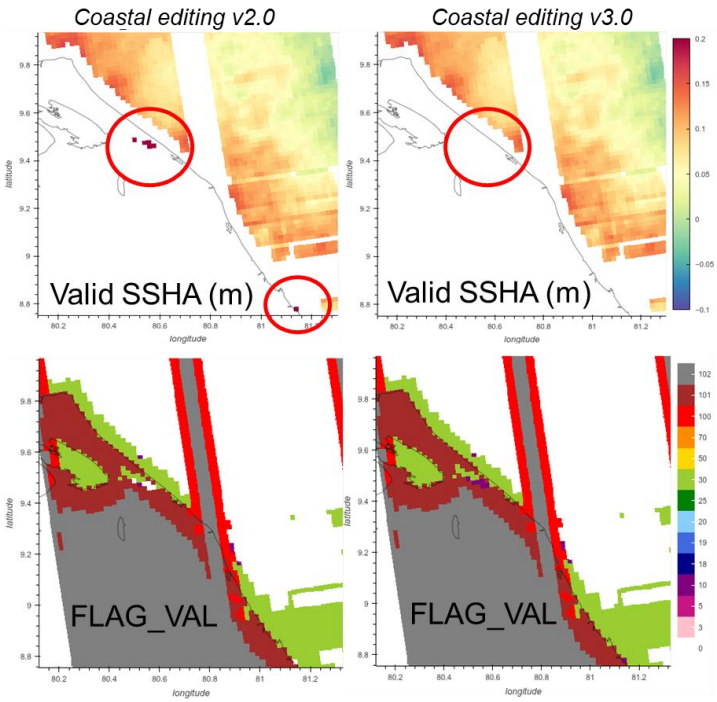

Figure 31: Example of coastal editing in V2 (left) and V3 (right). SSHA selected with flag_val value > 5 (top) and flag_val (bottom). Red circles show an example of invalid and inland SSHA pixels that were not rejected in V2 and now accurately rejected in V3 with dedicated "#10: suspected coastal pixels" flag_val value.

The granularity of the flag_val parameter was enhanced to better identify measurements affected by rain cells. To achieve this, independent precipitation rate estimates proposed by (Picard et al. 2025) were used to introduce a new

flag_val value #25, which marks measurements that were initially rejected based on the version 2 data selection criteria—primarily due to anomalies in the SSHA statistical distribution (e.g. Figure 32). The precipitation rate information is provided in the new "technical" product (see section 4.6.2)

Known limitations : the data selection criteria implemented in version 3 do not directly rely on precipitation rate. At this stage, precipitation rates are used solely to refine the potential origin of SSHA anomalies within the flag_val framework. A more integrated use of precipitation data should be considered for version 4 to enable consolidated data selection. Furthermore, the precipitation rates used in version 3 are not fully optimal. The two versions available have distinct strengths and weaknesses. Improved versions should be explored in future Level 3 KaRIn data production.

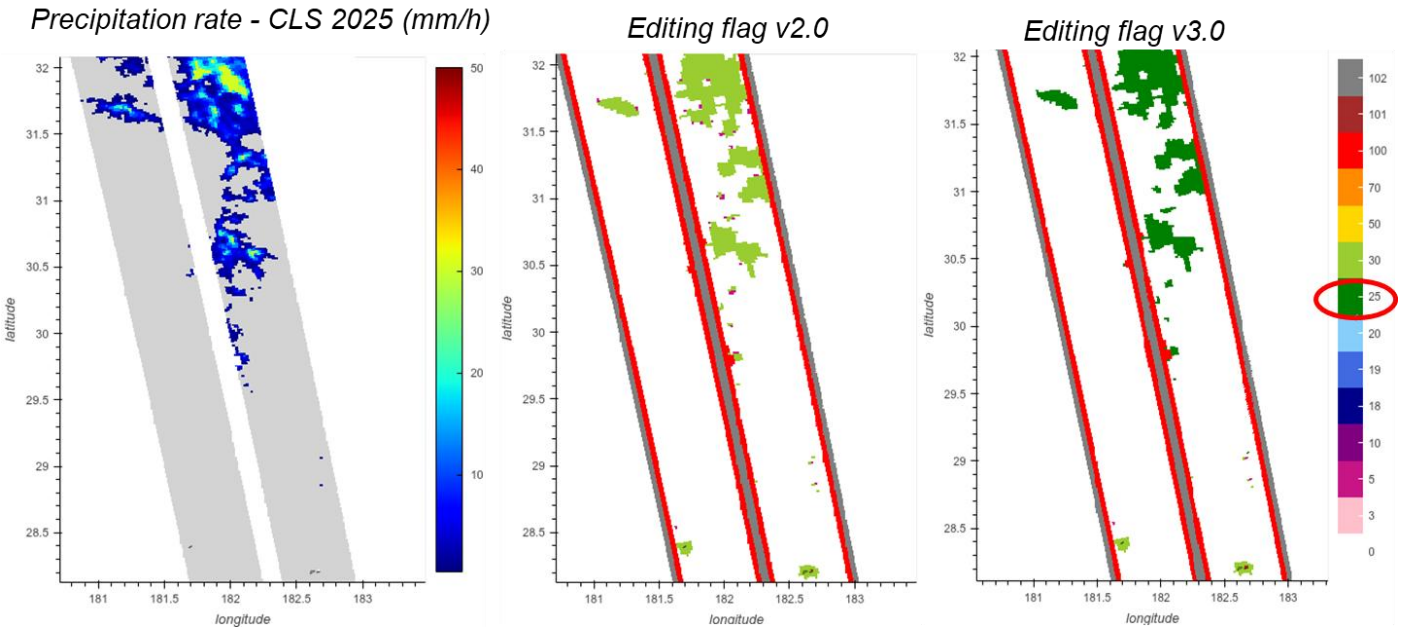

Figure 32: Example of refined flag_val granularity with #25 "rain event" value. Independent precipitaton rate (left), invalidated measurement in V2 using different data selection criteria (center), editing flag refined in V3 using precipitation rate (right).

4.6.1.4 Calibration improved

Calibration processing in the version 3 product was improved as follows:

- First, predictable calibration components are now more accurately identified and estimated using functions whose parameters are fitted to observational data. In future version 4 releases, this approach will be further refined to better account for the dependence of linear parameter on the beta angle.
- Second, the methodology for interpolating unpredictable calibration components in areas where direct estimation is not feasible has been enhanced. Version 3 now applies optimal interpolation to estimate gyro and long-wavelength KaRIn errors, replacing the previous polynomial approximation for roll errors. In future version 4 releases, this approach will be further refined to be adapted also on the bias errors.
- Third, estimation of an error associated to the calibration correction. This error is directly defined with the optimal interpolation methodology used. This information is mainly used for calibration validation purpose. It is not yet disseminated in the L3 product.

The benefits are mainly expected in marginal areas such as semi-enclosed seas, near-coastal zones, and polar oceans (e.g., Figure 33), where direct estimation is generally not possible.

Known limitations:

The improvements introduced in version 3 are intended to reduce the absorption of physical signals of interest by calibration corrections in the marginal regions. Nevertheless, the calibration process may still inadvertently absorb signals other than systematic KaRIn errors, which could continue to affect the physical signal of interest. The low frequence calibration component is available in the new technical product (see Section 4.6.2), enabling users to assess the impact of the calibration elements and selectively apply those relevant to specific applications.

The calibration correction presents a discontinuity linked to the residual biaises observed between Copernicus Marine Service L3 nadir products available in delayed time (MY DT-2024 series) and in Near Real Time. See section 5.8 for details.

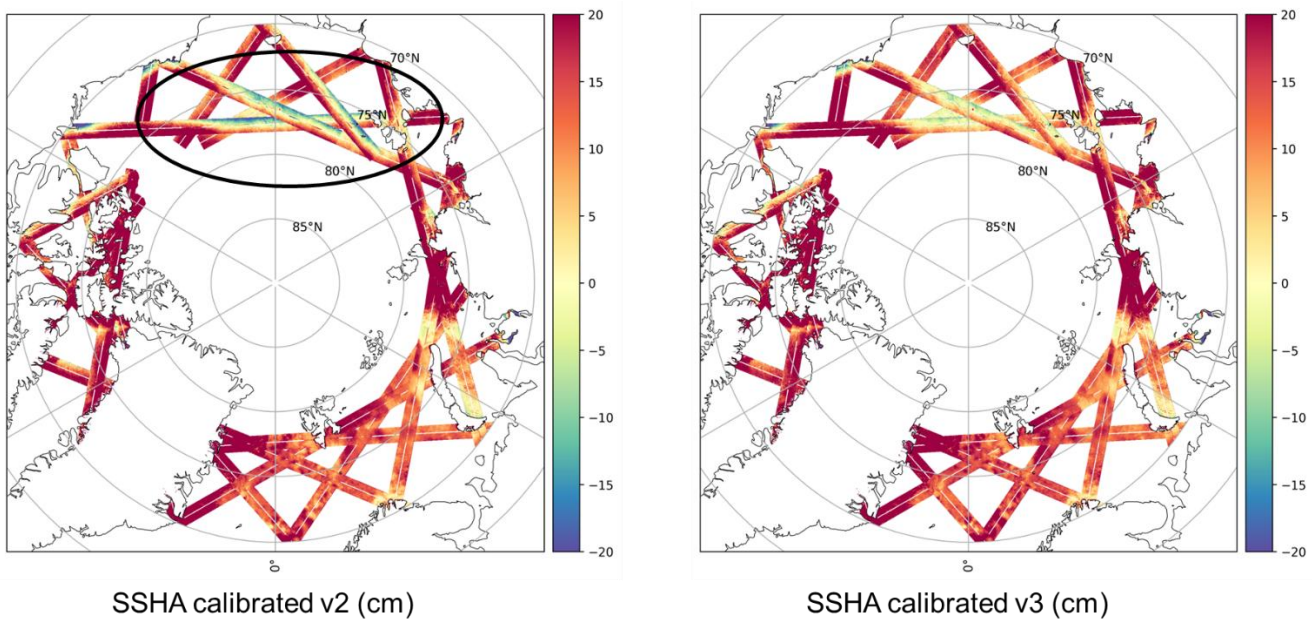

Figure 33: Example of calibrated SSHA in v2 (left) and V3 (right) product version (KaRIn cycle 9, passes 1-29). The black circle shows an area where calibration residual errors were high in V2. There are significantly reduced in V3.

4.6.1.5 Denoising improved

The 2 km denoising process was enhanced to reduce residual anomalies observed in the V2 product version (see section 5.4). Improvements to the U-net learning process included:

- Incorporating more realistic L3 editing in the simulated dataset
- Simplifying the training dataset in size and by going back on style-transferred noise
- Using a slower learning process, with appropriate parameters

Additionally, metrics to qualify the denoised SSHA were improved.

The new V3 denoising process eliminates noise signals considered as mainly uncorrelated. It also substantially reduces the artifacts observed in the V2 version (e.g. Figure 34), including:

- No regional biases introduced in the SSHA
- Significantly reduced absorption of physical signals at short wavelengths
- Greatly diminished discontinuities in the SSHA signal caused by denoising

Known limitations: The denoising process may still absorb signals other than uncorrelated noise. Residual small-scale wave signals and some MSS-related errors can be observed in the removed component. Users interested in wave signals, or those intending to combine SSHA with an MSS field different from the one used in the L3 processing, should work with SSHA prior to denoising.

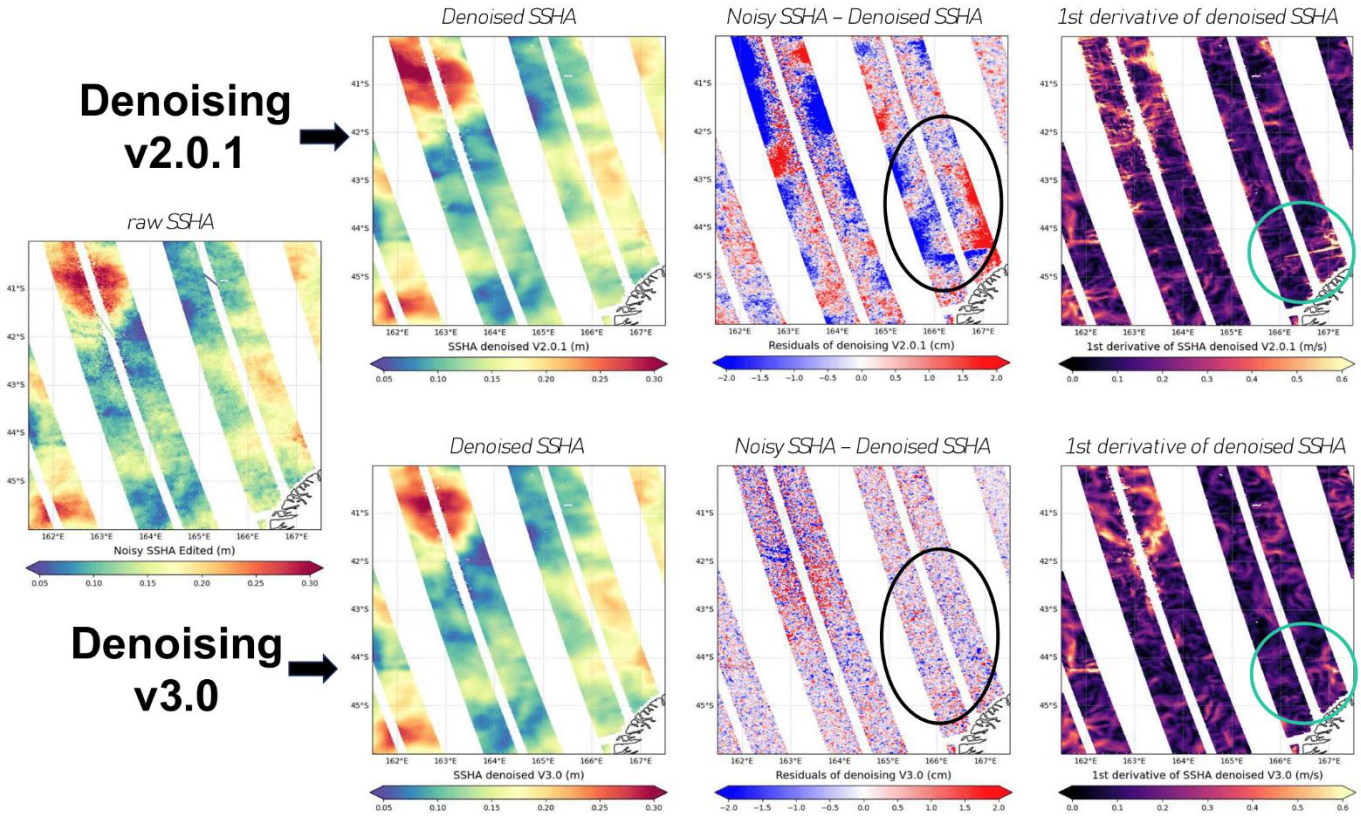

Figure 34: Example of denoised SSHA. The original raw (noisy) SSHA is shown on the left map. The denoised SSHA, the residual noise removed, and the first derivative of the denoised SSHA are presented in the three successive columns to the right, for version V2 (top) and version V3 (bottom) of the denoising process. The black circle highlights areas where regional biases were introduced by V2 (notably in regions of high SWH). The green circle indicates areas where SSHA discontinuities—clearly visible in the first derivative—were introduced in V2 denoising.

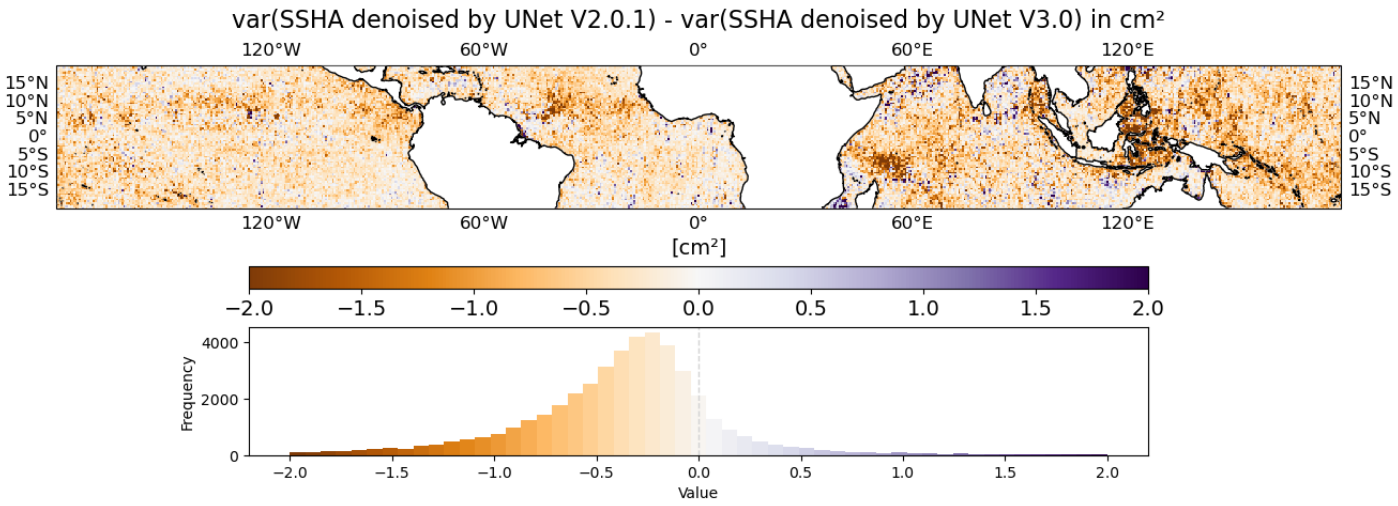

Figure 35: Mapping of difference of SSHA denoised variance between the SSHA denoised by the algorithm in V2.0.1 and the one in V3.0. Orange means that the SSHA denoised by the UNet V3.0 contains more variability (i.e. absorbing less signal) than in V2.0.1. We made the focus on the equatorial band where internal tides are well-known

4.6.1.6 Geostrophic current estimation improved

In version V3, the methodology for estimating geostrophic currents has been refined by integrating the 2D spline filtering technique proposed by (Tranchant et al. 2025). This approach enables selective filtering of short-wavelength signals that may include unbalanced motions inconsistent with the geostrophic approximation. The geostrophic velocity are then computed from the slope of the linear plane kernel fitted to 2D SSH observations Compared to V2, the resulting current fields are notably smoother.

Validation with independent drifter measurements confirms improved agreement, with KaRIn-derived geostrophic currents demonstrating stronger consistency. Notably, the Level-3 fitting method reduces the root mean square deviation (RMSD) by 10–20%, underscoring enhanced performance (Figure 36).

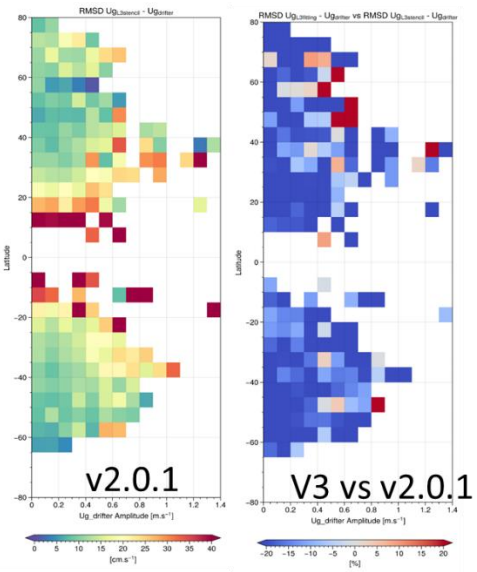

Figure 36: Intercomparison RMSD Karin velocity vs drifter velocity as a function of drifter velocity amplitude. Left: comparison between KaRIn currents available in v2.0.1 and drifters (units cm.s^{-1}); right: differences of RMSD when Karin v3 KaRIn currents are considered (units: %)

4.6.2 Technical

The L3 v3 KaRIn product is complemented by a 'Technical' product line. Its purpose is to provide access to additional geophysical parameters that may be relevant for targeted studies or specialized applications. This product may also include alternative solutions to core L3 outputs, particularly for variables not yet available in the Level-2 dataset.

4.6.2.1 Product overview

Currently offered at a spatial resolution of 2×2 km, the Technical product contains the variables listed in the 3.2.2

4.6.2.2 Goddard Ocean Tide GOT5.6

Goddard Ocean Tide (GOT5.6) is a new model proposed by (Ray 2025). It provides estimates of the amplitudes and phases of daily and sub-daily global ocean tides, derived from decades of radar altimetry data across multiple satellite missions. Over the majority of the deep ocean, between latitudes ±66°, the solution primarily relies on data from five satellites: TOPEX/Poseidon, Jason-1, Jason-2, Jason-3, and Sentinel-6A Michael Freilich. In contrast, data from additional satellite altimeters were incorporated for shallow seas and polar regions (Table 14).

Tidal analysis was conducted with respect to a prior reference model—mainly the Finite Element Solution FES2014 from Lyard et al. (2021)—with minor localized modifications.

Validation was performed using independent observations from several missions: Sentinel-6A, Sentinel-3A, HY2B, and SWOT nadir. An example of the comparative results is presented in Figure 37, revealing that:

- GOT5.6 yields greater variance reduction than FES2022b across most of the global ocean, though local variability is observed. The strongest improvements are found along the northern Australian coastline, in the Sea of Okhotsk, the South China Sea, and the northern Indian Ocean.
- FES2022b achieves superior variance reduction in certain regions, including the Patagonian shelf, Bering Strait, Greenland Sea, and North Sea. Additionally, FES2022b performs better in coastal proximity, notably within 20 km of the shoreline

Table 2: Solution domains used to construct GOT5.

Domain	Latitude extent	Satellites	Time span	# days
Main	±66°	Jason, S-6	2002–2023	7924
		Interleaved T/P-J	2002–2023	2961
		GFO	2000–2008	2459
		Envisat, SARAL	2002–2016	4280
		Sentinel-3A	2016–2023	2847
		Sentinel-3B	2018–2023	1860
Arctic	60°–90°N	CryoSat-2	2010–2021	3933
		GFO	2000–2008	2474
		Envisat	2002–2012	3502
		SARAL	2013–2022	3445
Antarctic	79°–60°S	CryoSat-2	2010–2021	3933
		GFO	2000–2008	2401
		Envisat	2002–2012	3502
		SARAL	2013–2022	3447
Ice shelves	86°–65°S	CryoSat-2	2010–2022	4285

Table 14: Solution domains used to construct GOT5 from (Ray 2025)

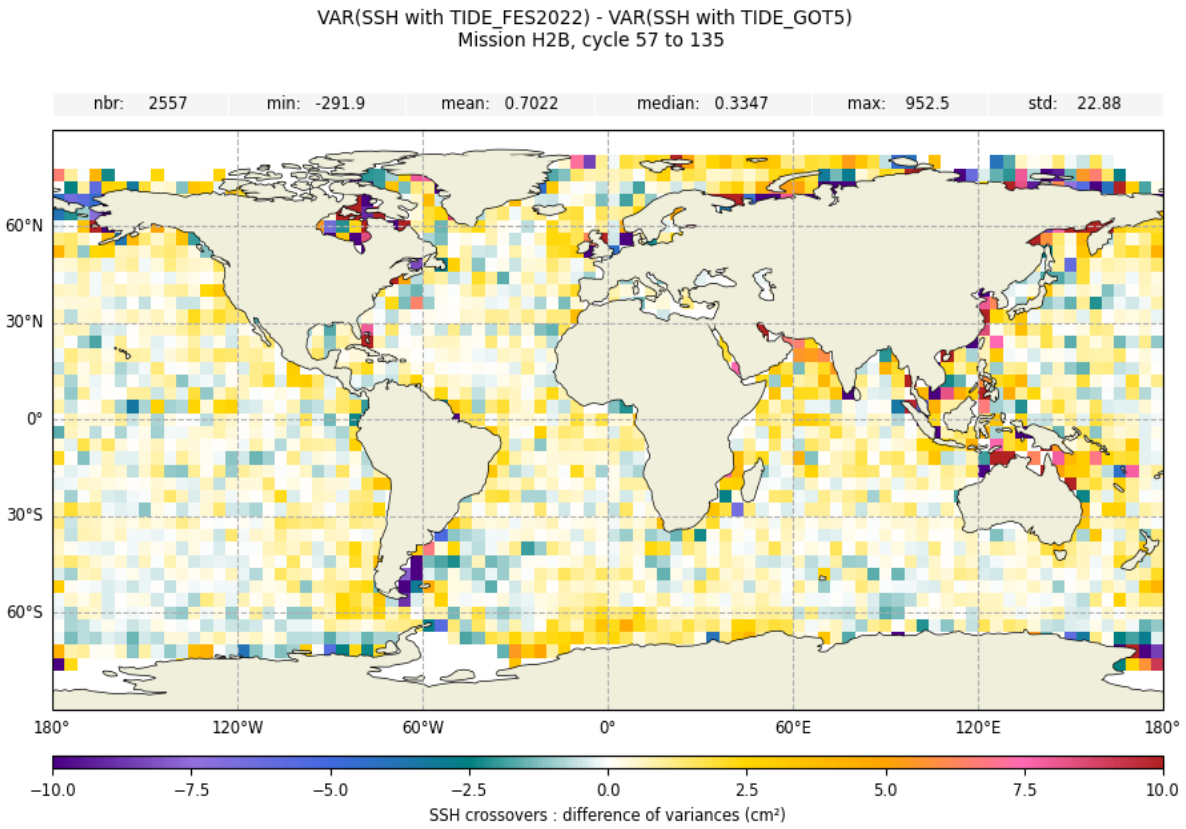

Figure 37: Difference of variance of SSH differences at HaiYang-2B crossover locations, when SSH is corrected from ocean tide with FES22 or with GOT5.6 model. (courtesy L. Carrere) (unit cm²)

4.6.2.3 Internal tide Zhao30y

ZHAO30yr is an internal tide model developed by (Zhao 2025), utilizing 30 years of satellite sea surface height (SSH) measurements spanning 1993 to 2022, processed using an enhanced mapping technique. As a next-generation model, ZHAO30yr decomposes the internal tide field and reveals numerous long-range internal tidal beams, which carry key information on the processes of generation, propagation, and dissipation. The ZHAO30yr atlases are available for the eight principal tidal constituents: M2, K1, S2, O1, N2, K2, P1, and Q1.

The ZHAO30yr internal tide model was evaluated in comparison with the HRET22 model, which is currently used in L3 KaRIn product generation, using SWOT-nadir observations (Figure 38). Results indicate that ZHAO30yr yields modest local variance reduction relative to HRET22 across tropical oceans, with more pronounced improvements observed east of Madagascar and throughout the Indonesian seas. Conversely, ZHAO30yr increases variance locally in several regions, including south of Japan, east of Australia, northern Indian Ocean, and west of Madagascar. Overall, the mean variance difference between the two models is minimal, estimated at just 0.03 cm²

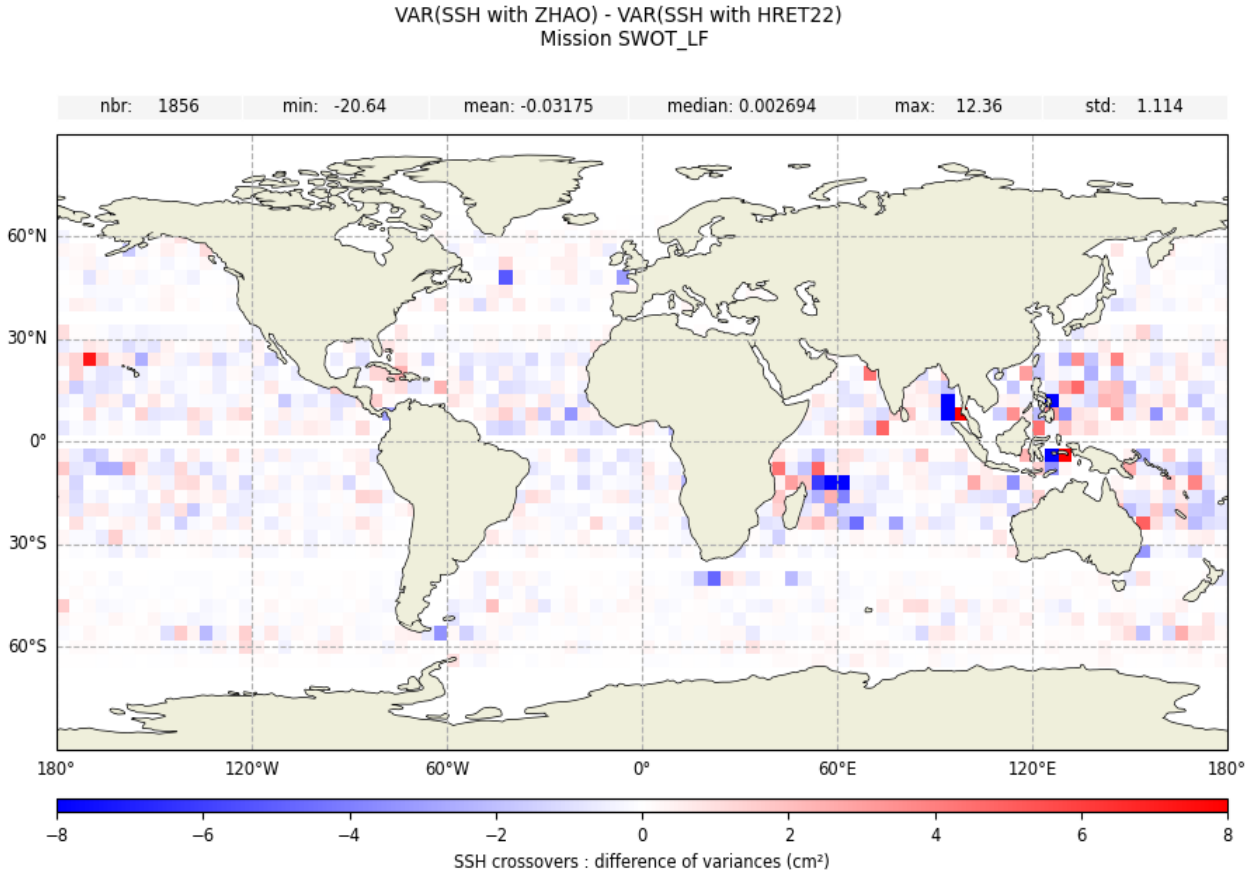

Figure 38: Difference of variance of SSH differences at SWOT-nadir crossover locations over the [2023, 2024] period, when SSH is corrected from internal tide with ZHAO30y or with HRET22 model. (courtesy L. Carrere) (unit cm²)

4.6.2.4 Internal tide MIOST-IT24

MIOST-IT24 is an internal tide model developed by (Tchilibou et al. 2025). It reconstructs the sea surface height (SSH) signature of coherent internal tides using a single-time inversion of a 28-year (1993–2020) along-track altimetry dataset. Leveraging a conjugate gradient algorithm, this single inversion approach simultaneously resolves internal tide contributions and mesoscale eddy variability—an advancement over conventional methods that rely on separate mesoscale estimates.

In contrast to its predecessor, MIOST-IT22 (Ubelmann et al. 2022), MIOST-IT24 incorporates mode-1 and mode-2 internal tide wavelengths computed from vertical stratification profiles provided by the GLORYS12v1 climatology (1993–2020). Atlases from MIOST-IT24 are available for four primary tidal constituents: M2, K1, S2, and O1.

MIOST-IT24 was evaluated against the HRET22 model, currently used in Level-3 KaRIn product generation, using SWOT-nadir observations (Figure 39). The results indicate that MIOST-IT24 generally outperforms HRET22, showing notable local variance reductions, particularly across the Indonesian region. However, slight degradation in performance is observed in some areas within the tropical band.

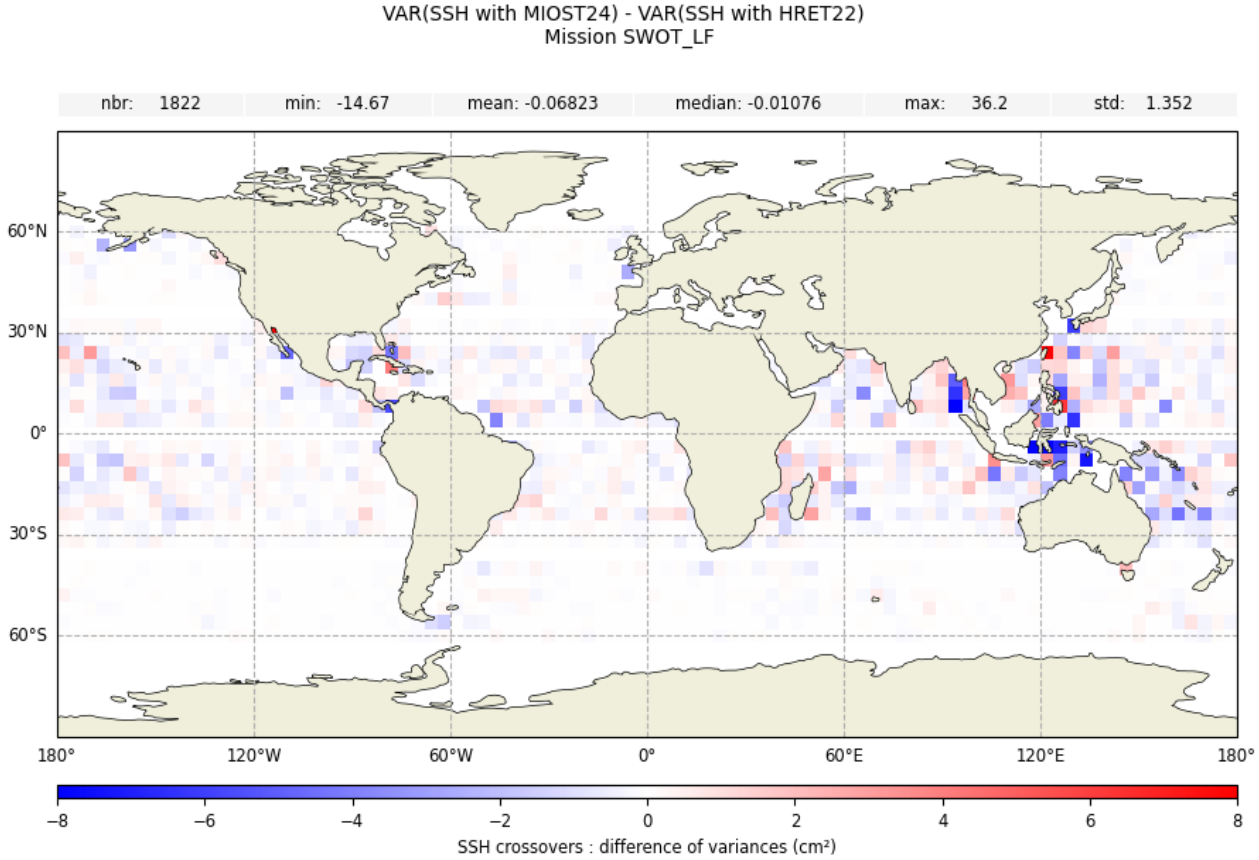

Figure 39: Difference of variance of SSH differences at SWOT-nadir crossover locations over the [2023, 2024] period, when SSH is corrected from internal tide with MOST-IT24 or with HRET22 model. (courtesy L. Carrere) (unit cm²)

4.6.2.5 Rain flagging and Precipitation rate (ITU 2025 & RF 2025):

Two different precipitation rate models, presented in (Picard et al. 2025) are propose:

- ITU 2025: This solution relies on physically based attenuation inversion using ITU-R models. It appears to be the more robust approach under extreme event conditions, but exhibits over-detection of precipitation rates in low-rain scenarios. Thresholds derived from FLUCTUS 2025 are used to define the precipitation flag included in the Technical product.
- RF 2025: This model is based on a supervised machine learning algorithm trained on collocated NEXRAD radar data. It performs better in detecting low precipitation rates but introduces discontinuities in the estimated precipitation field due to the segmentation scheme used during processing

4.6.2.6 Low frequency calibration

The objective of the calibration is to remove systematic errors from the satellite: uncorrected satellite roll angle, interferometric phase biases and thermo-elastical distortions in the instrument baseline and antennas. In practice, the calibration also absorbs residues of geophysical correction errors such as tide or SSB. In the technical product, a low-frequency calibration is provided. This is an alternative calibration that corrects the satellite's systematic errors less well but absorbs fewer residues of geophysical correction errors. In the following figure, we can see that there are fewer tidal residues absorbed in the v3.0 calibration but especially in the v3.0 low-frequency calibration.

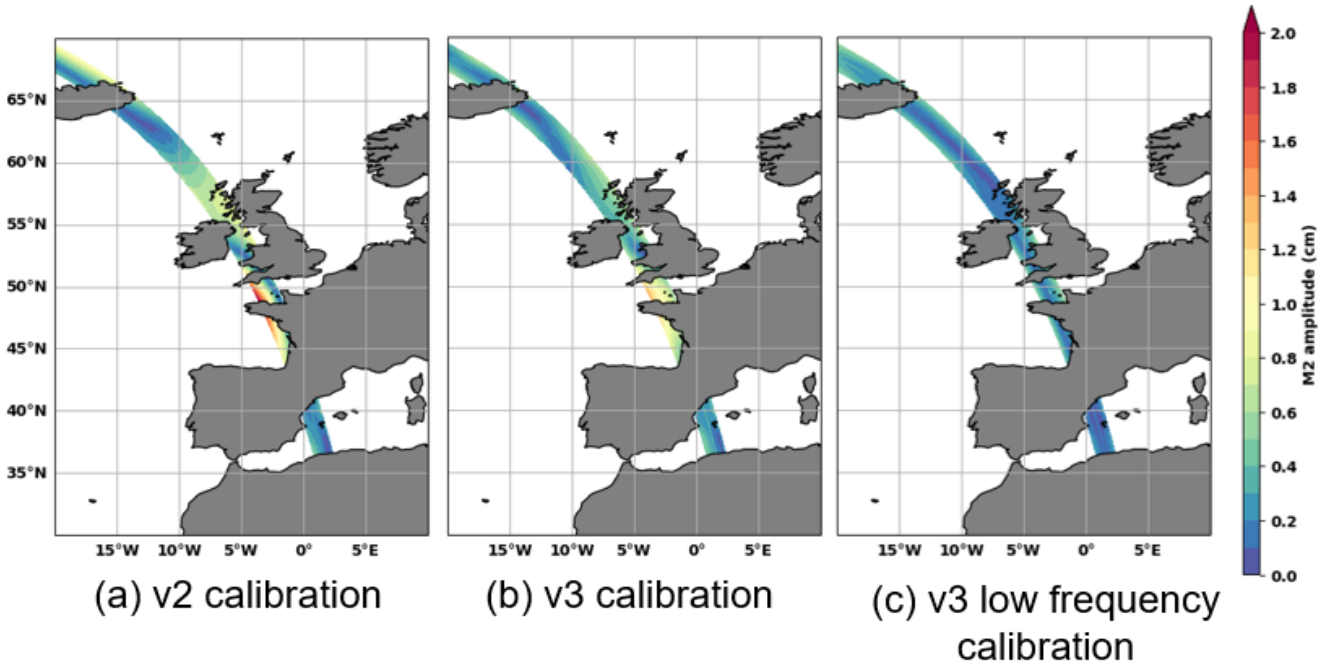

Figure 40: M2 amplitude in the v2, v3 and v3 low frequency calibrations for pass 348 (cm)

5 Known limitations and anomalies

We list in this section the known limitation or anomalies observed in the L3 KaRIn products

5.1 Missing estuaries in land-sea mask

Some areas (especially estuaries) are not well defined in OpenStreetMap and will show land where we would expect sea.

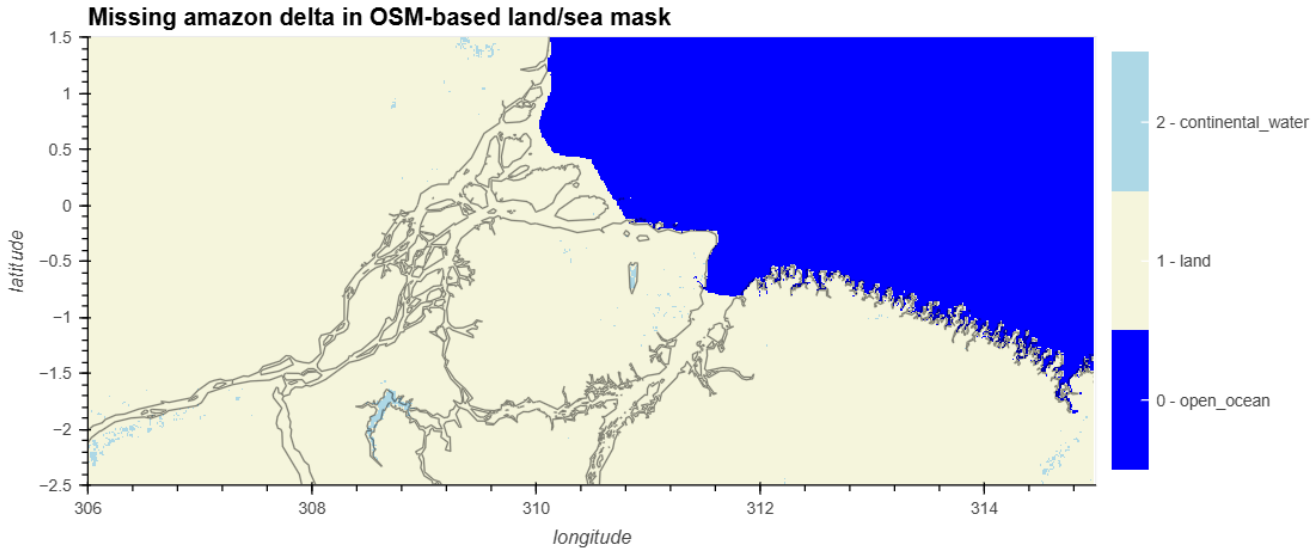

Figure 41: OpenStreetMap-derived land sea mask shows may classify some estuaries a land (yellow)

This issue has been mitigated

- in V2.0 (see section 4.4.1.2) by blending the L2 mask over the identified problematic areas, which include 43 estuaries. Additional problematic areas spotted by the users might be communicated to the AVISO team for further patching (refer to the Contact section 8).
- In v3.0 by introducing a new land-sea mask selection criterion (see section 4.6.1.3)

5.2 Discrepancy of valid domains for FES22 corrections in v2.0 and v2.0.1

In some particular areas, users might observe that some of Level-3 data is missing with respect to Level-2 data, and that the quality flag investigation is marked as no_data (see Figure 42)

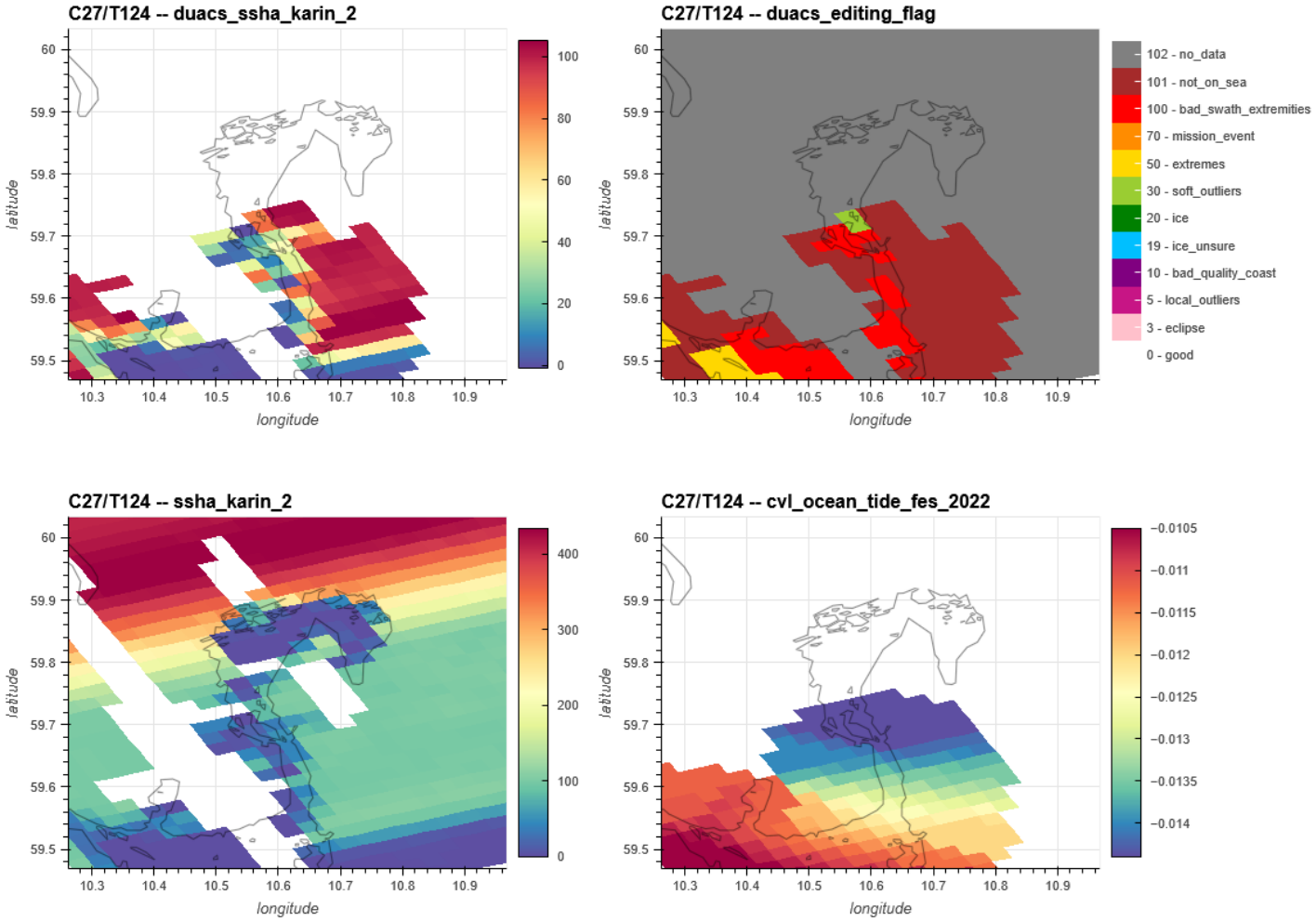

Figure 42: Missing points in L3 are observed when comparing the Sea Level Anomaly from Level-3 (top left) and Level-2 (bottom left) products. The quality flag (top right) indicates missing data in gray that are explained by missing data in the ocean tide correction (bottom right)

The missing data is introduced by the ocean tide correction FES 2022, which is not defined at the problematic location. Even if the ocean tide correction is the same in both the baseline C Level 2 product and the v2.0.1 Level 3 product, the source of the correction differs. Level-2 product uses an extrapolated cartesian grid whereas the Level-3 product uses the finite element meshes which has a smaller domain of definition. This is illustrated in the following Figure.

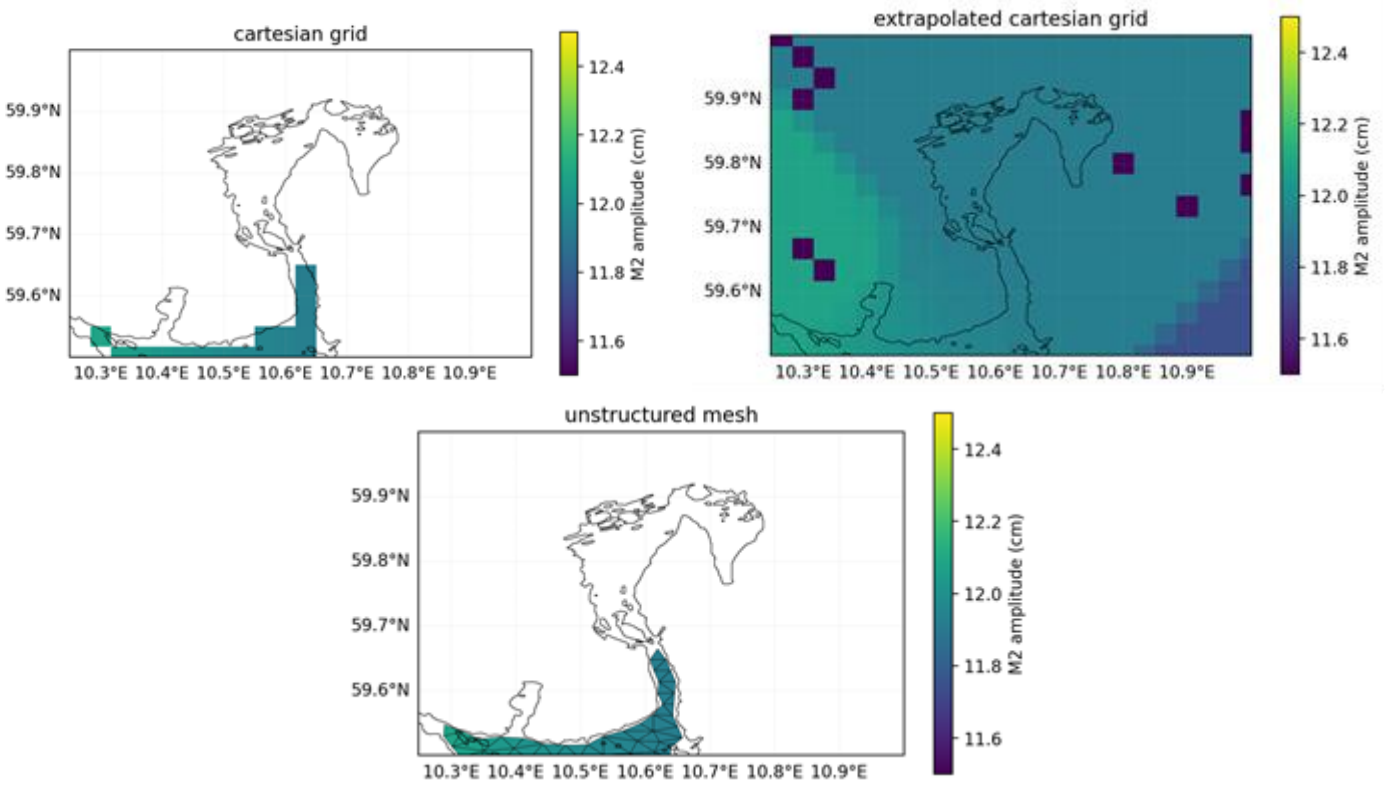

Figure 43: Difference in the definition of the FES2022 source data with (bottom) the original unstructured mesh used in the Level-3 product (top left) the cartesian grid interpolated from the mesh and (top right) the extrapolated cartesian grid used in the Level-2 product

This issue was mitigated in v3.0 by using the FES22 solution from extrapolated cartesian grid when the unstructured mesh solution is not available (see section 4.6.1.2)

5.3 Use of “ssha_filtered” and MSS in V2.0 and v2.0.1

The analysis of the constant content of the noise removed with the filtering can underline statics small scales structures linked to the MSS field used for the SSHA computation (see example in the following figure). Consequently, we recommend to users that may want to use a different MSS field than the one used in the L3 processing to work with the “ssha_unfiltered” field (i.e. before denoising processing) rather than “ssha_filtered” (i.e. after denoising processing)

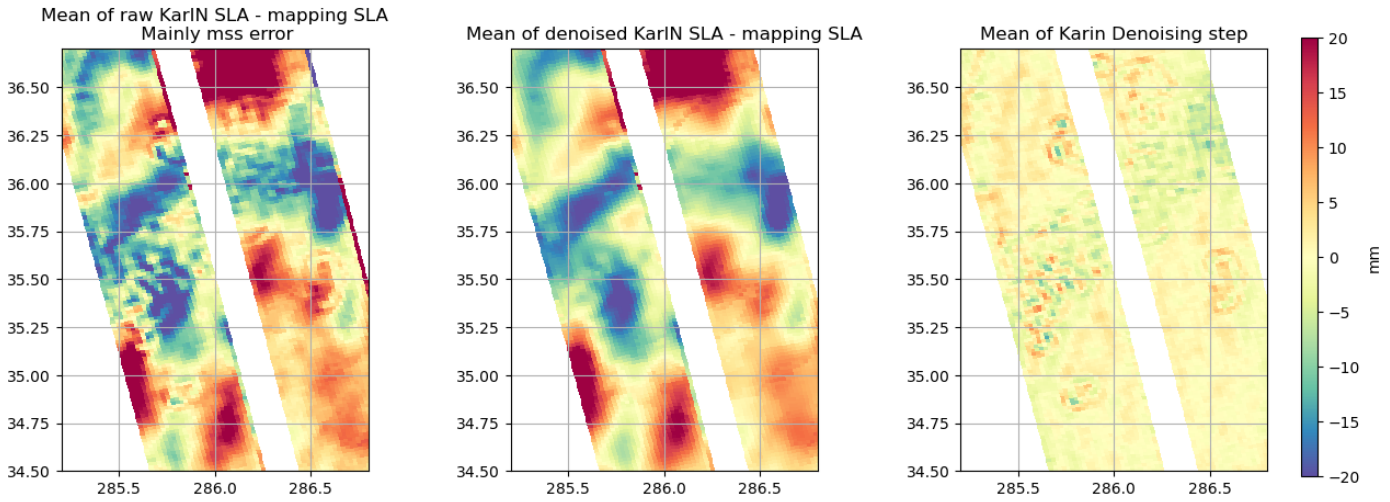

Figure 44: Mean structures remaining on SSHA during the CalVal phase period, before denoising (left) and after denoising (center). In this example, the mean content of the noise removed by the denoising processing (right) is dominated small scale static structures that are not corrected by the MSS used.

This issue was mitigated in v3.0 by using a new MSS (see section 4.6.1.1 for details)

5.4 “ssha_filtered” biases and discontinuities in v2.0 and v2.0.1

Regional biases in the ssha_filtered product were observed, primarily in areas of high SWH, where they can reach several centimeters (e.g. Figure 444). These biases are identified as anomalies introduced during the denoising process and are likely due to limitations in the current noise-modeling scheme. These biases are also visible in regions of strong variability, such as the Gulf Stream. The denoising versions V2.0 and V2.0.1 can absorb part of the oceanic structures and sometimes even amplify them. These biases can be so strong that they create a discontinuity in the predicted swaths (see Figure 44, purple circle).

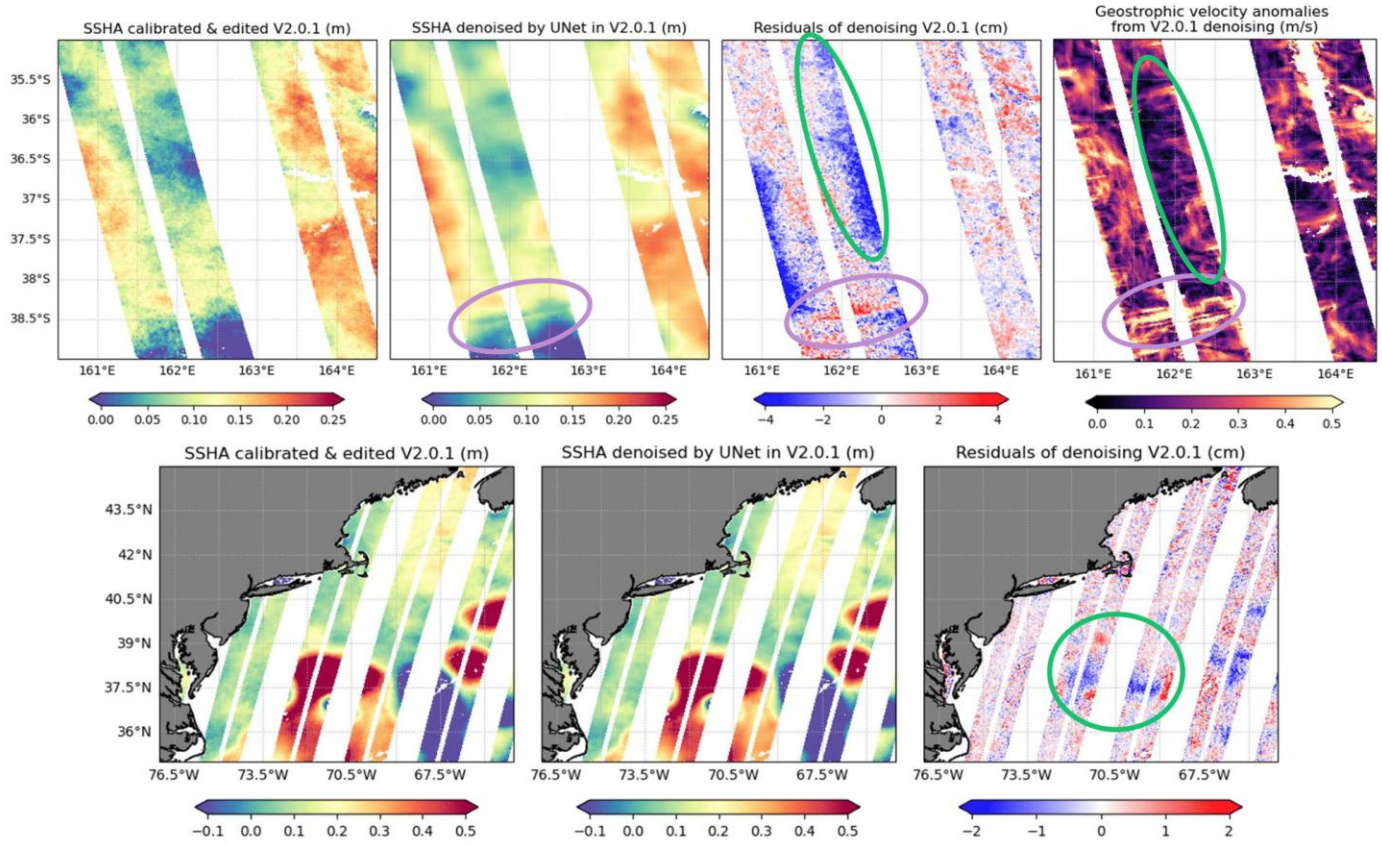

Figure 45: Example of regional biases induced by denoising processing in v2 version.

Certain physical structures may be attenuated by the denoising process implemented in version V2, particularly those associated with short-wavelength wave signals. This phenomenon is illustrated in Figure 45, where notable smoothing and signal loss are observed.

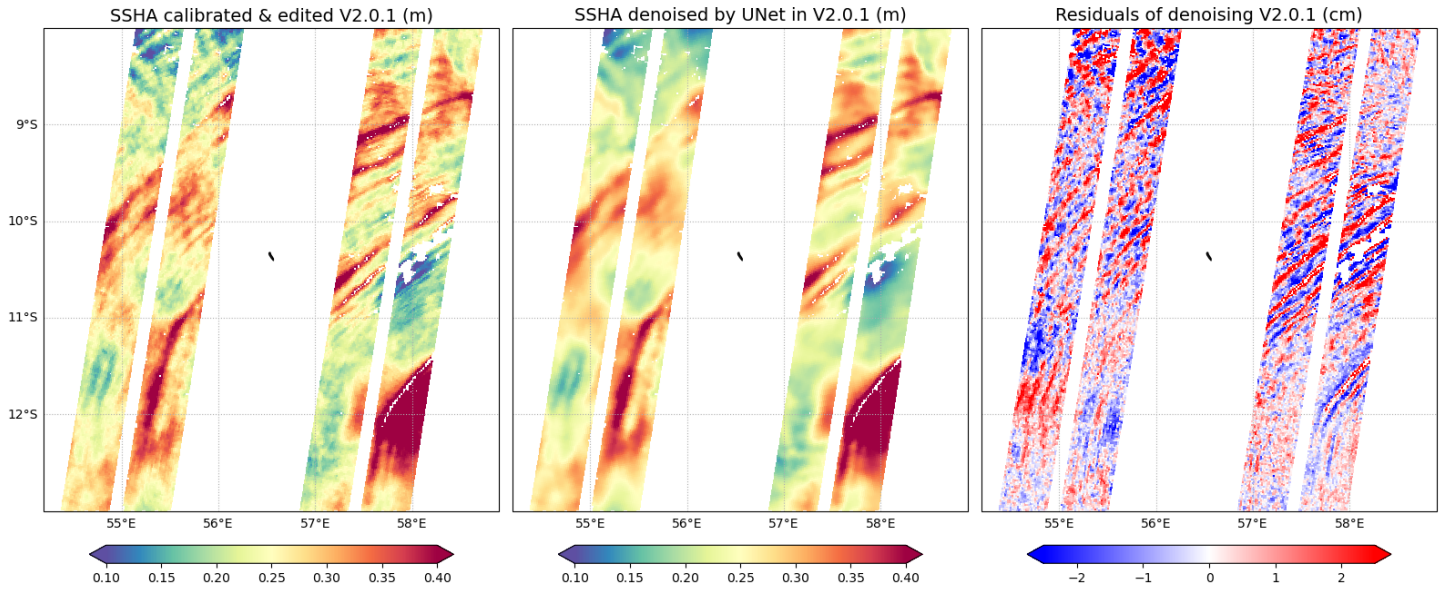

Figure 46: Example of waves attenuated by denoising processing in v2

These issues were mitigated in v3.0 by using an improved denoising (see section 4.6.1.5 for details)

5.5 SSHA restrictive quality flag during extreme events in v2.0, v2.0.1 and V3.0: Example of Hurricane Milton

The cycle 22, pass 216 intersects with the path of Hurricane Milton. Some pixels are rejected with flag #30 (SSHa pixels out of the expected statistical distribution) and #5 (SSHa pixels out of local distribution). This is mainly due to rain cells. For scientists who want to work on the Hurricane or on similar cases, we suggest applying flags higher than 30 (quality_flag variable) on the ssha_unedited variable.

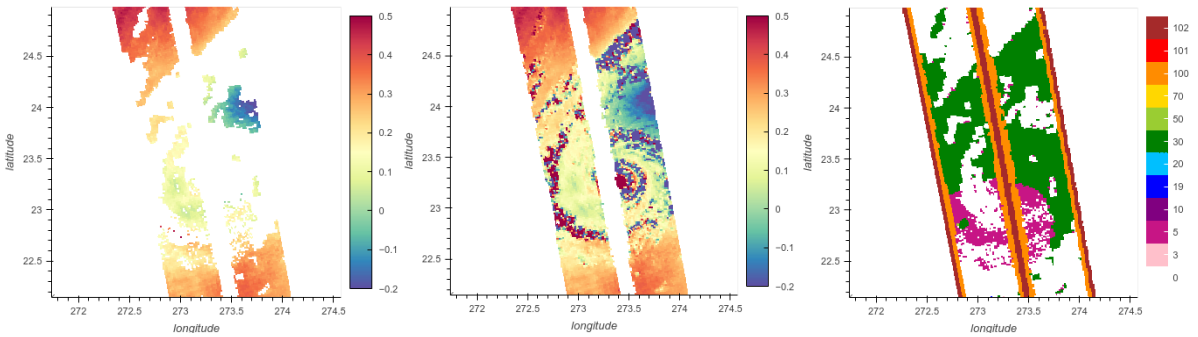

Figure 47: Example of Hurricane Milton. Left: ssha variable i.e. ssha with all flags applied. Middle: ssha with only flags > 30 applied. Right: quality flag

5.6 Small-scale discontinuities and errors in the calibration variable in v2.0.1 and v3.0

In some areas, when a L2 field (sc_yaw) is not defined, some small-scale terms of the calibration are reverted. This inversion causes small-scale discontinuities and errors inside the calibration variable. As these discontinuities and errors are small-scale, they are only visible if the calibration mean is removed. This issue only occurs when SSHA is not defined, thus this issue does not affect SSHA.

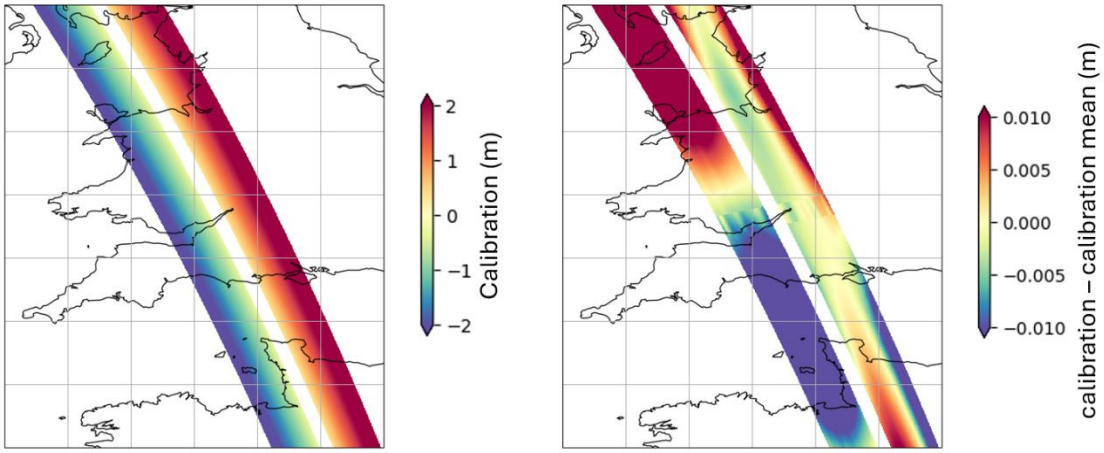

Figure 48: Example of small-scale discontinuities and errors in the calibration variable. Left: calibration variable. Right: difference between calibration variable and mean calibration variable.

5.7 Wrong editing flag in Unsmoothed product during eclipse transition

Some eclipse transitions in the Unsmoothed product are flagged with flag 30 ("SSHA pixels out of the expected statistical distribution") instead of flag 3 ("Eclipses"). These eclipses are not kept in the edited and filtered SSHA. There is therefore inhomogeneity between the Expert and Unsmoothed products.

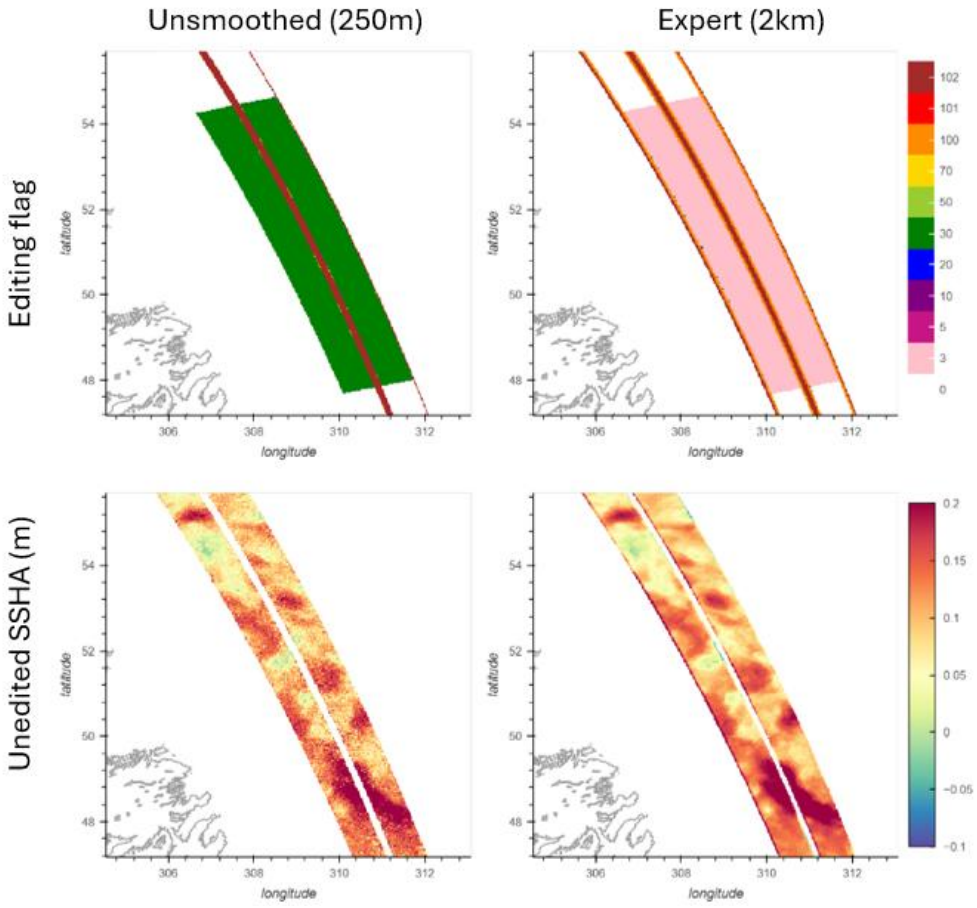

Figure 49: Example of eclipse transition with inhomogeneous flags between Expert and Unsmoothed products

5.8 SSHA calibration discontinuity in v3.0

The calibration correction presents a discontinuity related with the residual biases observed between Copernicus Marine Service L3 nadir products available in delayed time (MY DT-2024 series) and in Near Real Time (NRT). Indeed, for version 1.0.2 and 2.0.1, the KaRIn L3 data were calibrated from the Copernicus Marine Service L3 nadir products available in NRT. For version 3.0, an upgrade has been made in order to use L3 nadir MY products when available. The Copernicus Marine Service L3 nadir products based on MY DT-2024 standard are available in delayed time until May 2024 and, then in NRT after that date. Time evolving global and regional biases exist between L3 nadir MY and NRT series. The Figure 50 (left) illustrates the biases observed between L3 nadir MY and NRT series used for the L3 KaRIn v3 calibration. These biases propagate into the KaRIn calibration results as illustrated in the Figure 50 (right). To differentiate between the two calibration periods (based on L3 nadir MY or NRT), the L3 v3 KaRIn products are distributed in two separate directories:

- The "reproc" directory which contains L3 KaRIn products calibrated from the Copernicus Marine Service L3 nadir products available in delayed time (MY DT-2024 series);
- The "forward" directory which contains L3 KaRIn products calibrated from the Copernicus Marine Service L3 nadir products available in NRT (DT-2024 standards).

The bias between L3 nadirs in delayed time and in near real time products implies:

- A discontinuity in the SSHa calibrated at the junction of the "reproc" and "forward" repertoires
- A bias between the calibrated SSHa of v2.0.1 (based on L3 nadirs in near real time) and v3 of the "reproc" directory (based on L3 nadirs in delayed time).

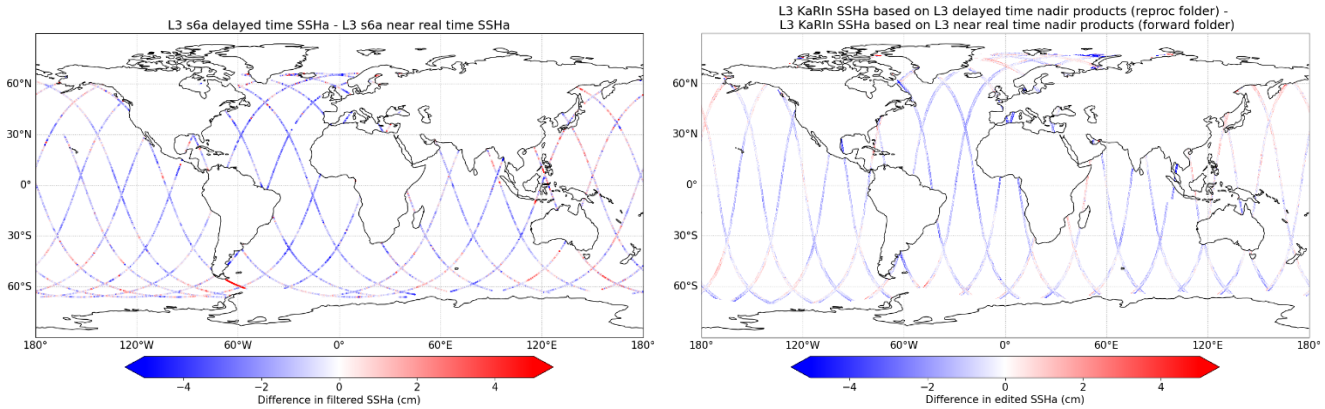

Figure 50: Bias between L3 s6a delayed time and near real time SSHa and its impacts on L3 KaRIn reproc and forward SSHA for the day of 2024/05/20

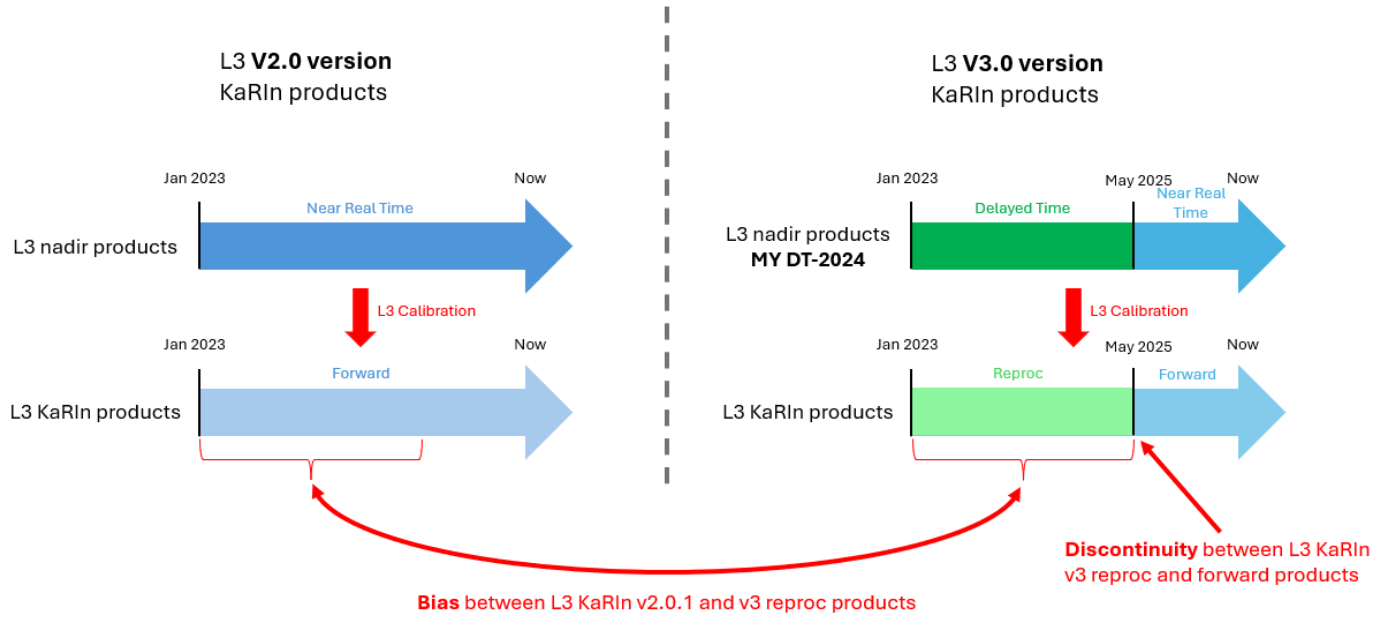

Figure 51: Impact diagram of L3 nadir inputs on L3 KaRIn products

6 Data format

This chapter presents the data storage format used for the products.

6.1 NetCDF

The products are stored using the NetCDF format.

NetCDF (network Common Data Form) is an interface for array-oriented data access and a library that provides an implementation of the interface. The netCDF library also defines a machine-independent format for representing scientific data. Together, the interface, library, and format support the creation, access, and sharing of scientific data. The netCDF software was developed at the Unidata Program Center in Boulder, Colorado. The netCDF libraries define a machine-independent format for representing scientific data. Please see Unidata NetCDF pages for more information, and to retreive NetCDF software package on:

https://www.unidata.ucar.edu/software/netcdf/

NetCDF data is:

- Self-Describing. A netCDF file includes information about the data it contains.
- Architecture-independent. A netCDF file is represented in a form that can be accessed by computers with different ways of storing integers, characters, and floating-point numbers.
- Direct access. A small subset of a large dataset may be accessed efficiently, without first reading through all the preceding data.
- Appendable. Data can be appended to a netCDF dataset along one dimension without copying the dataset or redefining its structure. The structure of a netCDF dataset can be changed, though this sometimes causes the dataset to be copied.
- Sharable. One writer and multiple readers may simultaneously access the same netCDF file.

The products are stored in **NetCDF** defined by the Cooperative Ocean/Atmosphere Research Data Service (COARDS) and Climate and Forecast (CF) metadata conventions.

The CF convention generalises and extends the COARDS convention but relaxes the COARDS constraints on dimension and order and specifies methods for reducing the size of datasets. A wide range of software is available to write or read NetCDF/CF files. API are made available by UNIDATA http://www.unidata.ucar.edu/software/netcdf:

- C/C++/Fortran
- Java
- MATLAB, Objective-C, Perl, Python, R, Ruby, Tcl/Tk

In addition to these conventions, the files are using a common structure and semantic as shown in the example below for expert product:

```
 netcdf SWOT_L3_LR_SSH_Expert_026_001_20241223T202047_20241223T211213_v2.0.0 {
dimensions:
      num_lines = 9860 ;
      num_pixels = 69 ;
      num_nadir = 1513 ;
variables:
      double time(num_lines) ;
            time:comment = "Time of measurement in seconds in the UTC time scale since 1 Jan 2000 00:00:00 UTC. [tai_utc_difference] is the difference between TAI and UTC reference time (seconds) for the first measurement of the data set. If a leap second occurs within the data set, the attribute leap_second is set to the UTC time at which the leap second occurs." ;
            time:leap_second = "0000-00-00T00:00:00Z" ;
            time:long_name = "time in UTC" ;
            time:standard_name = "time" ;
            time:tai_utc_difference = 37. ;
            time:calendar = "gregorian" ;
            time:units = "seconds since 2000-01-01 00:00:00.0" ;
      int calibration(num_lines, num_pixels) ;
            calibration:_FillValue = -2147483647 ;
            calibration:scale_factor = 0.0001 ;
            calibration:comment = "phase screen + phase_screen_static + phase_screen_orbit + xcal. the uncorrected ssha can be computed as follows: [uncorrected ssha]=[ssha from product] - [calibration]; see the product user manual for details.\n" ;
            calibration:coordinates = "longitude latitude" ;
```

calibration:long_name = "satellite calibration" ;
calibration:units = "m" ;
double cross_track_distance(num_pixels) ;
cross_track_distance:comment = "Distance of sample from nadir. Negative values indicate the left side of the swath, and positive values indicate the right side of the swath.\n" ;
cross_track_distance:coordinates = "longitude latitude" ;
cross_track_distance:long_name = "cross track distance" ;
cross_track_distance:units = "km" ;
cross_track_distance:valid_max = 75. ;
cross_track_distance:valid_min = -75. ;
short dac(num_lines, num_pixels) ;
dac:_FillValue = -32767s ;
dac:scale_factor = 0.0001 ;
dac:comment = "Model estimate of the effect on sea surface topography due to high frequency air pressure and wind effects and the low-frequency height from inverted barometer effect. The ssha in this file is already corrected for the dac; the uncorrected ssha can be computed as follows: [uncorrected ssha]=[ssha from product]+[dac]; see the product user manual for details.\n" ;
dac:coordinates = "longitude latitude" ;
dac:institution = "LEGOS/CNES/CLS" ;
dac:long_name = "dynamic atmospheric correction" ;
dac:source = "MOG2D" ;
dac:units = "m" ;
int internal_tide(num_lines, num_pixels) ;
internal_tide:_FillValue = -2147483647 ;
internal_tide:scale_factor = 0.0001 ;
internal_tide:comment = "The ssha in this file is already corrected for the internal_tide; the uncorrected ssha can be computed as follows: [uncorrected ssha]= [ssha from product]+[internal_tide]; We recommend to apply on ssha_unfiltered field. See the product user manual for details\n" ;
internal_tide:coordinates = "longitude latitude" ;
internal_tide:long_name = "Internal Tide signal from HRET14/HRET8 blend: coherent mode M2/K1/O1/S2/N2" ;
internal_tide:source = "HRET14/HRET8 blend" ;
internal_tide:units = "m" ;
internal_tide:disclaimer = "There are limitations of HRET14 in specific regions (see L3 handbook). Will likely be replaced by a new HRET algorithm in a future release\n" ;
int latitude(num_lines, num_pixels) ;
latitude:scale_factor = 1.e-06 ;
latitude:comment = "Latitude of measurement [-80,80]. Positive latitude is North latitude, negative latitude is South latitude." ;
latitude:long_name = "latitude (positive N, negative S)" ;
latitude:standard_name = "latitude" ;
latitude:units = "degrees_north" ;
int longitude(num_lines, num_pixels) ;
longitude:scale_factor = 1.e-06 ;
longitude:comment = "Longitude of measurement. East longitude relative to Greenwich meridian." ;
longitude:long_name = "longitude (degrees East)" ;
longitude:standard_name = "longitude" ;
longitude:units = "degrees_east" ;
int mdt(num_lines, num_pixels) ;
mdt:_FillValue = -2147483647 ;
mdt:scale_factor = 0.0001 ;
mdt:comment = "The mean dynamic topography is the sea surface height above geoid; it is used to compute the absolute dynamic topography adt=ssha+mdt. A -5cm bias is added to the MDT for consistency with DUACS nadir products. This bias is inherited from the change of reference period implemented in 2014 when DUACS products went from a 7-year reference [1993, 1997] to a 20-year reference [1993, 2012]\n" ;
mdt:coordinates = "longitude latitude" ;
mdt:long_name = "mean dynamic topography" ;
mdt:source = "HYBRID-CNES-CLS22-CMEMS2020 (https://doi.org/10.24400/527896/a01-2024.010)" ;
mdt:standard_name = "mean_dynamic_topography_cnes_cls" ;
mdt:units = "m" ;
int mss(num_lines, num_pixels) ;
mss:_FillValue = -2147483647 ;
mss:scale_factor = 0.0001 ;
mss:comment = "Mean sea surface height above the reference ellipsoid. The value is referenced to the mean tide system, i.e. includes the permanent tide (zero frequency)\n" ;
mss:coordinates = "longitude latitude" ;
mss:long_name = "mean sea surface height (CNES/CLS)" ;
mss:source = "Hybrid SIO/CNES_CLS22/DTU21 (https://doi.org/10.24400/527896/a01-2024.002)" ;
mss:units = "m" ;
int ocean_tide(num_lines, num_pixels) ;
ocean_tide:_FillValue = -2147483647 ;
ocean_tide:scale_factor = 0.0001 ;
ocean_tide:comment = "Geocentric ocean tide height. Includes the total sum of the ocean tide, the corresponding load tide and equilibrium long-period ocean tide height. The ssha in this file is already corrected for the ocean_tide; the uncorrected ssha can be computed as follows: [uncorrected ssha]=[ssha from product]+[ocean_tide]; see the product user manual for details.\n" ;
ocean_tide:coordinates = "longitude latitude" ;
ocean_tide:institution = "LEGOS/CNES" ;
ocean_tide:long_name = "geocentric ocean tide height (FES)" ;
ocean_tide:source = "FES2022 (https://doi.org/10.24400/527896/A01-2024.004)" ;
ocean_tide:units = "m" ;
ubyte quality_flag(num_lines, num_pixels) ;
quality_flag:comment = "Deduced from L3 DUACS processing; see the product user manual for details.\n" ;
quality_flag:coordinates = "longitude latitude" ;

quality_flag:flag_masks = 0LL, 3LL, 5LL, 10LL, 18LL, 19LL, 20LL, 30LL, 50LL, 70LL, 100LL, 101LL, 102LL ;
quality_flag:flag_meanings = "good eclipse local_outliers bad_quality_coast ocean_unsure ice_unsure ice soft_outliers extremes mission_event bad_swath_extremities not_on_sea no_data" ;
quality_flag:long_name = "Quality Flag" ;
quality_flag:standard_name = "valid_flag_for_data" ;
int sigma0(num_lines, num_pixels) ;
sigma0:_FillValue = -2147483647 ;
sigma0:scale_factor = 0.0001 ;
sigma0:comment = "Normalized radar cross section (sigma0) from KaRIn in real, linear units (not decibels). The value may be negative due to noise subtraction. The value is corrected for instrument calibration and atmospheric attenuation. A meteorological model provides the atmospheric attenuation (sig0_cor_atmos_model).\"\n" ;
sigma0:coordinates = "longitude latitude" ;
sigma0:long_name = "normalized radar cross section (sigma0) from KaRIn)" ;
sigma0:standard_name = "surface_backwards_scattering_coefficient_of_radar_wave" ;
sigma0:units = "1" ;
sigma0:valid_max = 10000000 ;
sigma0:valid_min = -1000 ;
int ssha_filtered(num_lines, num_pixels) ;
ssha_filtered:_FillValue = -2147483647 ;
ssha_filtered:scale_factor = 0.0001 ;
ssha_filtered:comment = "Height of the sea surface anomaly with all corrections applied and with calibration, data selection and noise reduction (using Unet model) applied; see the product user manual for details.\n" ;
ssha_filtered:coordinates = "longitude latitude" ;
ssha_filtered:long_name = "sea surface height anomaly calibrated, edited and filtered" ;
ssha_filtered:standard_name = "sea_surface_height_above_reference_ellipsoid" ;
ssha_filtered:units = "m" ;
string ssha_filtered:disclaimer = "Experimental algorithm. This parameter is the noise-mitigated counterpart of the 'ssha_unfiltered' variable. The noise was mitigated through a machine-learning algorithm (Treboutte et al., 2024). Caution is advised because the algorithm validation is still ongoing: some of the ocean features less than 50km in wavelength may also be affected by the de-noising algorithm\n" ;
int ssha_unedited(num_lines, num_pixels) ;
ssha_unedited:_FillValue = -2147483647 ;
ssha_unedited:scale_factor = 0.0001 ;
ssha_unedited:comment = "Height of the sea surface anomaly with all corrections applied and with calibration. Contains both valid and invalid measurements; see the product user manual for details.\n" ;
ssha_unedited:coordinates = "longitude latitude" ;
ssha_unedited:long_name = "sea surface height anomaly calibrated" ;
ssha_unedited:standard_name = "sea_surface_height_above_reference_ellipsoid" ;
ssha_unedited:units = "m" ;
int ssha_unfiltered(num_lines, num_pixels) ;
ssha_unfiltered:_FillValue = -2147483647 ;
ssha_unfiltered:scale_factor = 0.0001 ;
ssha_unfiltered:comment = "Height of the sea surface anomaly with all corrections applied and with calibration and data selection applied; It is equivalent to the Sea Level Anomaly (SLA) distribued in the nadir DUACS products; see the product user manual for details.\n" ;
ssha_unfiltered:coordinates = "longitude latitude" ;
ssha_unfiltered:long_name = "sea surface height anomaly calibrated and edited" ;
ssha_unfiltered:standard_name = "sea_surface_height_above_reference_ellipsoid" ;
ssha_unfiltered:units = "m" ;
int ugos_filtered(num_lines, num_pixels) ;
ugos_filtered:_FillValue = -2147483647 ;
ugos_filtered:scale_factor = 0.0001 ;
ugos_filtered:coordinates = "longitude latitude" ;
ugos_filtered:long_name = "Absolute geostrophic velocity: zonal component" ;
ugos_filtered:standard_name = "surface_geostrophic_eastward_sea_water_velocity" ;
ugos_filtered:units = "m/s" ;
ugos_filtered:comment = "Derived from [ssha_filtered] field and mean dynamic currents associated with the MDT field" ;
int ugosa_filtered(num_lines, num_pixels) ;
ugosa_filtered:_FillValue = -2147483647 ;
ugosa_filtered:scale_factor = 0.0001 ;
ugosa_filtered:coordinates = "longitude latitude" ;
ugosa_filtered:long_name = "Geostrophic velocity anomalies: zonal component" ;
ugosa_filtered:standard_name = "surface_geostrophic_eastward_sea_water_velocity_assuming_sea_level_for_geoid" ;
ugosa_filtered:units = "m/s" ;
ugosa_filtered:comment = "Derived from ssha_filtered field" ;
int ugosa_unfiltered(num_lines, num_pixels) ;
ugosa_unfiltered:_FillValue = -2147483647 ;
ugosa_unfiltered:scale_factor = 0.0001 ;
ugosa_unfiltered:comment = "Derived from ssha_unfiltered field" ;
ugosa_unfiltered:coordinates = "longitude latitude" ;
ugosa_unfiltered:long_name = "Geostrophic velocity anomalies: zonal component" ;
ugosa_unfiltered:standard_name = "surface_geostrophic_eastward_sea_water_velocity_assuming_sea_level_for_geoid" ;
ugosa_unfiltered:units = "m/s" ;
int vgos_filtered(num_lines, num_pixels) ;
vgos_filtered:_FillValue = -2147483647 ;
vgos_filtered:scale_factor = 0.0001 ;
vgos_filtered:coordinates = "longitude latitude" ;
vgos_filtered:long_name = "Absolute geostrophic velocity: meridian component" ;
vgos_filtered:standard_name = "surface_geostrophic_northward_sea_water_velocity" ;
vgos_filtered:units = "m/s" ;

```
        vgos_filtered:comment = "Derived from [ssha_filtered] field and mean dynamic currents associated with the MDT field" ;
    int vgosa_filtered(num_lines, num_pixels) ;
        vgosa_filtered:_FillValue = -2147483647 ;
        vgosa_filtered:scale_factor = 0.0001 ;
        vgosa_filtered:coordinates = "longitude latitude" ;
        vgosa_filtered:long_name = "Geostrophic velocity anomalies: meridian component" ;
        vgosa_filtered:standard_name = "surface_geostrophic_northward_sea_water_velocity_assuming_sea_level_for_geoid" ;
        vgosa_filtered:units = "m/s" ;
        vgosa_filtered:comment = "Derived from ssha_filtered field" ;
    int vgosa_unfiltered(num_lines, num_pixels) ;
        vgosa_unfiltered:_FillValue = -2147483647 ;
        vgosa_unfiltered:scale_factor = 0.0001 ;
        vgosa_unfiltered:comment = "Derived from ssha_unfiltered field" ;
        vgosa_unfiltered:coordinates = "longitude latitude" ;
        vgosa_unfiltered:long_name = "Geostrophic velocity anomalies: meridian component" ;
        vgosa_unfiltered:standard_name = "surface_geostrophic_northward_sea_water_velocity_assuming_sea_level_for_geoid" ;
        vgosa_unfiltered:units = "m/s" ;
    short i_num_line(num_nadir) ;
        i_num_line:comment = "alongtrack indice of the nearest karin pixel from the nadir data" ;
        i_num_line:long_name = "alongtrack indice of the nearest karin pixel from the nadir data" ;
        i_num_line:units = "count" ;
    byte i_num_pixel(num_nadir) ;
        i_num_pixel:comment = "acrosstrack indice of the nearest karin pixel from the nadir data" ;
        i_num_pixel:long_name = "acrosstrack indice of the nearest karin pixel from the nadir data" ;
        i_num_pixel:units = "count" ;

// global attributes:
        :Conventions = "CF-1.7" ;
        :Metadata_Conventions = "Unidata Dataset Discovery v1.0" ;
        :cdm_data_type = "Swath" ;
        :comment = "Sea Surface Height measured by Altimetry" ;
        :data_used = "SWOT KaRIn L2_LR_SSH PGC0/PIC0/PIC2 (NASA/CNES). DOI associated: https://doi.org/10.24400/527896/a01-2023.015" ;
        :doi = "https://doi.org/10.24400/527896/A01-2023.018" ;
        :geospatial_lat_units = "degrees_north" ;
        :geospatial_lon_units = "degrees_east" ;
        :geospatial_vertical_max = 0LL ;
        :geospatial_vertical_min = 0LL ;
        :geospatial_vertical_positive = "down" ;
        :geospatial_vertical_resolution = "point" ;
        :geospatial_vertical_units = "m" ;
        :institution = "CLS, CNES" ;
        :keywords = "Oceans > Ocean Topography > Sea Surface Height" ;
        :keywords_vocabulary = "NetCDF COARDS Climate and Forecast Standard Names" ;
        :platform = "Swot" ;
        :processing_level = "L3" ;
        :product_version = "2.0.1" ;
        :project = "SSALTO/DUACS" ;
        :reference_altimeter = "S6" ;
        :references = "Handbook: https://www.aviso.altimetry.fr/fileadmin/documents/data/tools/hdbk_duacs_SWOT_L3.pdf" ;
        :source = "Altimetry measurements" ;
        :ssalto_duacs_comment = "The reference mission used for the altimeter inter-calibration processing is Sentinel-6A" ;
        :standard_name_vocabulary = "NetCDF Climate and Forecast (CF) Metadata Convention Standard Name Table v37" ;
        :time_coverage_resolution = "PT0.3S" ;
        :title = "NRT SWOT KaRIn & nadir Global Ocean swath SSALTO/DUACS Sea Surface Height L3 product" ;
        :contact = "aviso@altimetry.fr" ;
        :creator_email = "aviso@altimetry.fr" ;
        :creator_name = "DUACS - Data Unification and Altimeter Combination System" ;
        :creator_url = "https://aviso.altimetry.fr" ;
        :license = "https://www.aviso.altimetry.fr/fileadmin/documents/data/License_Aviso.pdf" ;
        :time_coverage_start = "2024-12-23T20:20:47Z" ;
        :time_coverage_end = "2024-12-23T21:12:13Z" ;
        :geospatial_lat_min = -78.271942 ;
        :geospatial_lat_max = 78.272019 ;
        :geospatial_lon_min = 5.e-06 ;
        :geospatial_lon_max = 359.999986 ;
        :date_modified = "2025-01-10T11:03:59Z" ;
        :history = "2025-01-10T11:03:59Z: Created by DUACS KaRIn prototype" ;
        :date_created = "2025-01-10T11:03:59Z" ;
        :date_issued = "2025-01-10T11:03:59Z" ;
}
```

7 Accessibility of the products

If you already have an AVISO account, data access is available through the following services:

CNES AVISO FTP/SFTP (with AVISO+ credentials)

- FTP access: ftp-access.aviso.altimetry.fr:21
- SFTP access: ftp-access.aviso.altimetry.fr:2221
    - /swot_products/l3_karin_nadir/l3_lr_ssh/

CNES AVISO THREDDS Data Server, TDS

- TDS access: https://tds%40odatis-ocean.fr:odatis@tds-odatis.aviso.altimetry.fr/thredds/catalog/dataset-l3-swot-karin-nadir-validated/l3_lr_ssh/catalog.html

8 Contact

For more information, please contact:

Aviso+ User Services
E-mail: aviso@altimetry.fr
On Internet: https://www.aviso.altimetry.fr/

The user service is also interested in user feedback; questions, comments, proposals, requests are much welcome.

9 Bibliography

Arbic, Brian K., Robert B. Scott, Dudley B. Chelton, James G. Richman, et Jay F. Shriver. 2012. « Effects of Stencil Width on Surface Ocean Geostrophic Velocity and Vorticity Estimation from Gridded Satellite Altimeter Data ». *Journal of Geophysical Research: Oceans* 117 (C3): 2011JC007367. https://doi.org/10.1029/2011JC007367.

Cartwright, D. E., et Anne C. Edden. 1973. « Corrected Tables of Tidal Harmonics ». *Geophysical Journal International* 33 (3): 253‑64. https://doi.org/10.1111/j.1365-246X.1973.tb03420.x.

Cartwright, D. E., et R. J. Tayler. 1971. « New Computations of the Tide-generating Potential ». *Geophysical Journal International* 23 (1): 45‑73. https://doi.org/10.1111/j.1365-246X.1971.tb01803.x.

Charayron, R., P. Schaeffer, M. Ballaritta, et al. 2025. « Blending Data from SWOT KaRIn Science Phase and 30 Years of Nadir Altimetry to Improve Mean Sea Surface Models ». Oral presentation. EGU General Assembly 2025, Vienna, Austria, avril 30. https://meetingorganizer.copernicus.org/EGU25/EGU25-8570.html.

Chou, Min-Yang, Jia Yue, Jack Wang, et al. 2023. « Validation of Ionospheric Modeled TEC in the Equatorial Ionosphere During the 2013 March and 2021 November Geomagnetic Storms ». *Space Weather* 21 (6): e2023SW003480. https://doi.org/10.1029/2023SW003480.

Desai, Shailen, John Wahr, et Brian Beckley. 2015. « Revisiting the Pole Tide for and from Satellite Altimetry ». *Journal of Geodesy* 89 (12): 1233‑43. https://doi.org/10.1007/s00190-015-0848-7.

Jousset, S., et S. Mulet. 2020. « New Mean Dynamic Topography of the Black Sea and Mediterranean Sea from altimetry, gravity and in-situ data ». OSTST. https://ostst.aviso.altimetry.fr/fileadmin/user_upload/tx_ausyclsseminar/files/OSTST2020_JOUSSET_MULET_MDT.pdf.

Jousset, S., S. Mulet, John Wilkin, Eric Greiner, G Dibarboure, et N Picot. 2022. « New global Mean Dynamic Topography CNES-CLS-22 combining drifters, hydrological profiles and High Frequency radar data", OSTST 2022 ». https://doi.org/10.24400/527896/a03-2022.3292.

Jousset, Solène, Sandrine Mulet, Eric Greiner, et al. 2025. « New Global Mean Dynamic Topography CNES-CLS-22 Combining Drifters, Hydrography Profiles and High Frequency Radar Data ». *ESS Open Archive*, publication en ligne anticipée. https://doi.org/10.22541/essoar.170158328.85804859/v2.

Laloue, A, P Veillard, P Schaeffer, et al. 2024. « Merging recent Mean Sea Surface into a 2023 Hybrid model (from Scripps, DTU, CLS and CNES) ».

Loren Carrère, Florend Lyard, Mathilde Cancet, et al. 2023. « The new FES2022 Tidal atlas. Presented at the 2023 SWOT Science Team meeting (Toulouse). Available online (last access: 19 April 2024): https://doi.org/10.24400/527896/a03-2022.3287 ».

Lyard, F., L Carrere, M-L Dabat, et al. 2023. « Barotropic correction for SWOT: FES2022 and DAC ». Oral. SWOT-ST meeting, Toulouse. https://swotst.aviso.altimetry.fr/fileadmin/user_upload/SWOTST2023/20230921_ocean_3_tides/11h00-2_FES2022-DAC.pdf.

Picard, Bruno, Aurélien Colin, Aurélien Husson, et Gérald Dibarboure. 2025. *The Effects of Rain on a Ka-Band Swath Altimeter: Lessons Learned from the SWOT Mission*. avril 10. https://eartharxiv.org/repository/view/8950/.

Ray, R. D. 2025. « "Documentation for Goddard Ocean Tide Solution GOT5: Global Tides from Multimission Satellite Altimetry". NASA TM-20250002085, Goddard Space Flight Center, Greenbelt, Maryland, USA ». https://science.gsfc.nasa.gov/sed/content/uploadFiles/publication_files/GOT5-TechMemo.pdf.

Schaeffer, P., M-I Pujol, P Veillard, et al. 2023. « The CNES CLS 2022 Mean Sea Surface: Short Wavelength Improvements from CryoSat-2 and SARAL/AltiKa High-Sampled Altimeter Data ». *Remote Sensing* 15 (11): 2910. https://doi.org/10.3390/rs15112910.

Tchilibou, Michel, Simon Barbot, Loren Carrere, Ariane Koch-Larrouy, Gérald Dibarboure, et Clément Ubelmann. 2025. « M2 Monthly and Annual Mode 1 and Mode 2 Internal Tide Atlases from Altimetry Data and MIOST: Focus on the Indo-Philippine Archipelago and the Region off the Amazon Shelf ». *EGUsphere*, janvier 7, 1‑21. https://doi.org/10.5194/egusphere-2024-3947.

Tran, N. 2019. « Rapport Annuel d'activité SALP - Activité SSB ».

Tranchant, Yann-Treden, Benoit Legresy, Annie Foppert, Beatriz Pena-Molino, et Helen Elizabeth Phillips. 2025. « SWOT reveals fine-scale balanced motions and dispersion properties in the Antarctic Circumpolar Current ». *ESS Open Archive*, publication en ligne anticipée. https://doi.org/10.22541/essoar.173655552.25945463/v1.

Ubelmann, Clément, Loren Carrere, Chloé Durand, et al. 2022. « Simultaneous Estimation of Ocean Mesoscale and Coherent Internal Tide Sea Surface Height Signatures from the Global Altimetry Record ». *Ocean Science* 18 (2): 469‑81. https://doi.org/10.5194/os-18-469-2022.

Zaron E. et Elipot S. 2024. « Estimates of Baroclinic Tidal Sea Level and Currents from Lagrangian Drifters and Satellite Altimetry ». J. Atmoph. and Ocean. Tech.

Zaron, Edward D. 2019. « Baroclinic Tidal Sea Level from Exact-Repeat Mission Altimetry ». Journal of Physical Oceanography. *Journal of Physical Oceanography* 49 (1): 193‑210. https://doi.org/10.1175/JPO-D-18-0127.1.

Zhao, Zhongxiang. 2025. « A New-Generation Internal Tide Model Based on 30 Years of Satellite Sea Surface Height Measurements ». *Earth System Science Data Discussions*, janvier 20, 1‑37. https://doi.org/10.5194/essd-2024-611.